CUIMR-T-82-006 C. 2

CIRCULATING COPY
Sea Grant Depository

PB83-158709

Behavior of Submerged Multiple Bodies in Earthquakes

LOAN COPY ONLY

California Univ.
Berkeley

Prepared for

National Oceanic and Atmospheric Administration
Rockville, MD

Sep 82

NATIONAL SEA GRANT DEPOSITORY
PELL LIBRARY BUILDING
URI, NARRAGANSETT BAY CAMPUS
NARRAGANSETT, RI 02882

U.S. Department of Commerce
National Technical Information Service
NTIS

50272-101

REPORT DOCUMENTATION PAGE	1. REPORT NO. UCB/EERC-82/16	2.	3. Recipient's Accession No. PB83 158709
4. Title and Subtitle: The Behavior of Submerged, Multiple Bodies in Earthquakes			5. Report Date: September 1982
			6.
			8. Performing Organization Rept. No. EERC-82/16
7. Author(s): Wen-Gen Liao			10. Project/Task/Work Unit No.
9. Performing Organization Name and Address: Earthquake Engineering Research Center, University of California, Berkeley, 47th Street and Hoffman Blvd., Richmond, Calif. 94804			11. Contract(C) or Grant(G) No. (C) (G)
12. Sponsoring Organization Name and Address: NOAA, Office of Sea Grant, Department of Commerce			13. Type of Report & Period Covered
			14.

15. Supplementary Notes

16. Abstract (Limit: 200 words)

In order to investigate the nature of hydrodynamic interaction between two (or more) cylinders subjected to earthquake ground motion, a numerical analysis for determining the hydrodynamic forces on and the corresponding structural responses of a non-axisymmetrical offshore structure is presented.

With the assumption of potential flow theory, a finite element method is developed to solve the boundary value problem in the fluid domain, which because of symmetry is reduced to one half. A localized finite element method utilizing eigenfunction expansions is also outlined in detail. If the cylinders have uniform cross sections, the three-dimensional problem can be reduced to a two-dimensional one and the computation becomes much more efficient. A computer program is developed to analyze the hydrodynmaic forces and the structural responses according to the above mentioned analysis procedure, and illustrative examples are presented. Compared with the experiments of a physical model on an earthquake simulator, the results are generally in agreement.

The results established indicate that hydrodynamic interaction is relevant if the cylinders are close, and that this phenomenon depends on the characteristics of the structure, water depth, excitation frequency, amplitude of ground motion, and direction of excitation.

17. Document Analysis a. Descriptors

b. Identifiers/Open-Ended Terms

c. COSATI Field/Group

18. Availability Statement: Release Unlimited	19. Security Class (This Report)	21. No. of Pages 140
	20. Security Class (This Page)	22. Price

(See ANSI-Z39.18) See Instructions on Reverse OPTIONAL FORM 272 (Formerly NTIS-35) Department of Comm

PB83-156709

REPORT NO.
UCB/EERC-82/16
SEPTEMBER 1982

EARTHQUAKE ENGINEERING RESEARCH CENTER

THE BEHAVIOR OF SUBMERGED, MULTIPLE BODIES IN EARTHQUAKES

by

WEN-GEN LIAO

Report to NOAA, Office of Sea Grant, and
The State Resources Agency of California

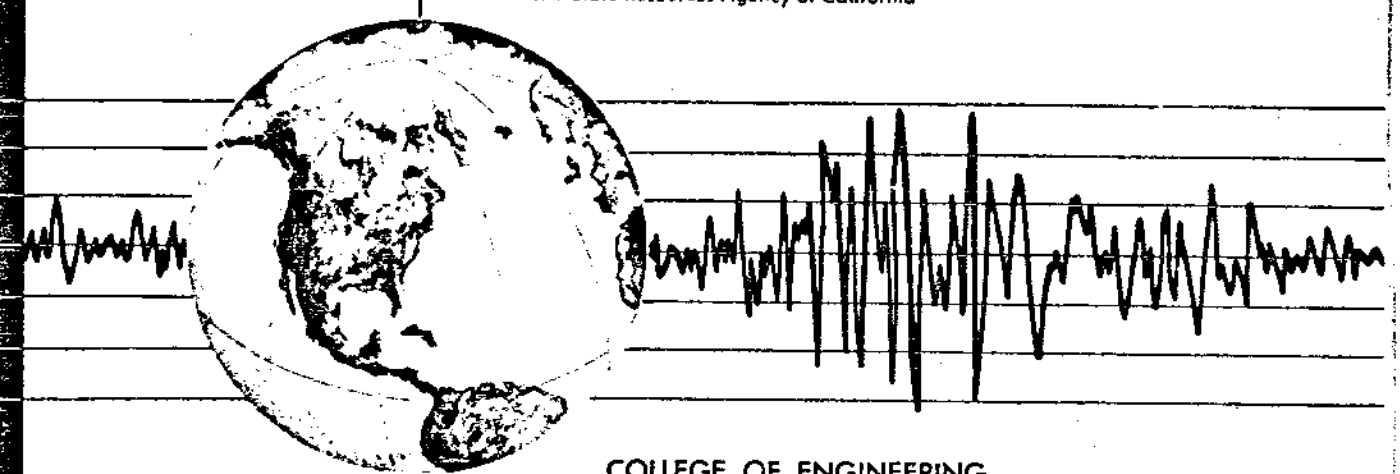

COLLEGE OF ENGINEERING

UNIVERSITY OF CALIFORNIA · Berkeley, California

REPRODUCED BY
NATIONAL TECHNICAL
INFORMATION SERVICE
US DEPARTMENT OF COMMERCE
SPRINGFIELD, VA. 22161

For sale by the National Technical Information Service, U.S. Department of Commerce, Springfield, Virginia 22161.

See back of report for up to date listing of EERC reports.

DISCLAIMER

Any opinions, findings, and conclusions or recommendations expressed in this publication are those of the author and do not necessarily reflect the views of the Sponsors or the Earthquake Engineering Research Center, University of California, Berkeley

THE BEHAVIOR OF SUBMERGED, MULTIPLE BODIES IN EARTHQUAKES

by

Wen-Gen Liao

Report to

NOAA, Office of Sea Grant
Department of Commerce, Washington, D.C.
and
The State Resources Agency of California

Report No. UCB/EERC-82/16
Earthquake Engineering Research Center
and
Hydraulic Engineering Laboratory
University of California
Berkeley, California

September 1982

j.a

ABSTRACT

In order to investigate the nature of hydrodynamic interaction between two (or more) cylinders subjected to earthquake ground motion, a numerical analysis for determining the hydrodynamic forces and the corresponding structural responses on a non-axisymmetrical offshore structure is presented.

With the assumption of potential flow theory, the finite element method is developed to solve the boundary value problem in fluid domain. Moreover, the principle of symmetry and antisymmetry is applied to the problem such that the fluid domain can be reduced to one half. A localized finite element method utilizing eigenfunction expansions is also outlined in detail. If the cylinders have uniform cross sections, the three-dimensional problem can be reduced to a two-dimensional one and the computation becomes much more efficient. A computer program is developed to analyze the hydrodynamic forces and the structural responses according to the above mentioned analysis procedure. Examples are presented to illustrate the points discussed. Comparing with the experiments of a physical model on an earthquake simulator, the results are generally in agreement.

From the results of the research, we arrive at the conclusion that the hydrodynamic interaction is relevant as the cylinders are closer. Also, this phenomenon depends on the characteristics of structures, water depth, the excitation frequency, the amplitude of ground motion, and the direction of excitation.

ACKNOWLEDGEMENTS

This work is a result of research sponsored by NOAA, Office of Sea Grant, Department of Commerce under Projects R/OT-1-WGL-SD-09/82 and E/G-2-WIEGEL-09/82, and by the State Resources Agency of California. The author sincerely appreciates their support.

This work also constitutes the author's doctoral dissertation submitted to the University of California, Berkeley. The dissertation committee consisted of Professors William C. Webster (Chairman), Joseph Penzien, Robert L. Wiegel and Alaa E. Mansour. The author is grateful to the professors in the committee for providing advices and invaluable suggestions.

Special thanks are extended to Professor William C. Webster who served as dissertation committee chairman, to Professor Joseph Penzien who served as academic advisor, and to Professor Robert L. Wiegel who served as program coordinator throughout the author's doctoral program.

The author is also thankful to Mr. G. R. Ansari for providing discussions and suggestions.

TABLE OF CONTENTS

LIST OF FIGURES

LIST OF TABLES

LIST OF NOTATIONS

a^j	=	radius of the j-th cylinder
A	=	projected area of cylinder in Morison's equation 2.1
$\underline{A}_l$	=	fluid stiffness matrix in localized finite element formulation, Eq. 4.43
$\underline{A}_{kl}$	=	submatrices of $\underline{A}_l$, Eqs. 4.41.a-d
$\underline{A}_m^*$	=	three-dimensional total generalized mass expression containing $\underline{A}_m$, Eq. 3.41
$\underline{A}_m$	=	generalized mass expression associated with ground acceleration, Eq. 3.32
$\underline{b}$	=	three-dimensional fluid loading vector, Eqs. 4.7,4.12
$\underline{b}_{1l},\underline{b}_{2l}$	=	fluid loading vectors in localized finite element formulation, Eq. 4.40
$\underline{b}_l$	=	two-dimensional fluid loading vector for the i-th mode of wave, Eq. 4.20
$\underline{B}_0$	=	amplitude of $\underline{b}$ due to unit ground acceleration, Eq. 4.13
$\underline{B}_{l0}$	=	amplitude of $\underline{b}_l$ due to unit ground acceleration, Eq. 4.25
$\underline{B}_k^j$	=	amplitude of $\underline{b}_l$ due to the k-th mode of structural vibration for the j-th cylinder, Eq. 4.25
$\underline{B}^j$	=	amplitude of $\underline{b}$ due to structural acceleration for rigid cylinders, Eq. 4.9.b
$\underline{B}_k^j$	=	amplitude of $\underline{b}$ due to the k-th mode of unit structural acceleration for flexible cylinders, Eq. 4.13
c_l	=	coefficient of hydrodynamic pressure expansion
C	=	velocity of sound in water
$\underline{C}^a$	=	hydrodynamic damping matrix of rigid structures, Eq. 3.25
$\underline{C}^j$	=	damping matrix of the j-th cylinder, Eq. 3.2.e
$\underline{C}_m^*$	=	total generalized hydrodynamic damping matrix of flexible structures, Eq. 3.41

$\underline{C}_m^*$	=	total generalized damping matrix of flexible structures, Eq. 3.41
$\underline{C}_n$	=	the n-th mode generalized damping matrix of flexible structures, Eq. 3.32
$\underline{C}^*$	=	total damping matrix of structures, Eq. 3.1
d	=	distance between cylinders
$\bar{d}$	=	$\frac{d}{a^1+a^2}$, relative distance
d.o.f.	=	degree of freedom
D	=	diameter of cylinder
$\underline{E}^U$	=	complex hydrodynamic effect matrix of rigid structures, Eq. 3.24
$\underline{E}^U_R, \underline{E}^U_I$	=	real and imagine parts of $\underline{E}^U$
E_{n0}	=	generalized hydrodynamic effect corresponding to the n-th mode of structural vibration due to the unit ground acceleration, Eq. 3.38
E_{nk}	=	generalized hydrodynamic effect corresponding to the n-th mode of structural vibration due to the unit modal acceleration on the k-th mode, Eq. 3.38
$f(x,y,z)$	=	source distribution function, Eq. 2.3
$\bar{f}(z)$	=	separated hydrodynamic pressure in Z-direction, Eq. 3.10
f_1	=	function defined in Eq. 4.29
F	=	hydrodynamic force in Morsion's equation, Eq. 2.1
F_n^j	=	element in $\underline{F}_n$
$\underline{F}^j$	=	hydrodynamic force matrix on the j-th cylinder, Eq. 3.2.e
$\underline{F}_n$	=	generalized hydrodynamic force on the n-th mode of structural vibration, Eq. 3.33.e
$\underline{F}^*$	=	total hydrodynamic force matrix containing $\underline{F}^j$, Eq. 3.1
$F(\bar{p}_{1i}, \bar{p}_{2i})$	=	functional defined in Eq. 4.33
δF	=	the variation of the functional F
g	=	acceleration of gravity
G	=	kernel of Green's function

h	=	water depth
H	=	height of cylinder
$H_n^{(1)}$	=	Hankel function of the first kind of order n
I	=	mass moment of inertia of rigid cylinder
k, k_0	=	wave number
k_i	=	coefficient of wave dispersion on the i-th mode, Eq. 3.13
K_c	=	Keulegan-Carpenter number
K_d	=	drag coefficient
K_m	=	added mass coefficient
$\bar{K}_l$	=	modified Bessel function of the second kind to the l-th order
$\underline{K}$	=	fluid stiffness matrix in three dimensions, Eq. 4.7
$\underline{K}_i$	=	fluid stiffness matrix in the i-th mode in two dimensions, Eq. 4.25
$\underline{K}^j$	=	stiffness matrix of the j-th cylinder, Eq. 3.2.d
$\underline{K}_m^*$	=	total generalized stiffness matrix of flexible structures, Eq. 3.41
$\underline{K}_n$	=	the n-th mode generalized stiffness matrix of flexible structures, Eq. 3.32
$\underline{K}^*$	=	total stiffness matrix of structures, Eq. 3.1
L	=	wave length
$m(z)$	=	unit mass of cylinder in Z-direction
$m_a^k(z)$	=	added mass effect defined in Eqs. 5.2,5.3
M	=	mass of rigid cylinder
$M_{ij,kl}$	=	added mass corresponding to the j-th d.o.f. of the i-th cylinder due to the unit acceleration on the l-th d.o.f. of the k-th cylinder as defined in Example V-A
$\underline{M}^a$	=	added mass matrix of rigid structures, Eq. 3.25

$\underline{M_g}$ — hydrodynamic effect matrix of rigid structures associated with ground acceleration, Eq. 3.25

$\underline{M^j}$ — mass matrix of the j-th cylinder, Eq. 3.2.b

$\underline{M_m}^e$ — total generalized added mass matrix of flexible structures, Eq. 3.41

$\underline{M_m}^g$ — total generalized hydrodynamic effect matrix of flexible structures due to unit ground acceleration, Eq. 3.41

$\underline{M_m}^*$ — total generalized mass matrix of flexible structures, Eq. 3.41

$\underline{M_n}$ — the n-th mode generalized mass matrix of flexible structures, Eq. 3.32

$\underline{M_{xy}}$ — added mass matrix in X-direction with respect to the d.o.f in Y-direction, Eq. 4.53

$\underline{M}^*$ — total mass matrix of structures, Eq. 3.1

$\overline{n}$ — unit vector in the direction of ground acceleration

n_l — number of eigenfunctions defined in outer domain in localized finite element formulation, Eq. 4.37

n_s — number of structural vibration modes

n_w — number of wave modes

$\underline{N}$ — shape function in finite element formulation

$p(x,y,z)$ — frequency dependent hydrodynamic pressure

$\overline{p}_{1i}$ — the i-th mode two-dimensonal hydrodynamic pressure in inner domain in the localized finite element formulation

$\overline{p}_{2i}$ — the i-th mode two-dimensional hydrodynamic pressure in outer domain in the localized finite element formulation

p_{as} — antisymmetrical hydrodynamic pressure

$\overline{p}_i(x,y)$ — amplitude of the i-th mode hydrodynamic pressure in two dimensions, Eq. 3.12

$p_i(x,y,z)$ — $c_i\overline{p}_i(x,y)\psi_i(z)$, Eq. 3.17.a

$p^j(z)$ — hydrodynamic forces on the j-th cylinder per unit height, Eq. 3.35

$p_k(z)$ — amplitude of hydrodynamic force on single flexible cylinder, Eq. C.22 or

$$\int_0^{2\pi}\left[\sum_{i=1}^{n_m} P_{ik}{}^1\psi_i(z)\right]a^1\cos\theta\, d\theta$$

p_s — symmetrical hydrodynamic pressure

$p^*(x,y,z;t)$ — time dependent hydrodynamic pressure

$\underline{p}$ — vector of nodal hydrodynamic pressure in finite element formulation

$\underline{p}^e$ — vector of nodal hydrodynamic pressure in each finite element

$\underline{P}_0$ — amplitude of three-dimensional hydrodynamic pressure due to unit ground acceleration, Eq. 4.15

$\underline{P}_{i0}$ — amplitude of two-dimensional hydrodynamic pressure on the i-th mode of wave, due to the unit ground acceleration, Eq. 4.26

$\underline{P}_{ik}{}^j$ — amplitude of two-dimensional hydrodynamic pressure on the i-th mode of wave, corresponding to the k-th mode of structural vibration for the j-th cylinder, Eq. 4.26

$\underline{P}^j$ — amplitude of hydrodynamic pressure on the j-th rigid cylinder, Eq. 4.10

$\underline{P}_k{}^j$ — amplitude of three-dimensional hydrodynamic pressure on the j-th cylinder, corresponding to the k-th mode of structural vibration, Eq. 4.15

$\underline{r}$ — pseudostatic influence coefficient vector

R — $\sqrt{x^2+y^2}$, central distance in polar coordinates

R_1, R_2 — inner and outer regions in localized finite element formulation

S — boundary of fluid domain

S_{as} — antisymmetrical boundary of fluid domain

S_b — boundary of bottom of fluid domain

S_f — far field boundary of fluid domain

S_{ij} — interface boundary on the j-th cylinder of fluid domain

S_s	=	symmetrical boundary of fluid domain
S_f	=	boundary of water surface
S_{tb}	=	transmitting boundary of fluid domain
T	=	period of wave
$u, \dot{u}, \ddot{u}$	=	water particle displacement, velocity and acceleration
$\ddot{u}_g$	=	ground acceleration
$\ddot{u}_{gx}, \ddot{u}_{gy}$	=	X- and Y-component of ground acceleration
$U(\omega), U$	=	frequency dependent total structural displacement vector
$\underline{\ddot{U}}^a$	=	$\underline{\ddot{U}}^t + \underline{r}\ddot{u}_g$, absolute structural response vector
$\underline{U}^j$	=	structural displacement vector for the j-th cylinder, Eq. 3.2.a
$\underline{U}^*(t)$	=	time dependent total structural displacement vector containing $\underline{U}^j$, Eq. 3.1
V	=	volume of fluid displaced by structure
V_s	=	base shear of structures
w^*	=	weighting function in finite element formulation
$\underline{Y}_m^*$	=	total generalized structural displacement vector of flexible structures, Eq. 3.41
$\underline{Y}_n$	=	the n-th mode generalized structural displacement vector for flexible structures, Eq. 3.32
z_c^j	=	height of center of gravity of the j-th cylinder
$\underline{Z}$	=	uncoupled generalized structural displacement vector, Eq. 3.48
β	=	inclined angle of the surface of cylinder, Eq. 4.6
δ	=	angle of ground acceleration
λ	=	constant in separation of variables, Eq. 3.11.a
ω	=	frequency of ground excitation
$\bar{\omega}$	=	submerged natural frequency of structures, Eq. 3.30

ω_n	=	the n-th mode natural frequency of structure in the air
$\bar{\omega}_m$	=	submerged natural frequency of structural vibration in generalized coordinate, Eq. 3.47
$\underline{\Omega}$	=	matrix of eigenvector with respect to $\underline{Z}$, Eq. 3.47
$\phi_k^j(z)$	=	the k-th mode shape of structural vibration in the air for the j-th cylinder
$\underline{\Phi}_m^*$	=	transformation matrix containing ϕ_k^j, Eq. 3.49.a
$\underline{\Phi}_s$	=	transformation matrix for rigid cylinder, Eq. 3.18
$\underline{\Phi}^*$	=	submerged mode shape of structural vibration, Eqs. 3.30,3.49.b
$\Phi_D(x,y,z)$	=	frequency dependent radiated velocity potential
$\Phi_D^*(x,y,z;t)$	=	time dependent radiated velocity potential
$\Phi^*(x,y,z;t)$	=	time dependent velocity potential
$\psi_i(z)$	=	the i-th mode shape of wave
Ψ_{ji}	=	element in $\underline{\Psi}_i$, Eq. 4.37
$\underline{\Psi}_i$	=	matrix of eigenvector associated with wave radiation, Eq. 4.37
ρ	=	mass density of water
θ	=	angle in polar coordinate
$\bar{\theta}$	=	angle which relative to the direction of ground acceleration
ξ	=	structural damping coefficient
$\_$	=	underline indicates vector or matrix

I. INTRODUCTION

Due to the development of offshore engineering in recent years, the need for an improved understanding of the effects of hydrodynamic forces on offshore structures becomes increasingly evident. The problem of a single vertical cylinder subjected to the hydrodynamic forces produced by surface waves, earthquake motions, and currents is reasonably well understood [1,2]*; however, the hydrodynamic interaction between two (or more) cylinders under these same conditions is not so well understood. Since most often offshore platforms have three or four cylindrical legs and they often support clusters of parallel riser pipes, this interaction was selected as the topic of the investigation reported herein.

A. Review of Past Work

Hydrodynamic forces on rigid bodies placed in a fluid have been a classic problem in the field of fluid dynamics [3,4,5]. An important paper by Morison et. al., discussed the problem of wave forces on a rigid vertical cylinder from the point of view of engineering [6]. An empirical formula for predicting wave forces was given in this paper which has been widely used in the design of offshore structures [7 3,9,10].

In a study of the hydrodynamic forces on cylinders and plates in an oscillating fluid, Keulegan and Carpenter introduced a new parameter for describing fluid behavior which now is called the Keulegan-Carpenter number [11].

Diffraction theory is another approach to finding hydrodynamic forces caused by wave diffraction and radiation [12]. An even more general method is to use an integral equation formulation which can be applied to bodies of arbitrary shape [13,14]. This formulation is the basis of the Green's function technique for solving the problem of fluid-structure interaction. Many hydrodynamic problems have been solved by this formulation, e.g. (1) the radiation problem of an elliptical cylinder oscillating at the free surface [15], (2) wave forces on vertical

* The numbers in [ ] refer to the corresponding items under "REFERENCES".

axisymmetrical bodies [16], (3) wave forces on large bodies of arbitrary shape [17,18,19,20], and (4) wave induced forces on various bodies in the diffraction regime [21]. The major difficulty in using the Green's function method is to evaluate the kernel in the integral equation formulation. The finite element method has been used to evaluate the kernel function by assuming a linear variation of source strength over each element [22,23]. All investigations mentioned above are based on the assumptions that the submerged body is rigid and the fluid is inviscid and incompressible.

Another technique for treating diffraction theory is to apply the finite element method to the governing differential equation directly. This method was introduced by Zienkiewicz, Iron and Nath on submerged structures [24] and by Zienkiewicz and Newton on flexible structures in compressible fluids [25]. The problem of earthquake response of an axisymmetrical tower surrounded by water was studied by Liaw and Chopra [26]. The effects of the diffracted surface wave and the compressiblity of the water are shown to be small in this case.

Bai and Yeung considered the three-dimensional and axisymmetrical decaying behavior of the local fluid disturbance caused by the presence of a rigid structure [27]. A localized finite element method was suggested which combined a finite element near field with an analytic solution of the far field to reduce the size of the fluid domain directly treated [28]. Mei [29] and Taylor [30] also discussed the same concept under the name of boundary series method. The application of this approach has been made by (1) Chen and Mei for ship wave and steady free-surface flow problems [31,32], (2) Bai for steady uniform flow in a canal [33], (3) Hall on arch dam [34], and (4) Nilrat for submerged axisymmetrical bodies [35]. The uniqueness of this approach has been proved by Aranha, Mei and Yue [36].

Using infinite elements is another approach to representing the radiation boundary condition in an unbounded fluid domain. Zienkiewicz and Bettess presented the numerical solution of diffraction and radiation of surface waves by using a combination of finite elements in the near field and infinite elements in the far field [37,38]. The shape function used in the infinite elements has an exponentially decreasing term in the direction away from the inner region.

However, the solutions were too sensitive with the choice of the decay length.

The fluid interaction produced between two (or more) cylinders has been investigated only in recent years. Spring and Monkmeyer considered the interaction of incident plane waves with vertical cylinders [39,40]. Yamamoto calculated the hydrodynamic forces on a group of cylinders due to uniform flow or long waves [41,42]. Isaacson studied the interference effect between large cylinders in a wave by diffraction theory and through experiment [43,44]. Chakrabarti extended the work of Spring and Monkmeyer for three and four cylinders [45]. In the study reported herein, the hydrodynamic forces on rigid cylinders subjected to plane waves are treated. The results presented show the manner in which interaction effects become important as the cylinders get closer together and they show how the hydrodynamic forces vary periodically with respect to the incident wave length.

B. Objective and Scope

The objective of this research is to develop a general and effective procedure to investigate the effects of hydrodynamic interaction between vertical flexible cylinders subjected to ground motion in different directions.

The structure-fluid system is considered as a combination of two subsystems which are the cylinders and the surrounding water. The dynamic responses of the cylinders are coupled with the associated hydrodynamic forces. In terms of modal coordinates of structural vibration, the amplitudes of the hydrodynamic forces are found by solving a boundary value problem in the frequency domain. Effects of surface waves are also examined. All theoretical considerations are based on steady state vibration conditions. The more general cases of transient state or random vibrations in time domain can in principle be obtained by Fourier integrals from frequency domain for all frequencies.

Two separate cylinders having arbitrary shapes are assumed and the fluid domain is modelled by using three-dimensional finite elements. A special case of uniform cylinders is also considered such that the vertical variation of hydrodynamic pressure can be expanded into

a set of orthogonal functions; thus, reducing the boundary value problem in the fluid domain into a two-dimensional problem. A modification of localized finite element method is applied to this problem.

A brief survey of this research is as follows. Chapter II investigates the nature of structural-fluid interaction. Chapter III establishes the mathematical models for both structural system and the surrounding fluid. Chapter IV derives the numerical procedures to evaluate the amplitude of hydrodynamic pressures in terms of the structural responses. Chapter V presents three examples in depth to illustrate the points discussed in the previous chapters. The conclusions are made in Chapter VI.

II. STRUCTURE-FLUID INTERACTION

Structure-fluid interaction is the coupling between structure response and fluid forces. For structures surrounded by water, hydrodynamic forces are often produced by wave action, current flow or earthquake ground motions. These forces are defined in terms of relative motions between the structure and its surrounding fluid. The distribution of hydrodynamic pressures for low frequency incident waves is significant only near the surface while the distribution of hydrodynamic pressures for high frequency ground motion increase with depth. The dynamic responses for structures subjected to ground motion become important especially in deep water.

A. Morison's Equation

As mentioned in the last chapter, this hydrodynamic force equation is essentially an empirical formula based on wave theory and confirmed by experiments [46].

The force exerted by an unbroken surface wave on a single vertical cylinder extending from the bottom upward beyond the wave crest, can be represented in two parts (1) a drag force proportional to the square of the velocity and (2) a virtual mass force proportional to the horizontal relative component of acceleration between water particle and cylinder. Two coefficients are involved in the formulation, namely the drag coefficient, K_d, and the added mass coefficient, K_m.

For a rigid cylinder, Morison's equation takes the form

$$F = \tfrac{1}{2} K_d \rho A |\dot{u}| \dot{u} + K_m \rho V \ddot{u} \tag{2.1}$$

where ρ is the mass density of fluid, A is the projected area perpendicular to the water particle velocity $\dot{u}$, $\ddot{u}$ is the water particle acceleration and V is the volume of fluid displaced by the cylinder.

This equation can be easily applied to a structure provided the drag and added mass coefficients are known. Many experiments have been performed to evaluate these coefficients for different structural configurations [47]. Table 2.1, after Bea and Lai, shows representative from experimental results using values of K_m and K_d derived from different wave theories [48].

The drag force can be interpreted as a combination of influencing factors. One of these being the viscosity of the fluid which produces a boundary layer on the cylinder. The other being the streamline separation which causes a decrease in pressure behind the cylinder. In the later case the wake behind the cylinder is essentially a region of dead water or vortices. For small amplitude displacements of the cylinder relative to fluid, separation of streamlines does not occur; thus, drag forces are small for fluids of low viscosity such as water.

B. Diffraction Theory

This theory describes the potential flow which results when drag forces are neglected. It is formulated in terms of a boundary value problem after making assumptions as follows: (1) small amplitude motion, (2) linear free surface boundary condition, and (3) inviscid fluid with irrotational motion. Because of the first and third assumptions, the drag term in Bernoulli's equation can be neglected. A relation between hydrodynamic pressure p^* and velocity-potential Φ^* can then be established in the three-dimensional form,

$$p^*(x,y,z;t) = -\rho \frac{\partial \Phi^*(x,y,z;t)}{\partial t} \tag{2.2}$$

The advantage of using pressure $p^*(x,y,z;t)$ as the independent variable in the fluid is that the resultant hydrodynamic forces on the structure can be found directly by integration. The second assumption is an approximation leading to a linear effect in the free surface boundary condition. It becomes significantly in error for shallow water subjected to large amplitude surface waves. It is sufficient here, however, to consider only the linear formulation resulting from the simplified boundary conditions since high order components for nonlinear conditions

die out rapidly with respect to water depth and since a more complicat· boundary condition could be represented by applying the principle of superposition to linear surface conditions. The third assumption allows the application of potential flow theory. The fluid is considered continuous and the eddies and wakes are neglected for low Reynold number.

To solve the boundary value problem for potential flow, three general approaches have been used, namely the multiple scattering method, the Green's function method, and the finite element method. The multiple scattering method can be applied to the rigid vertical cylinders easily [12,39,40]. With a known form of diffracted velocity potential and an unknown coefficient for a single rigid cylinder, the interaction among multiple cylinders can be found by superposing the velocity potential of each cylinder and matching the kinematic boundary conditions on all interfaces of the cylinders. As mentioned earlier, the Green's function method is suitable for structures of arbitrary shapes. Two steps are involved in this method. The first step involves finding a source distribution function f on the immersed surface of the structure by using the following integral Eq. (2.3). This function is usually evaluated numerically using the same concept as the finite element formulation [22,23]. The governing equation is given by

$$-f(x,y,z) + \frac{1}{2\pi}\int\int_s f(\xi,\eta,\zeta)\frac{\partial G}{\partial n}(x,y,z;\xi,\eta,\zeta)\,ds = 2\dot{u}_n(x,y,z) \tag{2.3}$$

where $\frac{\partial G}{\partial n}$ is the derivative of Green's function in the outward normal direction, G is the kernel of Green's function as derived by Wehausen and Laitone [13]. Both (x,y,z) and (ξ,η,ζ) denote the points on the interface. The velocity normal to the interface is given by $\dot{u}_n = \frac{\partial \Phi}{\partial n}$.

The second step involves calculating the velocity potential for the immersed surface using the equation

$$\Phi = \frac{1}{4\pi}\int\int_s f(\xi,\eta,\zeta)\,G(x,y,z;\xi,\eta,\zeta)\,ds \tag{2.4}$$

The above formulations are limited in frequency domain while a complete discussion of the Green's function method has been published by Garrison [20] so it will not be included herein.

The third method of treating fluid-structure interaction is to apply the finite element technique directly to the original differential equation. Compared with the conventional Green's function method, the finite element method has the definite advantage that the computations are fairly simple. This simplicity results from using banded matrices, transmitting boundaries and infinite elements. As shown subsequently, the finite element method for treating fluid-structure interaction is both efficient and flexible.

C. Limitations of Diffraction Theory

Hydrodynamic pressures on a submerged structure can be obtained by applying diffraction theory to the fluid domain. Diffraction theory is limited however due to the basic assumptions which have been discussed previously. It can be shown that the ratio of the cylinder diameter, D, to the wave length, L, categories the possible types of flow behavior. This parameter indicates the degree to which vortex sheddings are able to develop. For $\frac{D}{L} > 0.2$, viscous flow effects are small so that the hydrodynamic effects are caused by scattering or diffraction due to the presence of structure as shown in Fig. 2.1 [20].

Another important parameter as shown in Fig. 2.2 [52] is the Keulegan-Carpenter number, $K_c = \frac{\dot{u}T}{D}$ where T is the period of the wave, $\dot{u}$ is the water particle velocity, and D is the diameter of the cylinder. For large value of K_c , when water particle acceleration is small, inertia effects are negligible such that hydrodynamic force approaches to the drag force for cylinder in steady flow. For small value of K_c ($K_c < 2$ approx.), the drag force is negligible such that hydrodynamic force becomes the pure inertia force [21]. A detailed discussion about the relationship for the drag coefficient or added mass coefficient v.s. the Keulegan-Carpenter number can be found from Sarpkaya [49].

Considering the case of earthquake loading in high frequency excitation in deep water, the induced surface wave height becomes very small and the ratio of $\frac{D}{L}$ is always greater than 0.2 as shown in Fig. 2.1. Furthermore, because the drag force decreases with distance below the surface more rapidly than does the inertia force [6], it is reasonable to neglect the drag force in the analysis and compute the hydrodynamic forces by the diffraction theory.

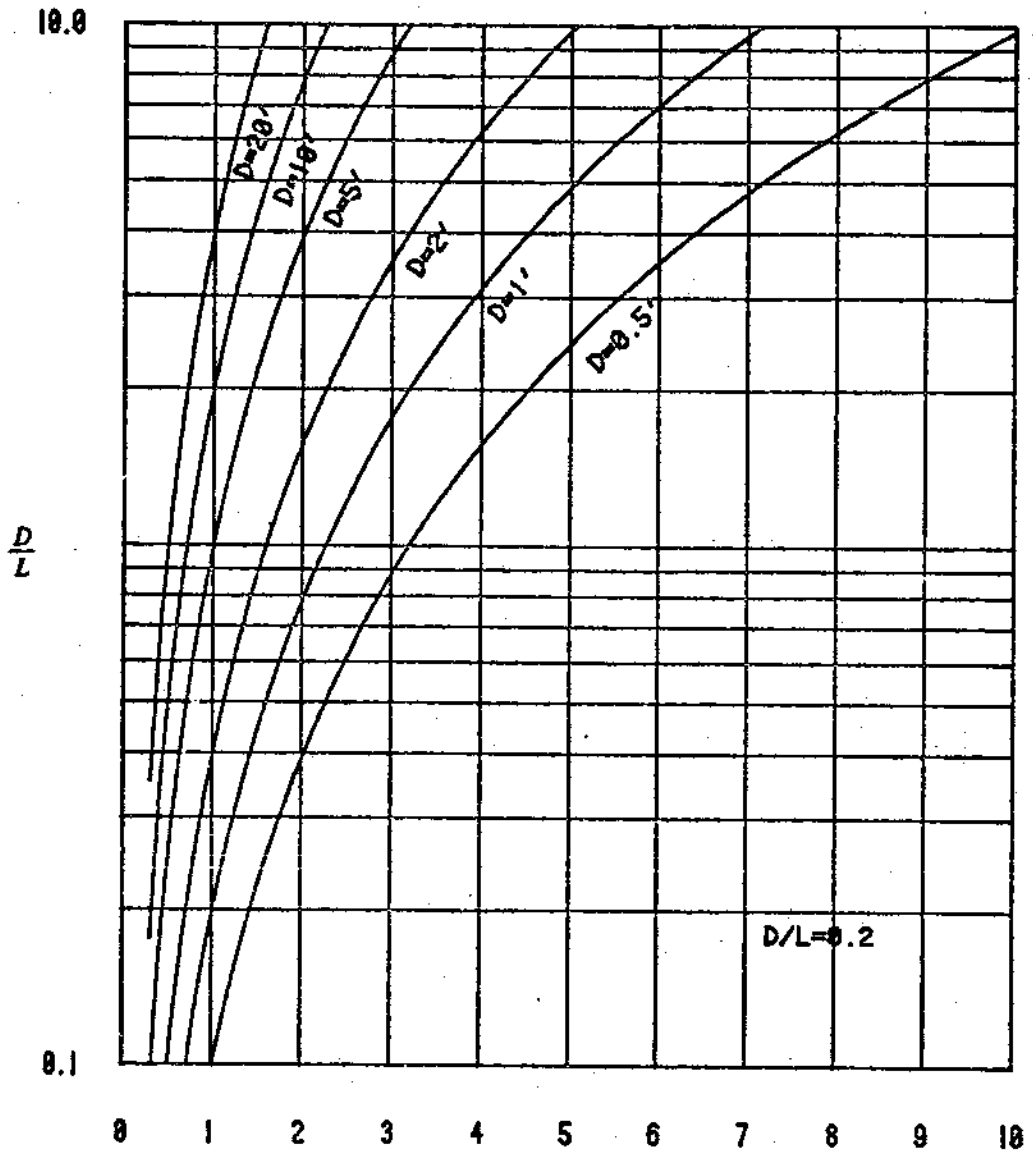

Figure 2.1 Diffraction Region : $\frac{D}{L}>0.2$

a. 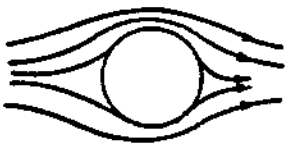

$K_c < 2$
No separation, amplitude of motion is less than cylinder diameter

b. 

$2 < K_c < 3$
Small separation, no eddy development yet

c. 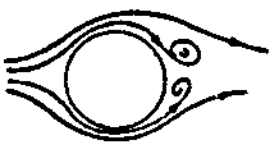

$K_c = 3$
First eddy shed, asymmetry starts, lift force begins to be non-zero

d. 

$3 < K_c < 4$
More than 2 eddies shed within half cycle (Von Karman street)

e. 

$5 < K_c < 7$
Wake becoming turbulent, additional eddies caused by wake when swept back

f. 

$7 < K_c$
Extremely turbulent

Figure 2.2 Wake Characteristics as a Function of Keulegan-Carpenter Number [52]

Force Coefficients			
Wave Theory	K_d	K_m	Remarks
Linear Theory	1.00	0.95	Mean values from ocean wave data on 13 and 24 in. diameter cylinders
	1.00-1.40	2.00	Recommanded design values based on a statistical analysis on published data with a 93% confidence level
Linear Filtering	0.60	1.50	Mean values from wave force data based on highest 50% of measured peak forces
Stokes Third Order	1.34	1.46	Mean values from laboratory oscillatory flow on 2 to 3 in. diameter cylinders
Stokes Fifth Order	0.57	3.10	Mean values from a statistical analysis
	0.50	1.20	Mean values from wave force data of small waves at 30 ft. water depth
	0.58	1.76	Mean values from wave force data of large waves at 100 ft. water depth
	0.80-1.00	2.00	Recommanded design values based on a statistical analysis of published data with a 98% confidence level

Table 2.1 Wave force coefficients (K_d and K_m) for a cylindrical member structure as pertaining to application of the Morison equation based on different wave theories [48]

III. MATHEMATIC MODEL

In dealing with this complicated structure-hydrodynamic interaction problem, it is necessary to make several simplifications. The complexity of the resulting theory depends greatly on the assumed flexibility and degrees of freedom of the structure. In the following development, we will investigate four separate cases:

(1) Rigid cylinder on rigid foundation

(2) Rigid cylinder connected flexibly to rigid foundation

(3) Flexible cylinder on rigid foundation

(4) Flexible cylinder on flexible foundation

As shown in Fig. 3.1, type (4) is the most realistic model for the offshore structures which are fixed at sea bottom. Either type (2) or type (3) is a better approximation than type (1) which is the most typical model used in the literatures and a special case to all the others.

The discussions in this chapter are devoted to the evaluation of structural responses. The basic equation of motion of structure is discussed in section A. The boundary value problem in the fluid domain is outlined in section B. The structural responses of type (2) rigid cylinders are discussed in section C and the type (3) flexible cylinders are discussed in section D. Fig. 3.2 shows the cylinders in the fluid and the associated coordinate system.

A. Equation of Motion

Planar vibration of two circular cylinders subjected to horizontal ground acceleration is considered. The equation of motion for the cylinders can be expressed as

$$\underline{M}^*\ddot{\underline{U}}^*(t)+\underline{C}^*\dot{\underline{U}}^*(t)+\underline{K}^*\underline{U}^*(t) = -\underline{M}^*\underline{r}\ddot{u}_g(t)-\underline{F}^*(t) \tag{3.1}$$

where $\ddot{u}_g$ is the horizontal ground acceleration, $\underline{r}$ is the pseudostatic influence-coefficient vector, the displacement of structural degrees of freedom is

$$\underline{U}^*(t) = \begin{Bmatrix} \underline{U}^1(t) \\ \underline{U}^2(t) \end{Bmatrix} \tag{3.2.a}$$

the mass matrix of structure is

$$\underline{M}^* = \begin{bmatrix} \underline{M}^1 & \underline{0} \\ \underline{0} & \underline{M}^2 \end{bmatrix} \tag{3.2.b}$$

the damping matrix of structure is

$$\underline{C}^* = \begin{bmatrix} \underline{C}^1 & \underline{0} \\ \underline{0} & \underline{C}^2 \end{bmatrix} \tag{3.2.c}$$

the stiffness matrix of structure is

$$\underline{K}^* = \begin{bmatrix} \underline{K}^1 & \underline{0} \\ \underline{0} & \underline{K}^2 \end{bmatrix} \tag{3.2.d}$$

the corresponding hydrodynamic forces are

$$\underline{F}^* = \begin{Bmatrix} \underline{F}^1 \\ \underline{F}^2 \end{Bmatrix} \tag{3.2.e}$$

and the superscripts 1 and 2 refer to the first and the second cylinder respectively. In the above expressions, $\underline{M}^j$, $\underline{C}^j$, $\underline{K}^j$ are structural characteristics of the j-th cylinder, while the hydrodynamic force $\underline{F}^j$ on the j-th cylinder is a function of structural responses for all the cylinders.

If the distance between cylinders is far enough, the effect of interaction between the cylinders will become small. In this case, the equation of motion (3.1) may be uncoupled into two separate equations. In terms of structural responses, the amplitude of hydrodynamic forces can be found by applying the diffraction theory. Then the structural responses may be solved by Eq. (3.1).

B. Hydrodynamic Forces

1. Boundary Value Problem in Three Dimensions

Assuming the water to be inviscid, the small amplitude irrotational motion in fluid domain is governed by three-dimensional wave equation:

$$\nabla^2 \Phi_D^*(x,y,z;t) = \frac{1}{C^2} \frac{\partial^2 \Phi_D^*}{\partial t^2}(x,y,z;t) \tag{3.3}$$

where C is the velocity of sound in water ($C = 4720$ ft per second).

Simplification can be made by assuming that the water is incompressible, i.e. neglecting the right hand side of Eq. (3.3). Thus, the following Laplace's equation is obtained.

$$\nabla^2 \Phi_D^*(x,y,z;t) = 0 \tag{3.4}$$

where Φ_D^* is the radiated velocity potential in fluid domain caused by the vibration of cylinders.

In a linear system, it is appropriate and sufficient to consider harmonic ground acceleration of the form

$$\ddot{u}_g(t) = \ddot{u}_g(\omega)\, e^{-i\omega t}$$

The dynamic responses can also be expressed in frequency domain. Linearity assumes that this motion has the same frequency, ω, as the ground motion excitation. Thus,

$$\Phi_D^*(x,y,z;t) = \Phi_D(x,y,z)\, e^{-i\omega t}$$

Applying the relationship in Eq. (2.2), Laplace's equation (3.4) becomes

$$\nabla^2 p(x,y,z) = 0 \tag{3.5}$$

where $p(x,y,z)$ is the hydrodynamic pressure in fluid.

The boundary condition at the bottom is

$$\frac{\partial p}{\partial z}(x,y,0) = 0 \tag{3.6.a}$$

It is assumed that the waves are of small amplitude, so that the dynamic and kinematic boundary conditions can be linearized to yield the following condition at the undisturbed free surface as

$$\frac{\partial p}{\partial z}(x,y,h) - \frac{\omega^2}{g}\, p(x,y,h) = 0 \tag{3.6.b}$$

At the far field, water extends to infinity in the radial direction. We insist that waves are outgoing (away from the cylinders) and the following radiation condition can be applied to the problem.

$$\lim_{R\to\infty} R^{1/2} \left(\frac{\partial p}{\partial r}(R,z) - ik\, p(R,z)\right) = 0 \tag{3.6.c}$$

where $R = (x^2+y^2)^{1/2}$ and k is the wave number which can be solved from the linearlized dispersion relation,

$$\omega^2 = kg \tanh kh$$

The kinematic boundary condition on the interface of structure and the fluid is

$$\frac{\partial p}{\partial n}(x,y,z) = -\rho \frac{\partial^2 u}{\partial t^2} \cos\bar{\theta} \tag{3.6.d}$$

where ρ is the mass density of water, $p(x,y,z)$ is the hydrodynamic pressure on the interface of cylinders, and u is the frequency dependent horizontal interface displacement at $\bar{\theta} = 0$ as

shown in Fig. 3.2.

The radiated wave propagating outward to infinity can be expressed as [13]:

$$\Phi(x,y,z) \infty \cosh(kz) H_n^{(1)}(kR) \cos(n\theta - \delta) \tag{3.7}$$

where δ is the direction of incident wave or ground motion, $H_n^{(1)}$ is the Hankel function of the first kind of order n, and k is the wave number. The asymptotic expansion of the Hankel function for large value of R is

$$H_n^{(1)}(kR) = (\frac{2}{\pi kR})^{1/2} e^{i(kR - \frac{n\pi}{2} - \frac{\pi}{4})} [1 - i\frac{n+1/4}{2kR}] + O(R^{-5/2}) \tag{3.8}$$

Substituting this relation into Eq. (3.7), the following expression can be derived;

$$\frac{\partial \Phi}{\partial R} = (-\frac{1}{2R} + ik)\Phi + O(R^{-5/2}) \tag{3.9}$$

This equation is consistent with the radiation boundary condition (3.6.c) and will be applied to the boundary value problem in Eq. (3.5) with the other boundary conditions Eqs. (3.6.a), (3.6.b) and (3.6.d).

2. Boundary Value Problem in Two Dimensions

If the cylinders have uniform cross section in Z-direction this problem can be reduced into two dimensions by separation of variables,

$$p(x,y,z) = \bar{p}(x,y)\ \bar{f}(z) \tag{3.10}$$

and the Eq. (3.5) is separated into two equations;

$$\nabla^2 \bar{p}(x,y) - \lambda \bar{p}(x,y) = 0 \tag{3.11.a}$$

and

$$\frac{\partial^2 \bar{f}}{\partial z^2}(z) + \lambda \bar{f}(z) = 0 \tag{3.11.b}$$

When Eq. (3.10) is inserted into the boundary conditions (3.6.a) and (3.6.b), the following expressions result;

$$p(x,y,z) = \sum_{i=0}^{n_w} c_i \bar{p}_i(x,y)\ \psi_i(z) \tag{3.12}$$

with

$$\nabla^2 \bar{p}_0(x,y) + k_0^2 \bar{p}_0(x,y) = 0 \tag{3.13.a}$$

$$\omega^2 = k_0 g \tanh k_0 h \tag{3.13.b}$$

$$\psi_0(z) = \cosh k_0 z \tag{3.13.c}$$

and for $i \geqslant 1$,

$$\nabla^2 \bar{p}_i(x,y) - k_i^2 \bar{p}_i(x,y) = 0 \tag{3.13.d}$$

$$\omega^2 = -k_i g \tan k_i h \tag{3.13.e}$$

$$\psi_i(z) = \cos k_i z \tag{3.13.f}$$

where n_w is the number of wave modes.

Thus the interface boundary (3.6.d) and the radiation boundary (3.9) are the only two conditions to be considered in a two-dimensional problem shown in Eqs. (3.13.a-f).

Considering the incompressibility of water and the high frequency wave generated by earthquakes, the corresponding wave lengths are very short. For slender cylinders and small

amplitude displacement [26], the problem can be simplified by reducing the surface boundary condition to

$$p(x,y,h) = 0 \tag{3.14.a}$$

and the radiation boundary condition to

$$\frac{\partial p}{\partial n}(x,y,z) = 0 \tag{3.14.b}$$

where n is the unit vector normal to the far field boundary.

A reduced two-dimensional boundary value problem is discussed in Appendix A in detail. In this case, we have the following decomposition

$$p(x,y,z) = \sum_{i=1}^{n_\infty} c_i \bar{p}_i(x,y)\, \psi_i(z) \tag{3.15}$$

with

$$\nabla^2 \bar{p}_i(x,y) - k_i^2 \bar{p}_i(x,y) = 0 \tag{3.16.a}$$

$$k_i h = (i - \frac{1}{2})\pi \tag{3.16.b}$$

and

$$\psi_i(z) = \cos k_i z \tag{3.16.c}$$

Since Eqs. (3.12) and (3.15) have the similar appearing expressions, the following general forms can be used for a reduced two-dimensional problem:

$$p(x,y,z) = \sum_{i=0}^{n_\infty} p_i(x,y,z) = \sum_{i=0}^{n_\infty} c_i \bar{p}_i(x,y) \psi_i(z) \tag{3.17.a}$$

$$\nabla^2 \bar{p}_i(x,y) - \lambda_i \bar{p}_i(x,y) = 0 \qquad (3.17.b)$$

where $\psi_i(z)$ is the mode shape of the wave, $\bar{p}_i$ (x,y) is the associated amplitude which can be solved from two-dimensional Helmholtz equations (3.17.a), c_i is the constant which can be combined within $\bar{p}_i(x,y)$, and $\bar{p}_0 = 0$ is for high frequency excitation.

The shapes of wave for the first six modes in both cases are shown in Fig. 3.3 where the mode shapes in Eq. (3.12) are the functions of vibration frequency and those in Eq. (3.15) are independent of frequency. The first mode has a shape of $\psi_0(z) = \cosh k_0 z$ which is obtained because of the surface wave effect in water depth of the order of the wave length. It is noted that the hydrodynamic pressures due to low frequency excitation are significant only near the water surface and decrease rapidly with the depth. On the other hand, the hydrodynamic pressures due to high frequency excitation will be zero on the water surface and increase with the depth.

In terms of the degrees of freedom of structure responses, the amplitude of hydrodynamic pressure $p(x,y,z)$ in three-dimensional problem as shown in Eq. (3.5), or $\bar{p}_i(x,y)$ in two-dimensional problem as shown in Eqs. (3.12) and (3.15), can be solved by applying the variation principle and the finite element method which will be discussed in the next chapter. The total hydrodynamic forces on structure will be the integration of $p(x,y,z)$ all over the interface on the cylinders.

In the case of rigid cylinders with two degrees of freedom, the hydrodynamic force will be

$$\underline{F}^j = \int_0^h \underline{\phi}_s{}^{jT} \int_{S_{ij}} \bar{p}(x,y,z)\, \vec{n}\, ds dz \qquad j=1,2 \qquad (3.18)$$

where $\underline{\phi}_s{}^j$ is the transformation matrix from horizontal degrees of freedom to structural degrees of freedom, i.e.

$$\underline{\phi}_s^j = \begin{bmatrix} 1 & z-z_c^j \end{bmatrix}$$

with z_c^j being the coordinate of center of gravity of the j-th cylinder, $\vec{n}$ is an unit vector in the direction of ground motion, and $\vec{p}(x,y,z)$ is normal to the interface on the cylinder.

In the case of flexible cylinders on rigid base, the generalized hydrodynamic force is

$$F_n^j = \int_0^h \int_{S_{ij}} \phi_n^j \vec{p}(x,y,z) \cdot \vec{n} \, ds dz \tag{3.19}$$

where ϕ_n^j is the n-th mode shape of cylinder vibration, and $p(x,y,z)$ can be obtained from either three-dimensional or two-dimensional considerations.

It should be pointed out here that the amplitude of hydrodynamic pressure becomes frequency independent in high frequency vibration. The associated added mass will be frequency independent also.

C. Structural Responses - Rigid Cylinders

As we stated before, when the excitation to a linear system is in simple harmonic motion, then the steady state response is also in simple harmonic motion at the same frequency. The amplitude and the phase of structural vibration can be described by the complex frequency response functions:

$$U(t) = U(\omega)\exp(-i\omega t) \tag{3.20.a}$$

$$\dot{U}(t) = -i\omega U(\omega)\exp(-i\omega t) \tag{3.20.b}$$

$$\ddot{U}(t) = -\omega^2 U(\omega)\exp(-i\omega t) \tag{3.20.c}$$

and the total acceleration is

$$\ddot{U}^t(\omega) = \ddot{U}(\omega) + r\ddot{u}_g(\omega) \tag{3.20.d}$$

The interface acceleration can be expressed as

$$\frac{\partial^2 u}{\partial t^2} = \underline{\phi}_s \ddot{\underline{U}}^j \tag{3.21}$$

where ϕ_s is the transfer matrix for rigid cylinders. Two degrees of freedom, translation and rotation for each cylinder are assumed to approximate the flexibility of the cylinder.

From Eq. (3.1), the equation of motion of the j-th cylinder can be expressed in frequency domain as

$$\underline{M}^j \ddot{\underline{U}}^j + \underline{C}^j \dot{\underline{U}}^j + \underline{K}^j \underline{U}^j = -\underline{M}^j \underline{r} \ddot{u}_g - \underline{F}^j \qquad j=1,2 \tag{3.22}$$

The hydrodynamic forces in Eq. (3.18) can be expressed in terms of the structural degrees of freedom for both cylinders. That is

$$\underline{F}^j = \left[\underline{E}^{j1} \underline{E}^{j2}\right] \begin{Bmatrix} \ddot{\underline{U}}^{1j} \\ \ddot{\underline{U}}^{2j} \end{Bmatrix} \qquad j=1,2 \tag{3.23}$$

In this expression, the hydrodynamic forces are complex frequency dependent functions. The energy is transmitted from the structure into far field during vibration. Furthermore, the following relation can be made:

$$\underline{E}^{ij} = \underline{E}^{ij}{}_R + i\, \underline{E}^{ij}{}_I \qquad i,j=1,2 \tag{3.24}$$

where $\underline{E}^{ij}{}_R$ and $\underline{E}^{ij}{}_I$ are the real and imaginary parts of $\underline{E}^{ij}$ respectively.

Combining all the equations of motion for both cylinders and applying the relation (3.24), one obtains

$$(\underline{M}^* + \underline{M}^a)\, \ddot{\underline{U}} + (\underline{C}^* + \underline{C}^a)\, \dot{\underline{U}} + \underline{K}^* \underline{U} = -(\underline{M}^* + \underline{M}_s)\, \underline{r} \ddot{u}_g \tag{3.25}$$

where M^*, C^*, K^* are the known physical properties of the structure as shown in Eqs. (3.2.b-

d), $\underline{M}^a$ is the added mass matrix of structure,

$$\underline{M}^a = \begin{bmatrix} \underline{E}^{11}{}_R & \underline{E}^{12}{}_R \\ \underline{E}^{21}{}_R & \underline{E}^{22}{}_R \end{bmatrix} \tag{3.26}$$

$\underline{C}^a$ is the hydrodynamic damping matrix,

$$\underline{C}^a = \omega \begin{bmatrix} \underline{E}^{11}{}_I & \underline{E}^{12}{}_I \\ \underline{E}^{21}{}_I & \underline{E}^{22}{}_I \end{bmatrix} \tag{3.27}$$

and $\underline{M}_g$ is the complex added mass matrix associated with ground acceleration,

$$\underline{M}_g = \begin{bmatrix} \underline{E}^{11} & \underline{E}^{12} \\ \underline{E}^{21} & \underline{E}^{22} \end{bmatrix} \tag{3.28}$$

The elements of $\underline{M}^a$,$\underline{C}^a$ are real matrices while those of $\underline{M}_g$ are complex. Each $\underline{E}^{ij}$ is a 2 x 2 submatrix which represents the hydrodynamic effect on the i-th cylinder subjected to the motion of the j-th cylinder.

In the frequency domain, the acceleration and the velocity can be referred to the displacement as shown in Eqs. (3.20.a-d) and the complex frequency response function will be in the following form:

$$\underline{U} = \left[-\omega^2(\underline{M}^* + \underline{M}^a) - i\omega(\underline{C}^* + \underline{C}^a) + \underline{K}^*\right]^{-1}\left[-(\underline{M}^* + \underline{M}_g)\underline{ii}_g\right] \tag{3.29}$$

Comparing with other terms, the damping matrices $\underline{C}^*$ and $\underline{C}^a$ are very small. It is therefore reasonable to calculate the submerged natural frequencies and shape functions by neglecting the damping matrices and solving the following eigenvalue problem:

$$\underline{K}^*\underline{\Phi}^* = \bar{\omega}^2(\underline{M}^* + \underline{M}^a)\underline{\Phi}^* \tag{3.30}$$

where $\underline{\phi}^*$ is the submerged mode shape and $\bar{\omega}$ is the submerged natural frequency of structures. A reduction of natural frequencies due to the presence of the surrounding water can be calculated.

D. Structural Responses - Flexible Cylinders

The solution shown above is based on the assumption of rigid cylinders with two degrees of freedom each. If flexible cylinders are considered, Eq. (3.19) will be modified by the generalized coordinates of structure,

$$\frac{\partial^2 u}{\partial t^2} = \ddot{u}_g + \sum_{k=1}^{n_s} \phi_k \ddot{Y}_k \tag{3.31}$$

where $\ddot{Y}_k$ is the amplitude of the generalized coordinates of the k-th mode of structure, ϕ_k is the shape function of structure in the air, and n_s is the number of structural vibration modes.

The cylinder can be treated as a beam type structure whose mode shapes of vibration, in the absence of water, are assumed to be known by applying a conventional finite element structural analysis. In the k-th mode, the shape function will be

$$\phi_k = \phi_k(z)$$

and the vibration will be in the same direction as the ground motion.

The following discussion is based on the reduced two-dimensional problem where $\psi_i(z)$ represents the mode shape of wave in Z-direction. In the three-dimensional case, the formulation can be derived easily by removing the $\psi_i(z)$ from the following equations. The summation of each individual wave mode of hydrodynamic pressure is also unnecessary. However, an increase on the effort of calculation in the three-dimensional formulation is expected.

The equation of motion in the n-th mode in the generalized coordinate becomes

$$\underline{M}_n \ddot{\underline{Y}}_n + \underline{C}_n \dot{\underline{Y}}_n + \underline{K}_n \underline{Y}_n = -\underline{A}_n \ddot{u}_g - \underline{F}_n \tag{3.32}$$

with

$$\underline{M}_n = \begin{bmatrix} M_n^1 & 0 \\ 0 & M_n^2 \end{bmatrix} \tag{3.33.a}$$

$$\underline{C}_n = \begin{bmatrix} C_n^1 & 0 \\ 0 & C_n^2 \end{bmatrix} \tag{3.33.b}$$

$$\underline{K}_n = \begin{bmatrix} K_n^1 & 0 \\ 0 & K_n^2 \end{bmatrix} \tag{3.33.c}$$

$$\underline{A}_n = \begin{Bmatrix} A_n^1 \\ A_n^2 \end{Bmatrix} \tag{3.33.d}$$

$$\underline{F}_n = \begin{Bmatrix} F_n^1 \\ F_n^2 \end{Bmatrix} \tag{3.33.e}$$

$$\underline{Y}_n = \begin{Bmatrix} Y_n^1 \\ Y_n^2 \end{Bmatrix} \tag{3.33.f}$$

and

$$M_n^j = \int_0^H m(z)\phi^j{}_n{}^2 dz \tag{3.34.a}$$

$$A_n^j = \int_0^H m(z)\phi^j{}_n dz \tag{3.34.b}$$

$$K_n^j = \omega_n^2 M_n^j \tag{3.34.c}$$

$$C_n^j = 2\xi_n \omega_n M_n^j \tag{3.34.d}$$

where $m(z)$ is the mass per unit length of cylinder, j refers to the j-th cylinder, ω is the natural frequency for the n-th mode, H is the height of cylinder and ξ_n is the damping coefficient.

For every i-th mode of wave, the hydrodynamic force per unit length on each cylinder can be computed as

$$p^j(z) = \int_{S_{ij}} \bar{p}(x,y,z)\, \vec{n}\, ds \tag{3.35}$$

where $\bar{p}(x,y,z)$ is the hydrodynamic pressure normal to the interface of the j-th cylinder and $\vec{n}$ is the direction of ground acceleration.

Recall from Eq. (3.17.a),

$$p(x,y,z) = \sum_{i=0}^{n_w} c_i \bar{p}_i(x,y)\psi_i(z) \tag{3.17.a}$$

and from the numerical analysis which will be discussed in the next chapter, we will obtain Eq. (4.26).

$$c_i \bar{p}_i(x,y) = \underline{P}_0 \ddot{u}_g + \sum_{k=1}^{n_s} \sum_{j=1}^{2} \underline{P}_{ik}^j \ddot{Y}_k^j \tag{4.26}$$

Substituting Eqs. (3.17) and (4.26) into Eq. (3.35), the total horizontal hydrodynamic force on the cylinder can be derived by numerical integration.

The generalized hydrodynamic force in the n-th mode of cylinder vibration will be

$$F_n^j = \int_0^h \phi_n^j(z)\, p^j(z)\, dz \tag{3.37}$$

where j refers to each cylinder, and h is the depth of water. In this expression, two different modal functions are involved, namely the mode shape of structure and the mode shape of wave.

Substituting Eq. (3.37) into Eq. (3.33.e), we have

$$\underline{F}_n = \underline{E}_{n0}\ddot{u}_g + \sum_{k=1}^{n_s} \underline{E}_{nk}\underline{\ddot{Y}}_k \tag{3.38}$$

where $\underline{\ddot{Y}}_k$ is a vector containing $\ddot{Y}_k^1$ and $\ddot{Y}_k^2$,

$$\underline{E}_{n0} = \begin{bmatrix} E_{n0}^1 \\ E_{n0}^2 \end{bmatrix} \tag{3.39.a}$$

is the hydrodynamic effect on the n-th mode of the generalized coordinate due to ground acceleration, and

$$\underline{E}_{nk} = \begin{bmatrix} E_{nk}^{11} & E_{nk}^{12} \\ E_{nk}^{21} & E_{nk}^{22} \end{bmatrix} \tag{3.39.b}$$

is the hydrodynamic effect on the n-th mode of the generalized coordinate due to the structural vibration in the k-th mode. The superscripts 12 and 21 refer to the coupling between the cylinders. Therefore, the following two equations are derived:

$$E_{n0}^j = \sum_{i=0}^{n_w} \int_0^h \phi_n^j(z)\psi_i(z)\,dz \int_0^{2\pi} P_{i0}(x,y)\cos\bar{\theta}\,a^j\,d\theta \tag{3.39.c}$$

and

$$E_{nk}^{ij} = \sum_{i=0}^{n_w} \int_0^h \phi_n^j(z)\psi_i(z)\,dz \int_0^{2\pi} P_{ik}^j(x,y)\cos\bar{\theta}\,a^j\,d\theta \tag{3.39.d}$$

where a^j is the radius of the j-th cylinder, P_0 and $P_{ik}{}^j$ are the amplitude of hydrodynamic pressure on the interface only.

Due to the coupling terms in the above expressions of hydrodynamic forces, the generalized equation of motion (3.32) is no longer uncoupled. Rewriting the complex frequency dependent function $\underline{E}_{nk}$ as

$$\underline{E}_{nk} = \underline{E}_{nk,R} + i\underline{E}_{nk,I} \tag{3.40}$$

and considering the first n_s modes of structural vibration, the following equations can be obtained by modifying Eqs. (3.24),(3.37) and rearranging Eq. (3.32).

$$(\underline{M}_m{}^* + \underline{M}_m{}^a)\ddot{\underline{Y}}_m{}^* + (\underline{C}_m{}^* + \underline{C}_m{}^a)\dot{\underline{Y}}_m{}^* + \underline{K}_m{}^*\underline{Y}_m{}^* = -(\underline{A}_m{}^* + \underline{M}_m{}^s)\ddot{u}_g \tag{3.41}$$

where

$$\underline{M}_m{}^* = \begin{bmatrix} \underline{M}_1 & \underline{0} & \cdot & \underline{0} \\ \underline{0} & \underline{M}_2 & \cdot & \underline{0} \\ \cdot & \cdot & \cdot & \cdot \\ \underline{0} & \underline{0} & \cdot & \underline{M}_{n_s} \end{bmatrix} \tag{3.42.a}$$

$$\underline{C}_m{}^* = \begin{bmatrix} \underline{C}_1 & \underline{0} & \cdot & \underline{0} \\ \underline{0} & \underline{C}_2 & \cdot & \underline{0} \\ \cdot & \cdot & \cdot & \cdot \\ \underline{0} & \underline{0} & \cdot & \underline{C}_{n_s} \end{bmatrix} \tag{3.42.b}$$

$$\underline{K}_m{}^* = \begin{bmatrix} \underline{K}_1 & \underline{0} & \cdot & \underline{0} \\ \underline{0} & \underline{K}_2 & \cdot & \underline{0} \\ \cdot & \cdot & \cdot & \cdot \\ \underline{0} & \underline{0} & \cdot & \underline{K}_{n_s} \end{bmatrix} \tag{3.42.c}$$

$$\underline{A}_m^* = \begin{Bmatrix} \underline{A}_1 \\ \underline{A}_2 \\ \cdot \\ \underline{A}_{n_s} \end{Bmatrix} \tag{3.42.d}$$

and $\underline{M}_m$, $\underline{C}_m$, $\underline{K}_m$ are the uncoupled matrices ($n \leq n_s$) which represent the assembled structural characteristics in the generalized coordinates as shown in Eqs. (3.33.a-d).

Also,

$$\underline{M}_m^a = \begin{bmatrix} \underline{E}_{11,R} & \underline{E}_{12,R} & \cdot & \underline{E}_{1n_s,R} \\ \underline{E}_{21,R} & \underline{E}_{22,R} & \cdot & \cdot \\ \cdot & \cdot & \cdot & \cdot \\ \underline{E}_{n_s1,R} & \cdot & \cdot & \underline{E}_{n_sn_s,R} \end{bmatrix} \tag{3.43}$$

is the generalized added mass matrix which is coupled between the modes as well as between the two cylinders.

$$\underline{C}_m^a = \omega \begin{bmatrix} \underline{E}_{11,I} & \underline{E}_{12,I} & \cdot & \underline{E}_{1n_s,I} \\ \underline{E}_{21,I} & \underline{E}_{22,I} & \cdot & \cdot \\ \cdot & \cdot & \cdot & \cdot \\ \underline{E}_{n_s1,I} & \cdot & \cdot & \underline{E}_{n_sn_s,I} \end{bmatrix} \tag{3.44}$$

is the generalized hydrodynamic damping matrix where ω is the frequency of ground acceleration. As expressed in Eq. (3.39), $\underline{E}_{nk,R}$ and $\underline{E}_{nk,I}$ are the 2 x 2 submatrices which indicate the coupling between two cylinders.

$$\underline{M}_m^g = \begin{Bmatrix} \underline{E}_{10} \\ \underline{E}_{20} \\ \cdot \\ \underline{E}_{n_s0} \end{Bmatrix} \tag{3.45}$$

is the complex generalized added mass term associated with ground acceleration.

$$\underline{Y}_m^s = \begin{Bmatrix} \underline{Y}_1 \\ \underline{Y}_2 \\ . \\ \underline{Y}_{n_s} \end{Bmatrix} \tag{3.46}$$

is a combination of the structural displacement in generalized coordinate which is shown in Eq. (3.33.f).

As discussed in the previous section, it is reasonable to neglect the damping terms which include both structural damping and hydrodynamic damping matrices so that Eq.(3.41) can be decoupled by solving the following eigenvalue problem,

$$\underline{K}_m^* \underline{\Omega} = \bar{\omega}_m^2 (\underline{M}_m^* + \underline{M}_m^a) \underline{\Omega} \tag{3.47}$$

where $\underline{\Omega}$ is the eigenvector with $2n_s$ elements and $\bar{\omega}_m$ is the submerged natural frequency in generalized coordinate.

Therefore, we know that

$$\underline{U} = \underline{\phi}_m^* \underline{Y}_m^* = \underline{\phi}_m^* \underline{\Omega} Z \tag{3.48}$$

is the structural response where

$$\underline{\phi}_m^* = \begin{bmatrix} \phi_1^1 & 0 & . . & \phi_{n_s}^1 & 0 \\ 0 & \phi_1^2 & . . & 0 & \phi_{n_s}^2 \end{bmatrix} \tag{3.49.a}$$

and

$$\underline{\phi}^* = \underline{\phi}_m^* \underline{\Omega} \tag{3.49.b}$$

is the submerged mode shape of structural vibration. The structural response $\underline{U}$ can be computed by decoupling the generalized Eq. (3.41) with

$$\underline{Y}_m^* = \underline{\Omega}\,\underline{Z} \tag{3.50}$$

and solving the following equation

$$\underline{\Omega}^T(\underline{M}_m^* + \underline{M}_m^a)\underline{\Omega}\,\ddot{\underline{Z}} + \underline{\Omega}^T(\underline{C}_m^* + \underline{C}_m^a)\underline{\Omega}\,\dot{\underline{Z}} + \underline{\Omega}^T\underline{K}_m^*\underline{\Omega}\,\underline{Z} = -\underline{\Omega}^T(\underline{A}_m^* + \underline{M}_m^s)\ddot{u}_g \tag{3.51}$$

Substituting $\underline{Z}$ from Eq. (3.51) into Eq. (3.48), the final response $\underline{U}$ can be determined.

If the cylinders are considered to be multi-degree-of-freedom systems, the conventional finite element analysis can be applied. Eq. (3.34) should be modified as

$$\begin{aligned} M_n^j &= \underline{\phi}_n^{jT}\underline{M}^j\underline{\phi}_n^j \\ K_n^j &= \omega_n^{j2}M_n^j \\ C_n^j &= 2\xi_n\omega_n^j M_n^j \\ A_n^j &= \underline{\phi}_n^{jT}\underline{M}^j\underline{r} \end{aligned} \tag{3.52}$$

where $\underline{M}^j$ is the mass matrix for the MDOF system of the j-th cylinder.

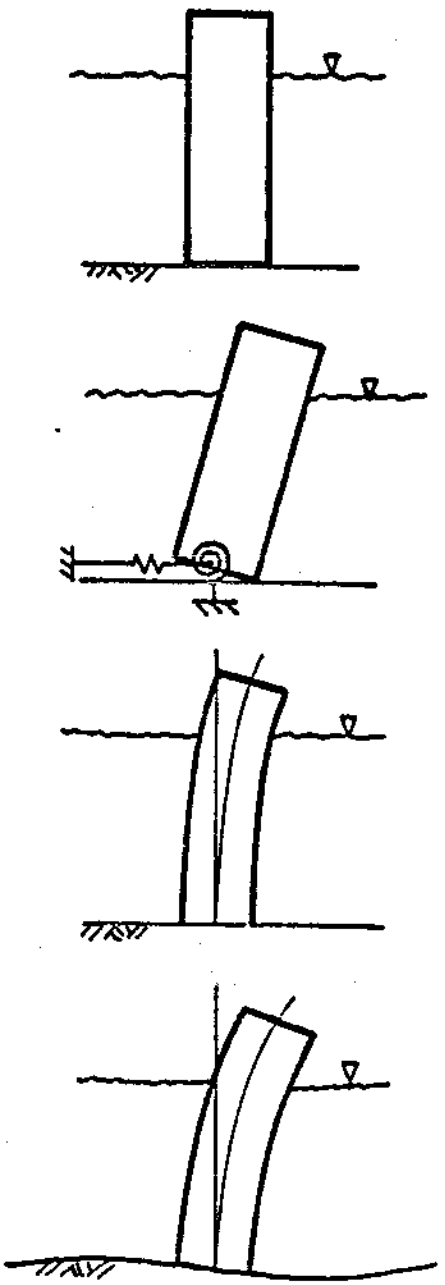

(1) Rigid Cylinder on Rigid Foundation

(2) Rigid Cylinder Connected Flexibly to Rigid Foundation

(3) Flexible Cylinder on Rigid Foundation

(4) Flexible Cylinder on Flexible Foundation

Figure 3.1 Models of Fixed Cylinder in Fluid

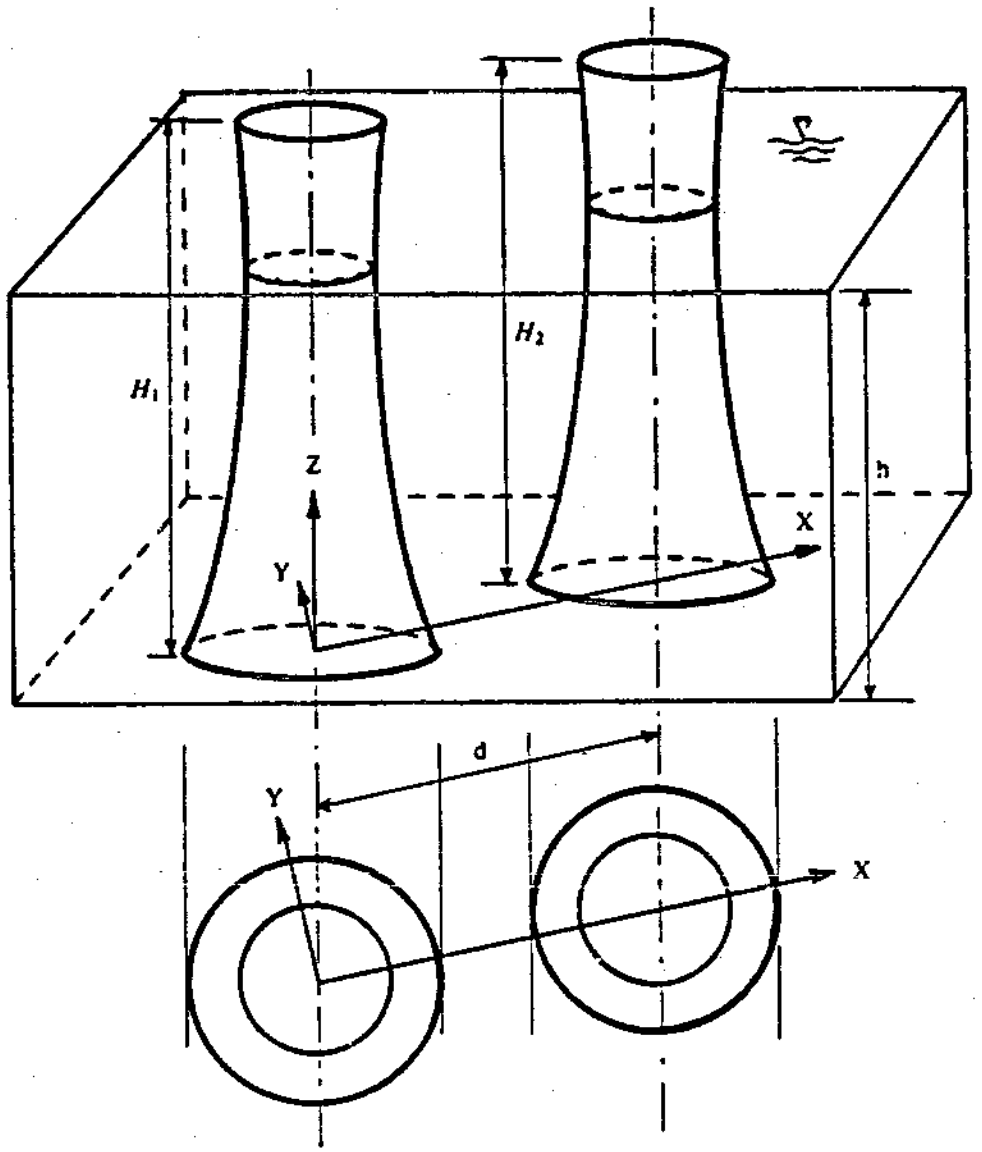

Figure 3.2 Structures in Fluid

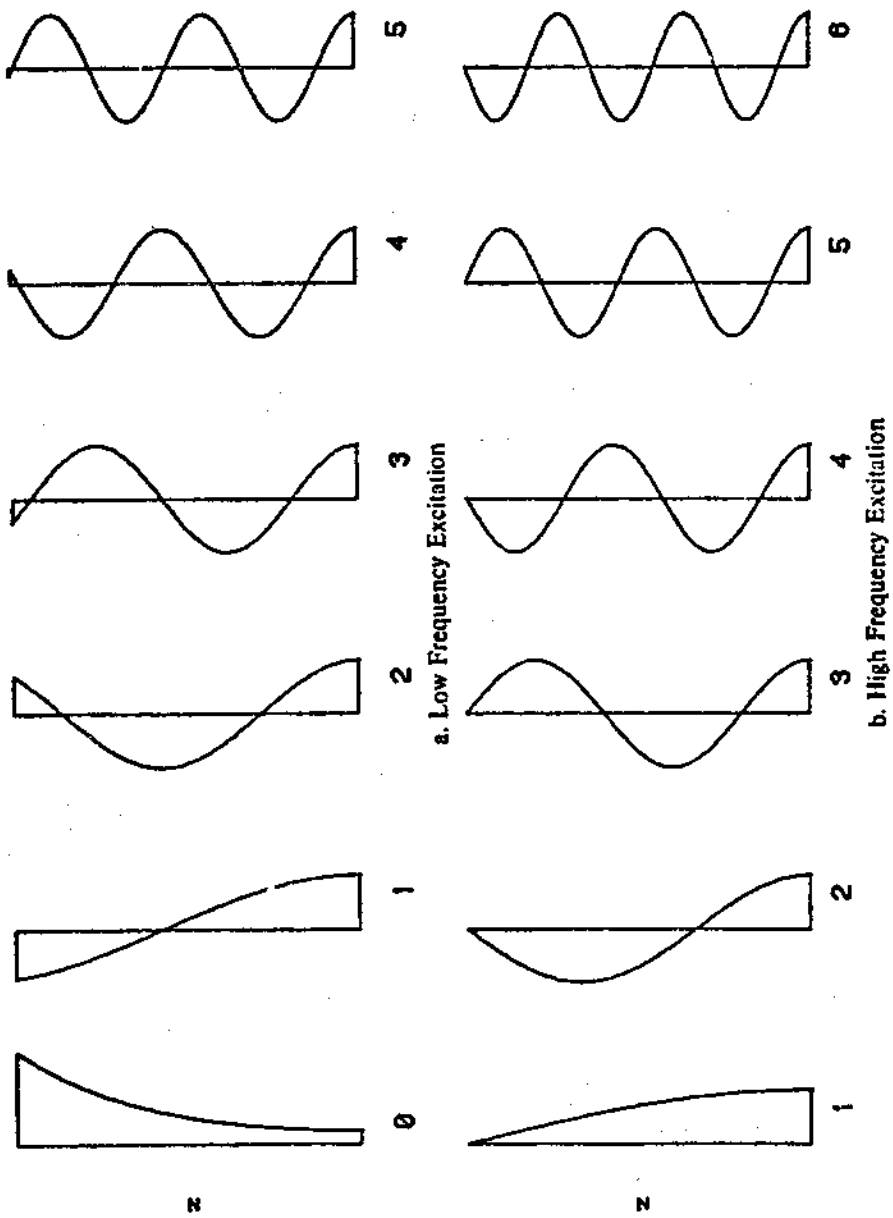

Figure 3.3 Mode Shape of Wave

IV. NUMERICAL ANALYSIS

In order to find the hydrodynamic pressure exerted on the interface of the structure, a variation principle and finite element method are applied to the boundary value problem [26]. The Laplace's equation (3.5) in the three-dimensional formulation and the Helmholtz equations (3.17.a),(3.17.b) in the reduced two-dimensional formulation, are considered with the associated boundary conditions. A localized finite element method [27] is also employed to reduce the fluid domain by utilizing the known analytic solutions in certain subdomains. The cases of symmetrical loading and antisymmetrical loading will be discussed later to further simplify the problem.

A. Finite Element Analysis in Three Dimensions

For a general three-dimensional problem (3.5), the fluid domain is divided into a finite number of elements as shown in Fig. 4.1. An interpolation function associated with each node is assumed such that each individual element can be represented by

$$p(x,y,z) = \sum_{i=1}^{n} N_i p_i^e \equiv \underline{N}\underline{p}^e \tag{4.1}$$

where $\underline{p}^e$ is a vector of the nodal values of hydrodynamic pressure in one element with n nodes.

In the standard Galerkin method, the weighting function w is chosen so that the weighted average error over the domain is forced to be zero. That is

$$\sum_e \int\int\int_V w^e \nabla^2 p(x,y,z)\, dV = 0 \tag{4.2}$$

and

$$w^e(x,y,z) = \sum_{i=1}^{n} N_i p_i^e \equiv \underline{N}\underline{p}^e \tag{4.3}$$

where the interpolation functions for the weighting function, w, are the same as those used for the hydrodynamic pressure.

After integrating by parts and applying the Green's Theorem, the weak form of Eq. (4.2) is obtained as follows:

$$\sum_e \int\int\int_V -\nabla \underline{N}^T \nabla \underline{N} dV \underline{p} = -\sum_e \int\int_S \underline{N}^T \frac{\partial p}{\partial n} dS \tag{4.4}$$

where $\underline{p}$ is a vector of nodal hydrodynamic pressure in the fluid domain.

The boundary of the fluid can be divided as shown in Fig. 4.1,

$$S = S_{f1} \cup S_{f2} \cup S_f \cup S_b \cup S_t \tag{4.5}$$

where S_{f1}, S_{f2} are the interface boundaries for each cylinder, S_f is the far field boundary, S_b is the boundary of the bottom of the fluid domain, and S_t is the free surface boundary.

With the boundary conditions, Eqs. (3.6.a-d), the right hand side of Eq. (4.4) becomes

$$\sum_e \int\int_S \underline{N}^T \frac{\partial p}{\partial n} dS = \sum_e \int\int_{S_t} \underline{N}^T \frac{\omega^2}{g} p dS + \sum_e \int\int_{S_f} \underline{N}^T \left(-\frac{1}{2R} + ik\right) p dS$$

$$+ \sum_{j=1}^{2} \sum_e \int\int_{S_{ij}} \underline{N}^T \left(-\rho \frac{\partial^2 u_j}{\partial t^2} \cos\bar{\theta}\right) \cos\beta \, dS \tag{4.6}$$

For rigid cylinder with two degrees of freedom, we have

$$\frac{\partial^2 u}{\partial t^2} = \underline{\phi} \cdot \ddot{\underline{U}}^t \tag{3.21}$$

Substituting Eq. (4.6) into Eq. (4.4), the following expression is obtained,

$$\underline{K} \, \underline{p} = \underline{b} \tag{4.7}$$

where $\underline{p}$ is the unknown nodal hydrodynamic pressure,

$$\underline{K} = \sum_e \int\int\int_V -\nabla \underline{N}^T \nabla \underline{N} dV + \sum_e \int\int_{S_0} \frac{\omega^2}{g} \underline{N}^T \underline{N} dS + \sum_e \int\int_{S_f} \underline{N}^T \underline{N} (-\frac{1}{2R} + ik)\, dS \qquad (4.8)$$

and

$$\underline{b} = -\sum_{j=1}^{2} \sum_e \int\int_{S_{ij}} \underline{N}^T \rho \underline{\phi}_s{}^j \cos\bar{\theta} \cos\beta \, dS \ddot{\underline{U}}^{j} \qquad (4.9.a)$$

or

$$\underline{b} = \sum_{j=1}^{2} \underline{B}^j \ddot{\underline{U}}^{j} \qquad (4.9.b)$$

and $\underline{B}^j$ is a $n \times 2$ matrix with n being the total nodal number. For those nodes which are not on the interfaces of cylinders, the values of the associated elements in $\underline{B}^j$ are zero.

In order to solve Eq. (4.7), the hydrodynamic pressure can be decomposed as

$$\underline{p} = \sum_{j=1}^{2} \underline{P}^j \ddot{\underline{U}}^{j} \qquad (4.10)$$

where $\underline{P}^j$ is the amplitude of hydrodynamic pressure with respect to the unit acceleration of the j-th cylinder.

Comparing Eq. (4.7) with Eq. (4.10), one can determine the amplitude of nodal hydrodynamic pressure by solving the following equations:

$$\underline{K}\, \underline{P}^j = \underline{B}^j \qquad j=1,2 \qquad (4.11)$$

Substituting $\underline{P}^j$ into Eq. (4.10), the hydrodynamic force applied to each cylinder can be found by picking up the nodal value on the interface of the cylinders and performing

numerical integration over the interface as discussed in Eq. (3.18). This procedure will lead to the expression in Eq. (3.23) and the solution of structure responses can be found accordingly.

In case of flexible cylinders on rigid foundation, the modification can be made by introducing the generalized coordinates

$$\frac{\partial^2 u}{\partial t^2} = \ddot{u}_g + \sum_{k=1}^{n_1} \phi_k(z)\, \ddot{Y}_k \tag{3.31}$$

and recalling that ϕ_k is the k-th mode shape of cylinder in air.

Substituting Eq. (3.31) into Eq. (4.6), we get

$$\underline{K}\, \underline{p} = \underline{b} \tag{4.12}$$

where $\underline{K}$ is the same term as shown in Eq. (4.8),

$$\underline{b} = \underline{B}_0 \ddot{u}_g + \sum_{k=1}^{n_1} \sum_{j=1}^{2} \underline{B}_k^j \ddot{Y}_k^j \tag{4.13}$$

with

$$\underline{B}_0 = \sum_{j=1}^{2} \sum_{e} \int\int_{S_{ij}} \rho \underline{N}^T \cos\bar{\theta} \cos\beta \, dS \tag{4.14.a}$$

$$\underline{B}_k^j = \sum_{e} \int\int_{S_{ij}} \rho \underline{N}^T \phi_k^j \cos\bar{\theta} \cos\beta \, dS \tag{4.14.b}$$

In the above expressions, j refer to the cylinder, k refer to the modes of vibration, and $\bar{\theta} = \theta - \delta$ is shown in Fig. 3.2.

Decomposing the hydrodynamic pressure in terms of modal amplitude and ground acceleration, we obtain

$$\underline{P} = \underline{P}_0 + \sum_{k=1}^{n_1} \sum_{j=1}^{2} \underline{P}_k^j \ddot{Y}_k^j \tag{4.15}$$

Substituting this expression into Eq. (4.12), the amplitude of hydrodynamic pressure can be solved. Thus,

$$\underline{K}\ \underline{P}_0 = \underline{B}_0 \tag{4.16.a}$$

and

$$\underline{K}\ \underline{P}_k^j = \underline{B}_k^j \tag{4.16.b}$$

where k and j are the same as those in Eq. (4.15).

B. Two-Dimensional Approximation

For a reduced two-dimensional problem, i.e. the cross sections of cylinders are uniform, then the boundary conditions on the free surface and on the bottom are not involved in the boundary integral in the finite element formulation. The weak form of the integral of the Helmholtz equation (3.17.b) will be

$$\sum_e \int\int_A (-\nabla \underline{N}^T \nabla \underline{N} - \lambda \underline{N}^T \underline{N})\, dA\, \bar{\underline{p}}_i = -\sum_e \int_S \underline{N}^T \frac{\partial \bar{p}_i}{\partial n}(x,y)\, dS \tag{4.17}$$

where $\lambda_i = -k_i^2$ for $i = 0$, $\lambda_i = k_i^2$ for $i \geq 1$, k_i can be solved from the dispersion relation in Eq. (3.13) for low frequency excitation or from Eq. (3.16) for high frequency excitation, $\bar{p}_i(x,y)$ is the two-dimensional hydrodynamic pressure on the interface for the i-th mode of the wave, and $\bar{\underline{p}}_i$ is a vector of nodal hydrodynamic pressures in the i-th mode.

The boundary in the two-dimensional domain becomes

$$S = S_{f1} \cup S_{f2} \cup S_f \tag{4.18}$$

with S_{ij} on the interface and S_f on the far field. Therefore, the boundary integral in Eq. (4.17) will be

$$\sum_e \int_S \underline{N}^T \frac{\partial \bar{p}_i}{\partial n} dS - \sum_{j=1}^{2} \sum_e \int_{S_{ij}} \underline{N}^T \frac{\partial \bar{p}_i}{\partial n} dS + \sum_e \int_{S_f} \underline{N}^T \frac{\partial \bar{p}_i}{\partial n} dS \tag{4.19}$$

Applying the appropriate boundary conditions and rearranging terms, the following equation is obtained,

$$\underline{K}_i \underline{\bar{p}}_i = \underline{b}_i \tag{4.20}$$

where

$$\underline{K}_i = \sum_e \int \int_A (-\nabla \underline{N}^T \nabla \underline{N} - \lambda_i \underline{N}^T \underline{N})\, dA + \sum_e \int_{S_f} \underline{N}^T \underline{N} (-\frac{1}{2R} + ik_0)\, dS \tag{4.21}$$

The interface boundary condition will be applied by substituting Eq. (3.12) into Eq. (3.6.d), such that the hydrodynamic pressure can be expressed in terms of structure responses as

$$\sum_{i=0}^{n} c_i \frac{\partial \bar{p}_i}{\partial n}(x,y)\psi_i(z) = -\rho \frac{\partial^2 u}{\partial t^2}(z)\cos\bar{\theta} \tag{4.22}$$

again, $\psi_i(z)$ is the i-th mode shape of the wave.

Since ψ's are orthogonal functions, the Fourier series expansion can be applied in order to find the modal coefficients:

$$c_i \frac{\partial \bar{p}_i}{\partial n}(x,y) = \frac{4k_i}{\sin 2k_i h + 2k_i h} \int_0^h -\rho \frac{\partial^2 u}{\partial t^2}(z)\cos\bar{\theta}\psi_i(z)\, dz \tag{4.23}$$

For the rigid cylinder with two degrees of freedom each, we have

$$\frac{\partial^2 u}{\partial t^2} = \underline{\phi}_r \underline{\ddot{U}}^I \tag{3.21}$$

while for the flexible cylinder with rigid base, we have

$$\frac{\partial^2 u}{\partial t^2} = \ddot{u}_g + \sum_{k=1}^{n_i} \phi_k(z)\, \ddot{Y}_k \tag{3.31}$$

However, only the second case will be considered here since the formulations for the first one are straightforward.

Introducing the generalized coordinates in terms of Eq. (3.31) to Eq. (4.23) for each cylinder in each i-th mode of wave, we have

$$c_i \frac{\partial \bar{p}_i}{\partial n}(x,y) = -\frac{2\rho}{h}\cos\bar{\theta}\left(\int_0^h \psi_i(z)\, dz \ddot{u}_g + \sum_{k=1}^{n_i}\int_0^h \phi_k \psi_i(z)\, dz \ddot{Y}_k\right) \tag{4.24}$$

Applying the same procedure of decomposition as discussed in the three-dimensional case, the following expression can be derived from Eqs. (4.19) and (4.20).

$$\underline{K}_i c_i \underline{\bar{p}}_i = \underline{B}_{i0} \ddot{u}_g + \sum_{k=1}^{n_i}\sum_{j=1}^{2} \underline{B}_{ik}{}^j \ddot{Y}_k{}^j \tag{4.25}$$

where

$$\underline{B}_{i0} = \frac{2\rho}{h}\int_0^h \psi_i(z) \sum_e \int_{S_{f1} \cup S_{f2}} \underline{N}^T \cos\bar{\theta}\, dS$$

$$\underline{B}_{ik}{}^j = \frac{2\rho}{h}\int_0^h \phi_k \psi_i(z)\, dz \sum_e \int_{S_{ij}} \underline{N}^T \cos\bar{\theta}\, dS$$

Decomposing the hydrodynamic pressure in terms of modal amplitude and ground acceleration, we get

$$c_i\underline{\bar{P}}_i(x,y) = \underline{P}_0\ddot{u}_g + \sum_{k=1}^{n_s}\sum_{j=1}^{2}\underline{P}_k^j\ddot{Y}_k^j \tag{4.26}$$

The amplitude of hydrodynamic pressure for each mode of wave can be found by solving the following equations

$$\underline{K}_i(x,y)\underline{P}_0 = \underline{B}_0 \tag{4.27.a}$$

and

$$\underline{K}_i(x,y)\underline{P}_k^j = \underline{B}_k^j \tag{4.27.b}$$

where k is the mode of structural vibration, j refers to the j-th cylinder and i is the mode of wave.

Substituting the results of Eqs. (4.27.a-b) into Eqs. (4.26) and (3.12), we can compute the amplitude of three-dimensional hydrodynamic pressures.

C. Localized Finite Element Method

In order to reduce the fluid domain, the following procedures are suggested: 1) introducing a transmitting boundary to separate the fluid into the inner and outer domains, 2) connecting the inner and outer domains by the continuity conditions on the transmitting boundary, 3) using a finite number of orthogonal functions, which are derived from the analytic solution of diffraction problem, to represent the hydrodynamic pressures in the outer domain, 4) applying the finite element technique only to the inner domain with appropriate boundary conditions. Once these procedures are made, the rest of the numerical analyses can be performed without difficulty.

For simplicity, we will only consider the two-dimensional problem in Eqs. (3.17.a) and (3.17.b) where the fluid domain is governed by a series of Helmholtz equations.

1. Inner and Outer Domains

As shown in Fig. 4.2, a transmitting boundary S_m was located near the structure in order to separate the infinite fluid domain into inner domain R_1 and outer domain R_2. Let p_1 and p_2 denote the hydrodynamic pressure in R_1 and R_2 respectively, then we have the following two-dimensional problems where the boundary conditions on the water surface and at the bottom are reduced.

In the inner domain, we have $S = S_{f1} \bigcup S_{f2} \bigcup S_m$ and

$$\nabla^2 \bar{p}_{1i}(x,y) - \lambda_i \bar{p}_{1i}(x,y) = 0 \tag{3.13.a}$$

with the boundary condition on the interface of cylinders being

$$\frac{\partial p_1}{\partial n}(x,y,z) = -\rho \frac{\partial^2 u}{\partial t^2}(z)\cos\bar{\theta} \tag{3.6.d}$$

Recalling that

$$p_1(x,y,z) = \sum_{i=0}^{n_m} \bar{p}_{1i}(x,y)\psi_i(z) \tag{3.12}$$

we obtain

$$\frac{\partial \bar{p}_{1i}}{\partial n}(x,y) = f_i \tag{4.29}$$

where

$$f_i = -\frac{2\rho}{c_i h}\cos\bar{\theta}\int_0^h \ddot{u}(z)\psi_i(z)\,dz$$

In the outer domain, we have $S = S_{tb} \bigcup S_f$

and

$$\nabla^2 \bar{p}_{2i}(x,y) - \lambda_i \bar{p}_{2i}(x,y) = 0 \tag{4.30}$$

with the far field boundary condition for low frequency excitation as

$$\lim_{R \to \infty} R^{1/2}\left(\frac{\partial \bar{p}_{2i}}{\partial r}(R) - ik_0 \bar{p}_{2i}(R)\right) = 0 \tag{4.31}$$

On the transmitting boundary, we require that

$$\bar{p}_{1i} = \bar{p}_{2i} \tag{4.32.a}$$

and

$$\frac{\partial \bar{p}_{1i}}{\partial n} = -\frac{\partial \bar{p}_{2i}}{\partial n} \tag{4.32.b}$$

where the normal vector is taken outwards from the fluid domain which is being considered. With these boundary conditions, $\bar{p}_{1i}$ and $\bar{p}_{2i}$ can have unique solutions.

2. The Functional in Inner Domain

Using the principle of variation, the following functional in the inner domain is formulated for each mode of wave:

$$F(\bar{p}_{1i}, \bar{p}_{2i}) = \tfrac{1}{2}\int\int_{R_1} ((\nabla \bar{p}_{1i})^2 + \lambda_i \bar{p}_{1i}^2)\, dxdy - \sum_{j=1}^{2}\int_{S_{fj}} \bar{p}_{1i} f_i^j\, dS$$

$$+ \int_{S_{tb}} (\bar{p}_{1i} - \tfrac{1}{2}\bar{p}_{2i})\bar{p}_{2in}\, dS \tag{4.33}$$

where $\bar{p}_{1in}$ and $\bar{p}_{2in}$ denote $\frac{\partial \bar{p}_{1i}}{\partial n}$ and $\frac{\partial \bar{p}_{2i}}{\partial n}$ respectively.

Applying Green's Theorem to $\bar{p}_{2i}$ and $\delta\bar{p}_{2i}$ in the outer domain, we have the following variation:

$$\delta F = -\int\int_{R_1} (\nabla^2\bar{p}_{1i} - \lambda_i\bar{p}_{1i})\delta\bar{p}_{1i}dxdy + \sum_{j=1}^{2}\int_{S_{ij}} (\bar{p}_{1in} - f_i')\delta\bar{p}_{1i}dS$$

$$+ \int_{S_w} (\bar{p}_{1in} + \bar{p}_{2in})\delta\bar{p}_{1i}dS + \int_{S_w} (\bar{p}_{1i} - \bar{p}_{2i})\delta\bar{p}_{2in}dS \tag{4.34}$$

where $\delta\bar{p}_{1i}$, $\delta\bar{p}_{2i}$ are the variations for $\bar{p}_{1i}$ and $\bar{p}_{2i}$.

Since the Eqs. (4.28), (4.29), and (4.32) are obtained by letting $\delta F = 0$, the values of $\bar{p}_{1i}$ derived from the functional, Eq. (4.33), will be the solution of the problem.

3. Boundary Value Problem

Let the inner domain R_1 be divided into finite element mesh with nodal points in each element. Introducing the interpolation function associated with each node such that each element can be represented by

$$\bar{p}_{1i}(x,y) = \sum_{l=1}^{n} N_l\bar{p}_{1i}{}^{l} \equiv \underline{N}\bar{p}_{1i} \tag{4.35}$$

According to Wehausen and Laitone [13], the radiated hydrodynamic pressure in the far field can be expressed in terms of the eigenfunctions $\Psi_i(x,y)$ with unknown coefficients $\bar{p}_{2i}$.

From three-dimensional hydrodynamic pressure

$$p_2(x,y,z) = \sum_{i=0}^{n_w} \bar{p}_{2i}(x,y)\psi_i(z) \tag{4.36}$$

and for each i-th mode of wave,

$$\bar{p}_{2i}(x,y) = \sum_{l=0}^{n_f-1} \Psi_{il}(x,y)\bar{p}_{2i}{}^{l} \equiv \underline{\Psi}_i\bar{p}_{2i} \tag{4.37}$$

when $l = 0$ we have

$$\Psi_{0l}(x,y) = H_l^1(k_0R)\cos(l\theta-\delta) \tag{4.38.a}$$

when $l \geq 1$ we have

$$\Psi_{1l}(x,y) = \bar{K}_l(k_lR)\cos(l\theta-\delta) \tag{4.38.b}$$

where H_l^1 is the Hankel function of the first kind to the l-th order, $\bar{K}_l$ is the modified Bessel function of the second kind to the l-th order, and $\psi_l(z)$ is the mode shape of wave, Eqs. (3.13) and (3.16).

The stationary point of the functional, Eq. (4.33), with respect to $\bar{p}_{1l}$ and $\bar{p}_{2l}$ can be found by the following equations:

$$\frac{\partial F(\bar{p}_{1l},\bar{p}_{2l})}{\partial \bar{p}_{1l}} = 0 \tag{4.39.a}$$

and

$$\frac{\partial F(\bar{p}_{1l},\bar{p}_{2l})}{\partial \bar{p}_{2l}} = 0 \tag{4.39.b}$$

where $\bar{p}_{1l}$ is a vector of nodal hydrodynamic pressures in R_1, and $\bar{p}_{2l}$ is a vector of coefficients in Eq. (4.37).

The following set of algebraic equations is then formulated for each mode of wave:

$$\begin{bmatrix} \underline{A}_{11} & \underline{A}_{12} \\ \underline{A}_{21} & \underline{A}_{22} \end{bmatrix}_l \begin{Bmatrix} \bar{p}_{1l} \\ \bar{p}_{2l} \end{Bmatrix} = \begin{Bmatrix} \underline{b}_{1l} \\ \underline{b}_{2l} \end{Bmatrix} \tag{4.40}$$

where

$$\underline{A}_{11} = \sum_e \int\int_{R_1} (\nabla \underline{N}^T \nabla \underline{N} + \lambda (\underline{N}^T \underline{N})\, dA \tag{4.41.a}$$

$$\underline{A}_{22} = \sum_e \int_{S_{ij}} \tfrac{1}{2} (\underline{\Psi}_{in}{}^T \underline{\Psi}_i + \underline{\Psi}_i{}^T \underline{\Psi}_{in})\, dS \tag{4.41.b}$$

$$\underline{A}_{12} = -\sum_e \int_{S_{ij}} \underline{N}^T \underline{\Psi}_{in}\, dS \tag{4.41.c}$$

$$\underline{A}_{21} = \underline{A}_{12}{}^T \tag{4.41.d}$$

$$\underline{b}_{1i} = \sum_{j=1}^{2} \sum_e \int_{S_{ij}} \underline{N}^T f_i{}^j\, dS \tag{4.41.e}$$

$$\underline{b}_{2i} = \underline{0} \tag{4.41.f}$$

also the cylindrical coordinates are applied to R_2 and $\underline{\Psi}_{in}$ denotes $\frac{\partial \underline{\Psi}_i}{\partial n}$.

Recall the expansion of the interface boundary condition (4.22) for both cylinders the matrix $\underline{b}_{1i}$ can be represented as follows by the same procedure discussed before,

$$\underline{b}_{1i} = \underline{B}_{i0} \ddot{u}_g + \sum_{k=1}^{n_s} \sum_{j=1}^{2} \underline{B}_{ik}{}^j \ddot{Y}_k{}^j \tag{4.42}$$

where cylinders are considered to be flexible, k refers to the k-th mode of structural vibration and j refers to the j-th cylinder.

The algebraic equation (4.40) can be simplified as

$$\underline{A}_i \underline{\tilde{p}}_i = \underline{B}_{i0} \ddot{u}_g + \sum_{k=1}^{n_s} \sum_{j=1}^{2} \underline{B}_{ik}{}^j \ddot{Y}_k{}^j \tag{4.43}$$

Decomposing the hydrodynamic pressure in terms of $\ddot{u}_g$ and $\ddot{Y}_k$

$$\underline{\tilde{p}}_i = \underline{P}_{i0} \ddot{u}_g + \sum_{k=1}^{n_s} \sum_{j=1}^{2} \underline{P}_{ik}{}^j \ddot{Y}_k{}^j \tag{4.44}$$

the amplitude of hydrodynamic pressure for each mode of wave will be solved from the following equations,

$$\underline{A}_i \underline{P}_0 = \underline{B}_0 \tag{4.45.a}$$

$$\underline{A}_i \underline{P}_k^J = \underline{B}_k^J \tag{4.45.b}$$

Thus the three-dimensional hydrodynamic pressure can be found by Eq. (3.12).

It should be noted that if the transmitting boundary is taken at a far distance from the structure, then $\bar{p}_2$ can be represented only by the first few terms of the series in Eq. (4.37).

For the case of high frequency excitation, the far field boundary condition is reduced to

$$\frac{\partial p}{\partial n}(x,y) = 0 \tag{3.14.b}$$

Therefore, the eigenfunction expansions in the outer domain [34] can be represented by

$$\Psi_l(x,y) = e^{-k_l r}\cos(l\theta - \delta) \tag{4.46}$$

and the method discussed above is modified in Appendix B. However, the amplitude of pressure wave due to high frequency excitation decreases rapidly with the traveling distance. We can solve numerically the radiation problem by choosing a proper boundary at far field and applying finite element technoque in the inner domain only [26].

D. Symmetrical Loading and Antisymmetrical Loading

The discussions in the previous sections are for the general consideration that the ground motion can be in any direction. The steady state structural responses are assumed in the same direction as the ground motion. By using the appropriate conditions of symmetry and antisymmetry, the fluid domain is reduced to one half so that the computation of hydrodynamic pressure is simplified and becomes much more efficient.

If the structures are symmetrical with respect to the X-axis as shown in Fig. 4.3, an arbitrary ground motion can be decomposed into X-component and Y-component,

$$\ddot{\vec{u}}_g = \ddot{\vec{u}}_{gx} + \ddot{\vec{u}}_{gy}$$

Therefore, the hydrodynamic pressure consists of two parts - the one induced by $\ddot{u}_{gx}$ is symmetrical to the X-axis and the one induced by $\ddot{u}_{gy}$ is antisymmetrical to the X-axis:

$$p = p_s + p_{as}$$

The total responses of structures can be obtained by combining of the solutions from those two reduced problems as follows:

$$\vec{u} = \vec{u}_x + \vec{u}_y$$

For the symmetrical responses, the direction of ground motion becomes $\delta = 0$ and $\ddot{\theta} = \theta$. The boundary for the integral domain in finite element formulation reduces to the following form as shown in Fig. 4.3

$$S = S_s \cup S_{fl} \cup S_{\infty} \cup S_f \tag{4.47}$$

where S_s is the symmetrical boundary on X-axis, S_{fl} is the interface boundary, and S_f is the far field boundary.

On the symmetrical boundary, S_s, we have the following condition:

$$\frac{\partial \bar{p}_i}{\partial n} = 0 \tag{4.48}$$

Thus the boundary integrals, Eqs. (4.C) and (4.19), vanish and the computation is greatly simplified.

As for the antisymmetrical responses, the direction of ground motion becomes $\delta = \frac{\pi}{2}$ and $\bar{\theta} = \theta - \frac{\pi}{2}$. The hydrodynamic pressure in the positive Y-direction will be opposite to that in the negative Y-direction. The boundary for this case is (Fig. 4.3)

$$S = S_{as} \cup S_{f1} \cup S_{f2} \cup S_f \tag{4.49}$$

where S_{as} is the antisymmetrical boundary.

associated with the boundary condition,

$$\bar{p}_{as} = 0 \tag{4.50}$$

the boundary integral on S_{as} becomes

$$\int_{S_{as}} \underline{N}^T \frac{\partial \bar{p}_i}{\partial n}(x,y)\, dS = \int_{S_{as}} \underline{N}^T \frac{\partial N}{\partial n} dS\ \bar{p}_i \tag{4.51}$$

which will be added to the the right hand side of Eq. (4.8).

It is worth mentioning that, for the antisymmetrical problem, the structural responses in the direction perpendicular to the ground motion becomes significant if one considers the second-order terms in the fluid flow.

If we decompose the structural response such as

$$u = u_x \cos\theta + u_y \sin\theta \tag{4.52}$$

and consider the degrees of freedom for both X- and Y-directions, an added mass matrix will be constructed as follows:

$$\underline{M}^e = \begin{bmatrix} \underline{M}_{xx} & \underline{M}_{xy} \\ \underline{M}_{yx} & \underline{M}_{yy} \end{bmatrix} \tag{4.53}$$

where $\underline{M}_{xy}$ is the coupled added mass matrix in the X-direction due to the unit structural acceleration on the degree of freedom in the Y-direction for both cylinders.

However, the coupled added mass matrices $\underline{M}_{xy}$ and $\underline{M}_{yx}$ will vanish in a linear fluid formulation and the antisymmetrical problem is uncoupled into two parts. Since the component of ground motion is in the Y-direction, we need to solve this problem for the Y-direction only. The assumption that the structural responses have the same direction as the ground motion is assured.

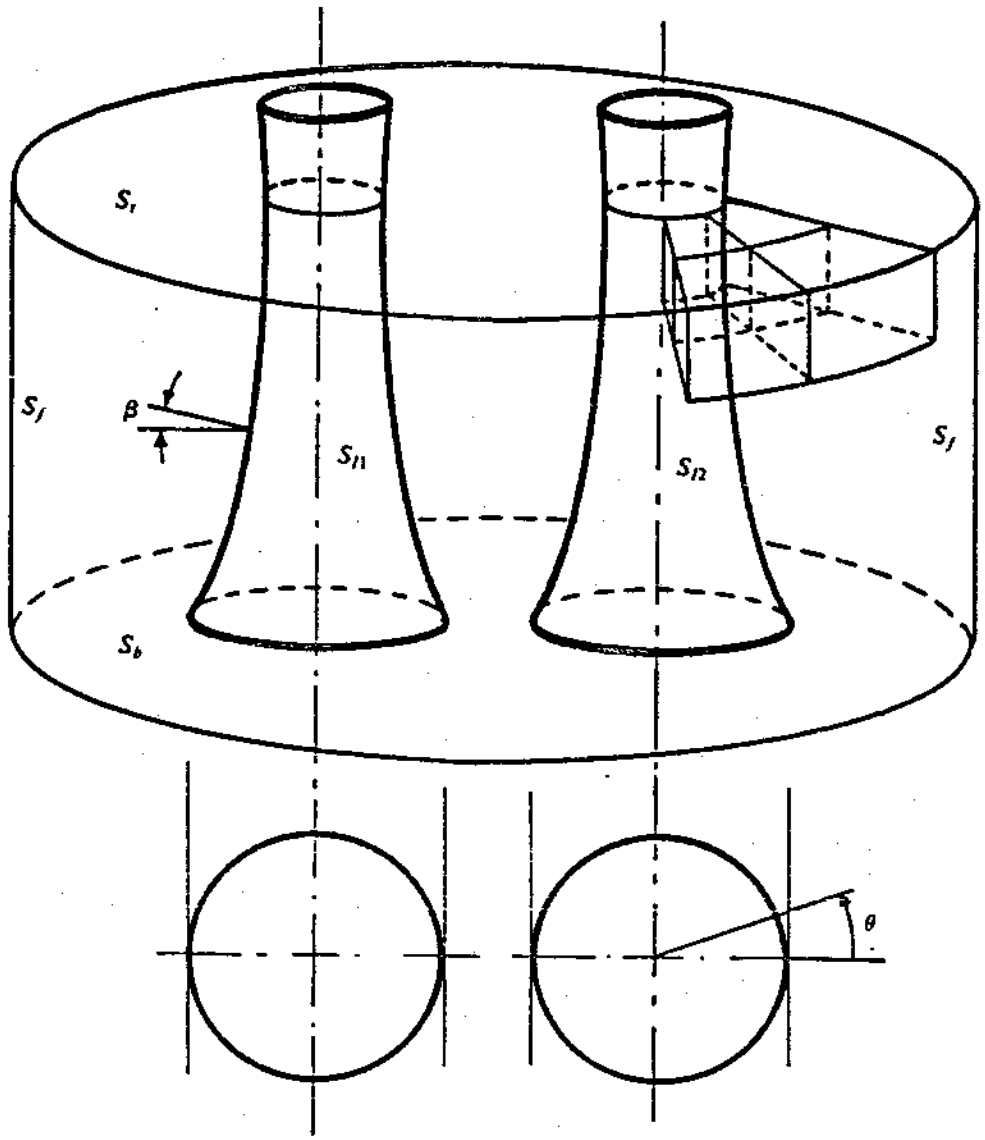

Figure 4.1 Three-Dimensional Fluid Domain

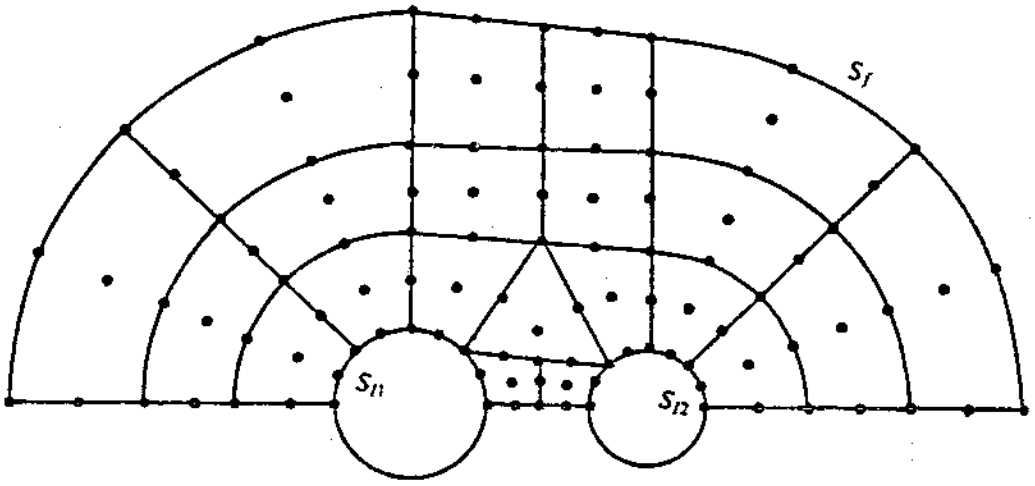

a. Conventional Finite Element Discretization

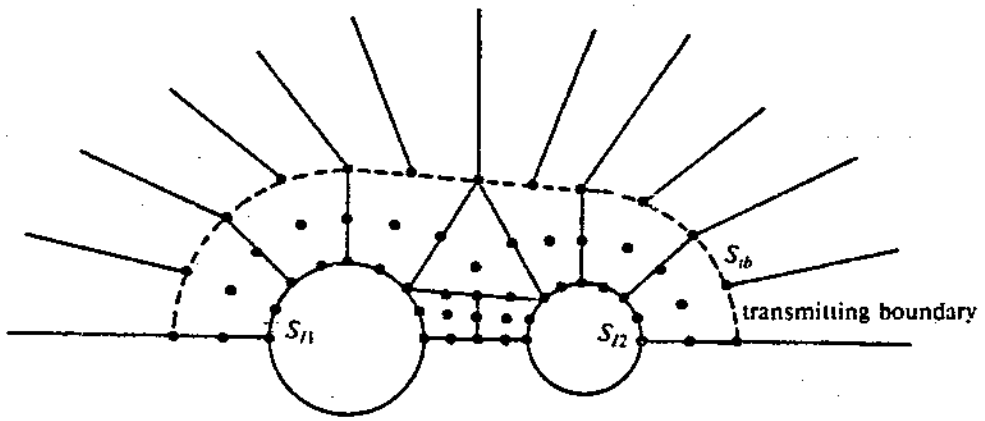

b. Localized Finite Element Discretization

Figure 4.2 Reduced Two-Dimensional Fluid Domain in Localized Finite Element Method

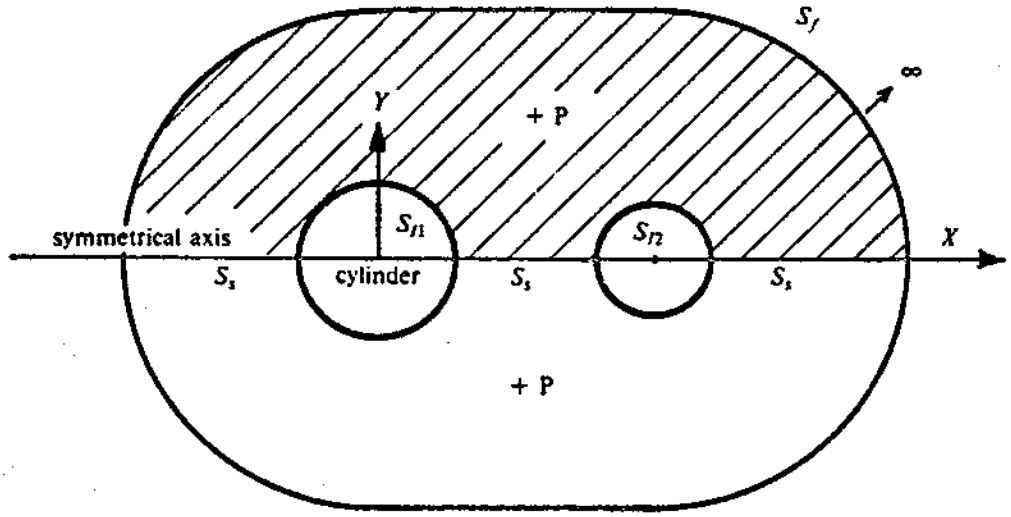

a. Ground Motion in X-Direction : Symmetry

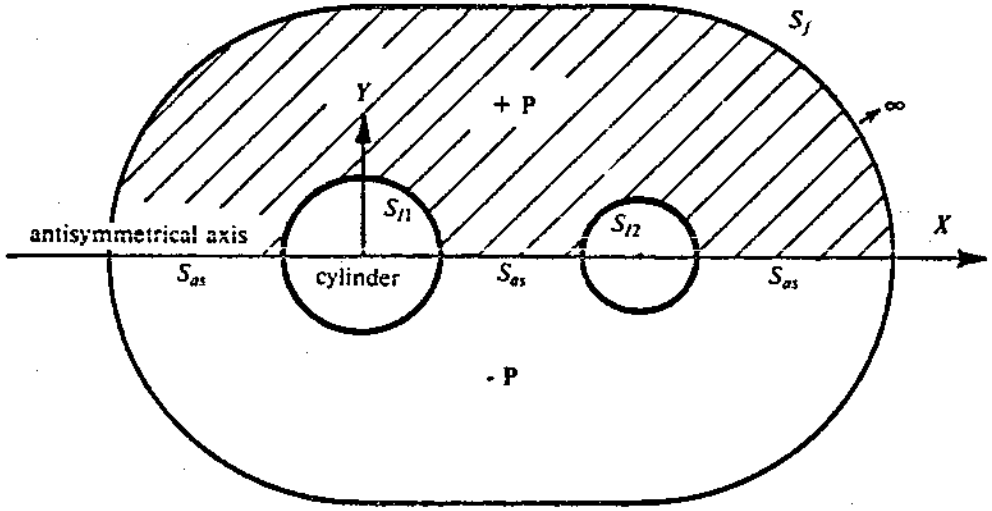

b. Ground Motion in Y-Direction : Antisymmetry

Figure 4.3 Symmetrical and Antisymmetrical Fluid Domain

V. EXAMPLES AND RESULTS

The method discussed in the previous chapters was programmed for a high speed computer. Here, we will illustrate three examples for numerical calculations. In Example A, the structural system is assumed to be the same as that in the experiments [51] which were performed in the Earthquake Engineering Research Center in University of California at Berkeley. Then, the comparison of results from numerical analyses and experiments is made. In Example B, the results of finite element analysis for a single flexible cylinder is used to compare with those from theoretical analysis [26]. Example C is an extension of Example B, with the assumption of two flexible cylinders.

A. Rigid Cylinders of Type (2)*

We assume that there are two identical rigid circular cylinders connected to a rigid foundation as shown in Fig. 3.1 and Fig. 5.1, where each cylinder has two degrees of freedom, namely translation and rotation. If the harmonic ground acceleration is either from X-direction or from Y-direction, then the principle of symmetry and antisymmetry can be applied to reduce the fluid domain to one half. For ground acceleration with high frequencies, i.e. 6 Hz to 10 Hz, the induced wave length is small and the ratio of $\frac{D}{L}$ is large as shown in Fig. 2.1. It implies that the validity of diffraction theory is assured. Furthermore, a simplification of the far field boundary can be made by assuming

$$\frac{\partial p}{\partial n} = 0 \tag{5.1}$$

i.e. the radiation effect due to the surface wave propagation is neglected for high frequency vibration.

* refers to the definition in Chapter III.

The number of wave modes is chosen to be six by taking the first six terms from the series shown in Eq. (3.15). Fig. 3.3.b exhibits the variation of hydrodynamic forces in the vertical direction with respect to each of the six modes. Fig. 5.2 shows how the amplitude of hydrodynamic forces decreases as the number of modes increases in the cases of high frequency (8 Hz) excitation. It also shows that the hydrodynamic forces on each cylinder due to the vibration on the neighboring one can be as high as 40 percent of those due to the vibration of the translational degree of freedom on itself. Since the forces decrease very fast for higher modes, they are negligible when the mode number is greater than six.

By the assumption of the uniform cross section in the vertical direction, the boundary value problem in the fluid domain can be reduced to two-dimensional problem as discussed in Chapter III. A finite element system of 129 nodes which correspond to 29 Lagrange quadratic elements is formed to investigate the hydrodynamic effect around the cylinders as shown in Fig. 5.3. Also, the variation of the relative structural responses with respect to the size of finite element mesh is examined. From Fig. 5.4, it implies that the change of structural displacement is less than 5 percent as the ratio of the radius of the far field boundary to the radius of cylinder is greater than 7. In order to insure the convergence of the results in this example, the ratio of $\frac{r}{a}$ is chosen to be 10 wnich is twice as much as the effective diffraction distance of a single cylinder under high frequency vibration [26].

The natural frequency of each cylinder in the air is 26 Hz for the first vibration mode. Figure 5.1 displayes the mass matrix and the stiffness matrix of the cylinders. Rayleigh damping of structure has been assumed with a damping ratio being 5 percent. The translation and rotation of structural displacements are shown in Fig. 5.5 and Fig. 5.6 respctively. With the definition of relative distance as the ratio of the distance between the centers of cylinders to the sum of the radius of cylinders, it is clear that the hydrodynamic interaction becomes important as relative distance is less than 4. Also, the extent of interaction depends on the frequency of excitation, the amplitude of ground motion, the characteristics of structures and the depth of water.

Fig. 5.7 shows the variation of base shear of the cylinders. When the cylinders get closer, the structural reactions and deformations will decrease if the ground acceleration is in the X-direction and increase if the ground motion is in the Y-direction. The variation in high frequency excitation can be in the range from a 20 percent decrease for the symmetrical case to a 60 percent increase for the antisymmetrical case.

In Fig. 5.7, it also presents the results from the experiments [51] to compare with the numerical analyses. As clearly shown, these two results are quite close to each other except some minor discrepancies. These discrepancies may be caused by the following reasons: (1) the linearization of the boundary value problem in numerical analysis, (2) the square basin being constructed to simulate the unbounded fluid domain, and (3) the uncertainties in laboratory works. The experimental equipments, techniques and results are discussed in great detail in a report by Ansari [51].

The interaction for the added mass in this example changes in the same pattern as that for structural responses. Fig. 5.8 and Fig. 5.9 present the normalized added mass for the case of symmetry and antisymmetry respectively. The added mass of the degrees of freedom between the two cylinders is negligible for relative distance greater than about 4. The interaction of added masses for degrees of freedom of the same cylinder can be as high as 30 percent when the cylinders contact each other for both cases of symmetry and antisymmetry.

B. Single Flexible Cylinder of Type (3)

This problem was solved analytically by Liaw and Chopra [26] with the principle of axisymmetry. A reduced two-dmensional numerical procedure discussed in the previous chapters is now applied to the same problem for comparison.

At first, the fluid domain is investigated by a finite element mesh with 63 nodes and 12 quadratical elements as shown in Fig. 5.10. Secondly, let the ratio of outside radius to the height of a slender cylinder, $\frac{a}{H}$ be 0.05, and the ratio of wall thickness to the outside radius, $\frac{t}{a}$ be 0.2 which is a typical value for many towers. Next, assign a value of 5 million psi to

Young's modulus E, a value of 155 pcf to the unit weight of concrete and a value of 0.05 to the modal damping ratio. The frequencies and mode shapes of vibration can then be obtained by the assumption of uniform cantilever beams governed by elementary beam theory.

The detail of the analytical solution is presented in Appendix C. We are considering the case when the cylinder is with no surrounding water or is fully submerged for the dynamic responses of the first two modes. As shown in Fig. 5.11, by using six modes of wave, the numerical solution of structural acceleration gives a very good approximation to the analytic solution.

The effect of surrounding water on the dynamics of towers in the first mode of vibration is given by

$$m_a^1(z) = \frac{p_1(z)}{\phi_1(z)} \tag{5.2}$$

where $m_a(z)$ is defined as an additional mass per unit height of the cylinder, $p_1(z)$ is the hydrodynamic forces which can be derived either from the analytic solution by Eq. (C.22), or from the numerical procedures in Eqs. (3.17.a), (3.35) and (4.26) for the first vibration mode where $\ddot{u}_g$ is the unit ground acceleration, and ϕ_1 (z) is the shape function of the first mode vibration of the cylinder.

The "added excitation" due to the hydrodynamic effect with respect to the ground motion can be represented as

$$m_a^0(z) = p_0(z) \tag{5.3}$$

where p_0 can also be derived either from the analytic solution, Eq. (C.22), or from the numerical solution.

The comparison of added mass distribution between analytic solution and numerical solution is shown in Fig. 5.12. It proves that the numerical solution, by using six modes of wave,

is a very good approximation to the analytic solution.

C. Flexible Cylinders of Type (3)

This example will investigate two identical flexible cylinders of type (3) under high frequency horizontal ground excitation. For each cylinder, it has the same structural characteristics as shown in example B. The reduced two-dimensional numerical analysis is still applied to the symmetrical and antisymmetrical cases as the previous examples.

The fluid domain is divided into finite element mesh which is the same as the mesh outlined in example A. However, the hydrodynamic pressure and the structural responses are calculated herein by using the first six modes of wave and the first two mode of structural vibration. While the convergence of hydrodynamic forces with respect to the modes of wave has been examined in example A, the convergence of structural responses with respect to the modes of structural vibration is exhibited in Fig. 5.13. Since the cylinders in this example are very stiff, the first vibration mode dominates the dynamic structural behavior. As the number of modes increases, the structural responses will change within a variation of one percent.

Fig. 5.14 shows how the structural responses vary with the relative distance, which is defined as the ratio of the distance between the centers of the cylinders to the sum of the radius of cylinders. It is obvious that the interaction is negligible as relative distance exceeds 4. Also, the difference of the responses between the symmetrical case and the antisymmetrical case becomes greater as the relative distance decreases. Fig. 5.15 exhibits that the symmetrical structural responses are shifting to higher frequency as the relative distance decreases, i.e. it approaches to 1. Fig. 5.16 shows that the antisymmetrical structural responses are shifting to lower frequency as the distance decreases. Also shown in Figs. 5.17-20, if we move the condition of relative distance from a big value to a small value so that the interaction is important, the submerged natural frequency will change with the variation of 10 percent decrease in the symmetrical case and 10 percent increase in the antisymmetrical case. Clearly, the variation of structural responses for the higher mode of structural vibration is greater than those for the

lower mode.

The change of structural responses with respect to water depth is shown in Fig. 5.21. In the antisymmetrical case, the responses to the fully-submerged cylinders are six times greater than those with zero water depth. While, in the symmetrical case, the responses to the fully-submerged cylinders are only three times greater than those to the dry cylinders. The difference of the first modal response in both cases is negligible as water depth is less than 40 percent of the height of cylinder.

The distribution of hydrodynamic forces in the vertical direction is shown in Figs. 5.22-25 for the first six modes of wave. Two sets of calculations which correspond to different relative distances, are presented. From those figures, we can find that the forces are decreasing gradually by the ascending order of modes. Again, the influences of the cases of symmetry and antisymmetry are clearly shown. The dimensionless values of the amplitude of hydrodynamic forces are listed in Table 5.1 for comparison.

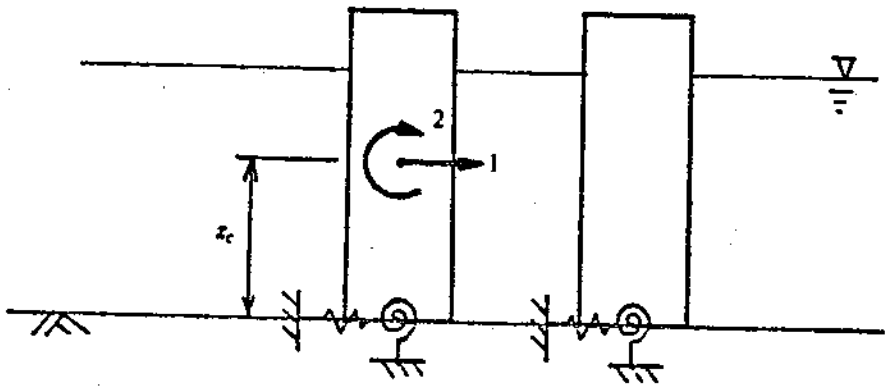

$$\text{Mass Matrix} = \begin{bmatrix} 0.549 \ \frac{lb}{ft} sec^2 & 0 \\ 0 & 0.595 \ lb-ft-sec^2 \end{bmatrix}$$

$$\text{Stiffness Matrix} = \begin{bmatrix} 99600 \ \frac{lb}{ft} & -141940 \ lb \\ -141940 \ lb & 253240 \ lb-ft \end{bmatrix}$$

$$z_c = 1.6837 \ ft$$

Figure 5.1 Structural Configuration and Characteristics of Example A

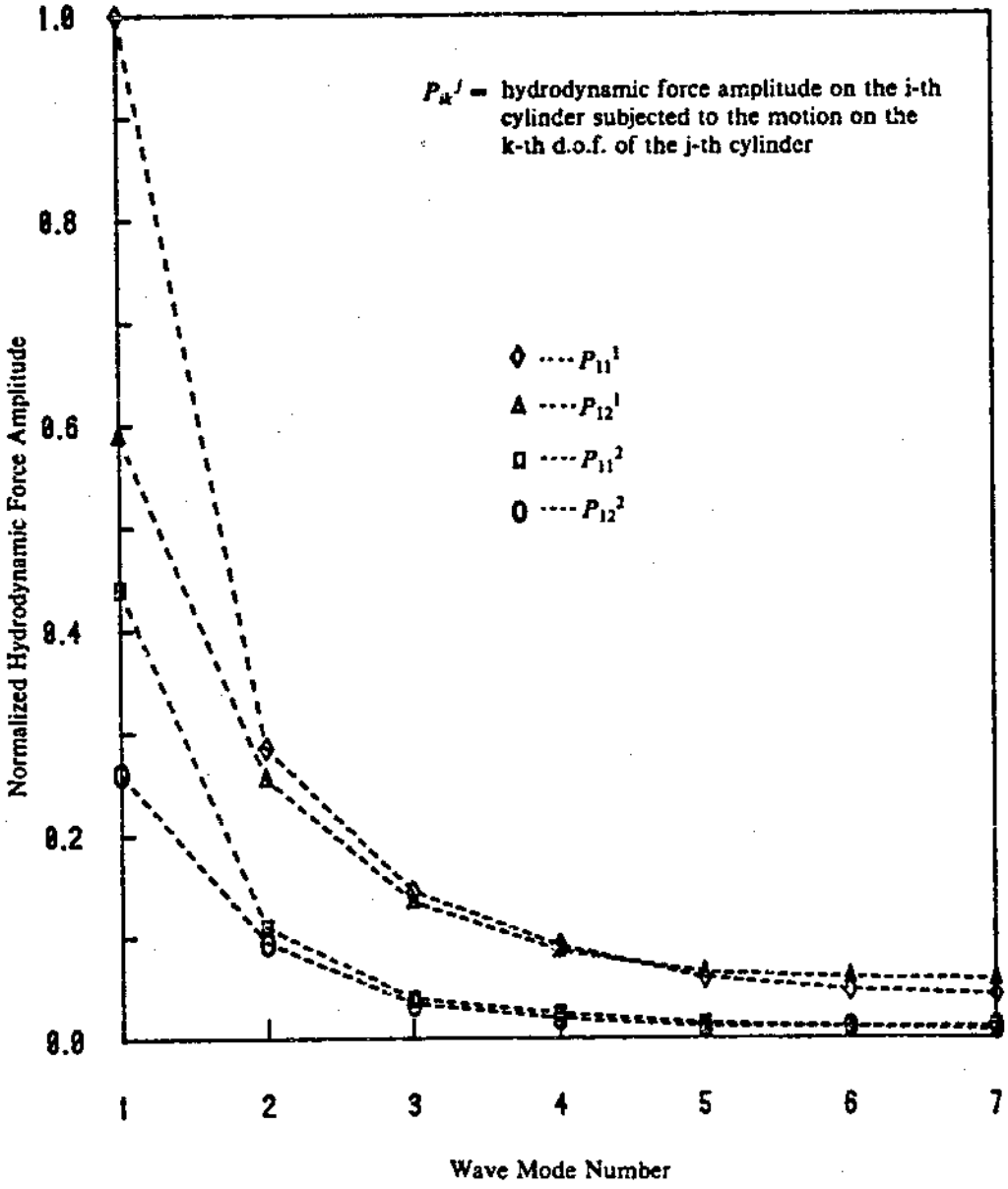

Figure 5.2 Convergence of Hydrodynamic Force Amplitude

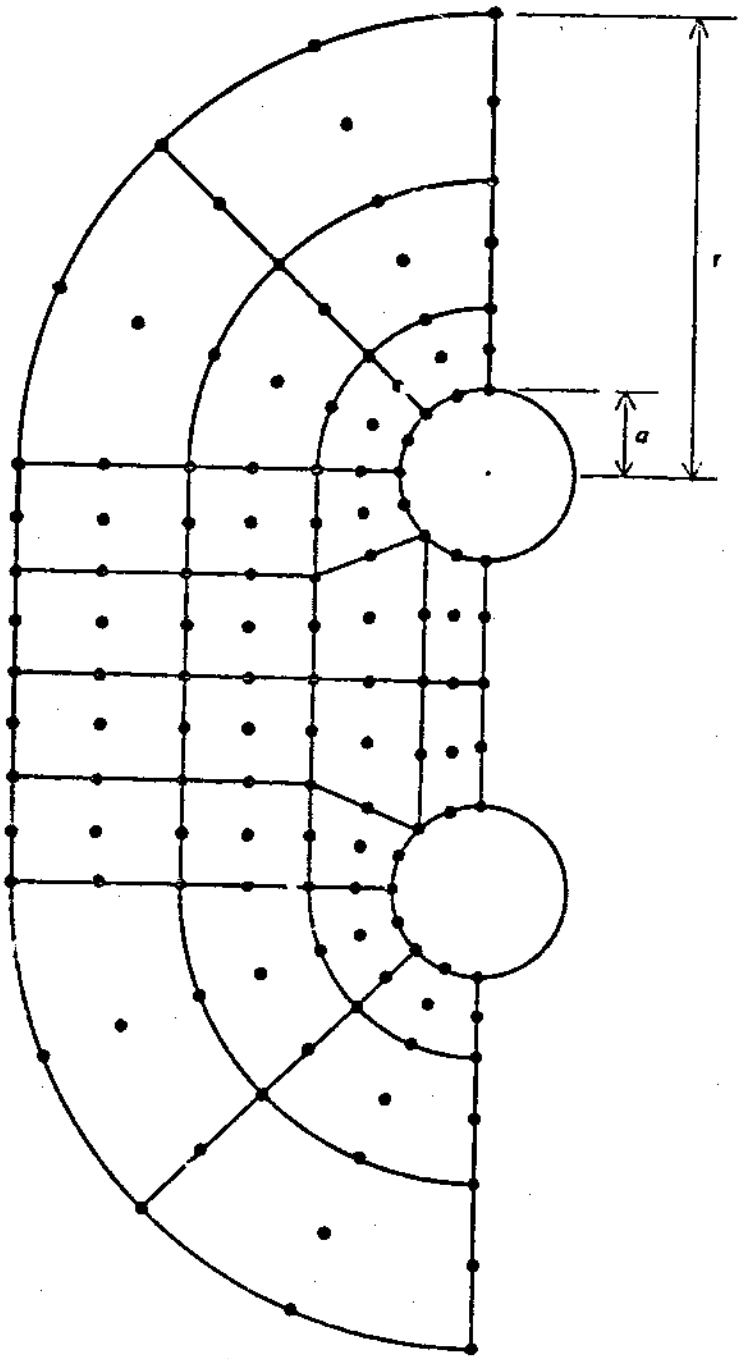

Figure 5.3 Finite Element Mesh of Example A

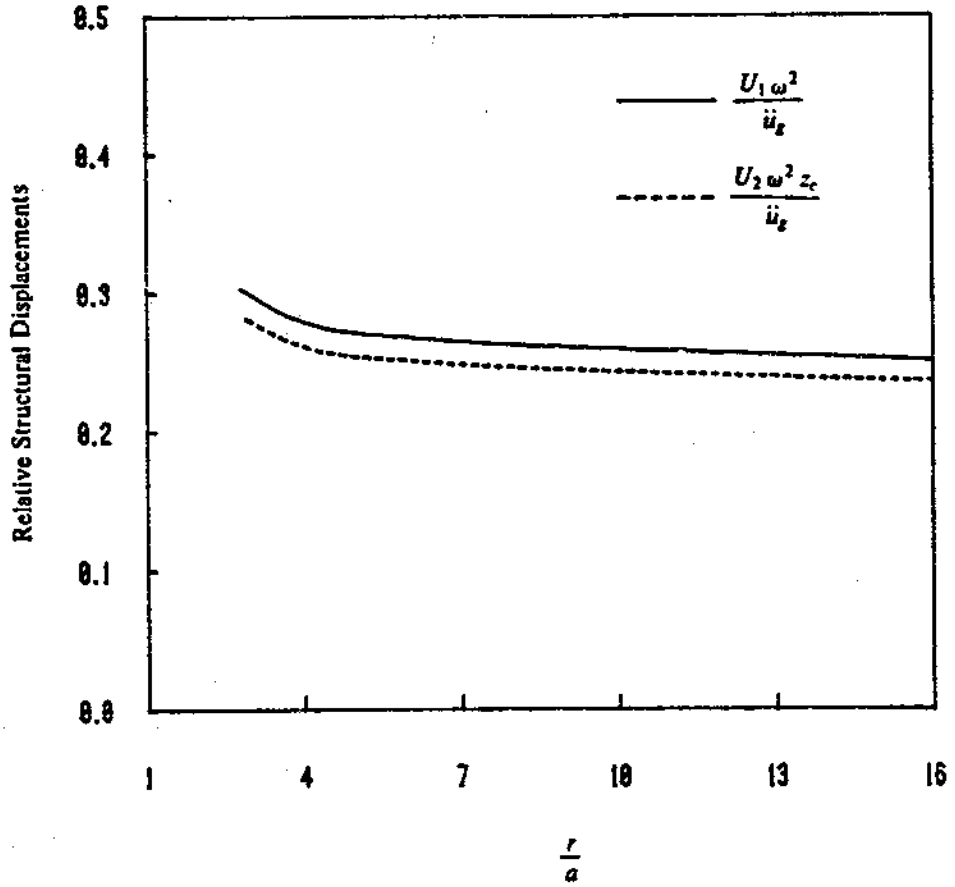

Figure 5.4 Decay of Structural Responses ($\bar{d}$=2.667, $\frac{h}{z_c}$=1.782, $\frac{\omega}{\omega_1}$=0.384, *symmetry*)

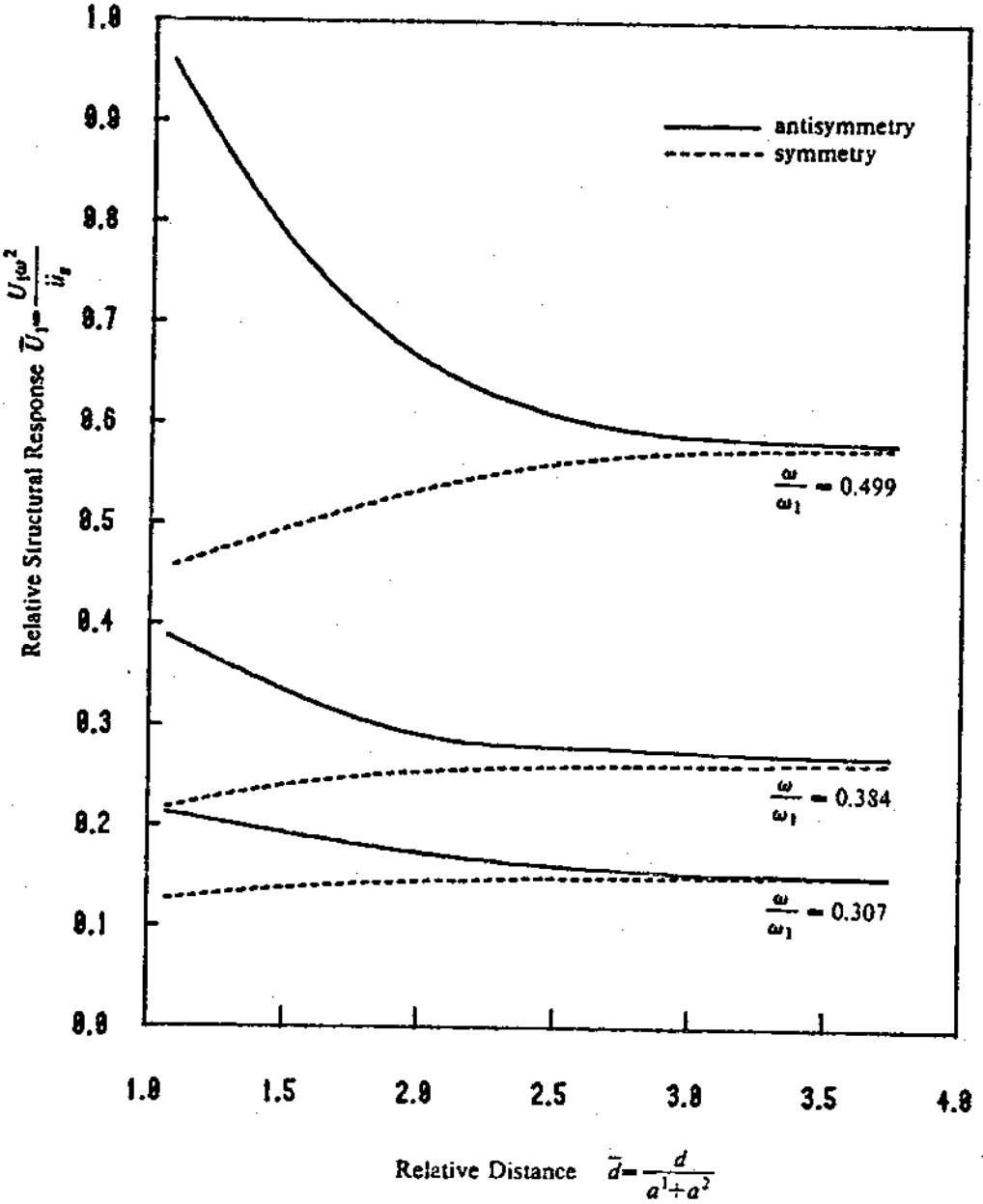

Figure 5.5 Relative Structural Response $\bar{U}_1,(\frac{h}{z_c}=1.782)$

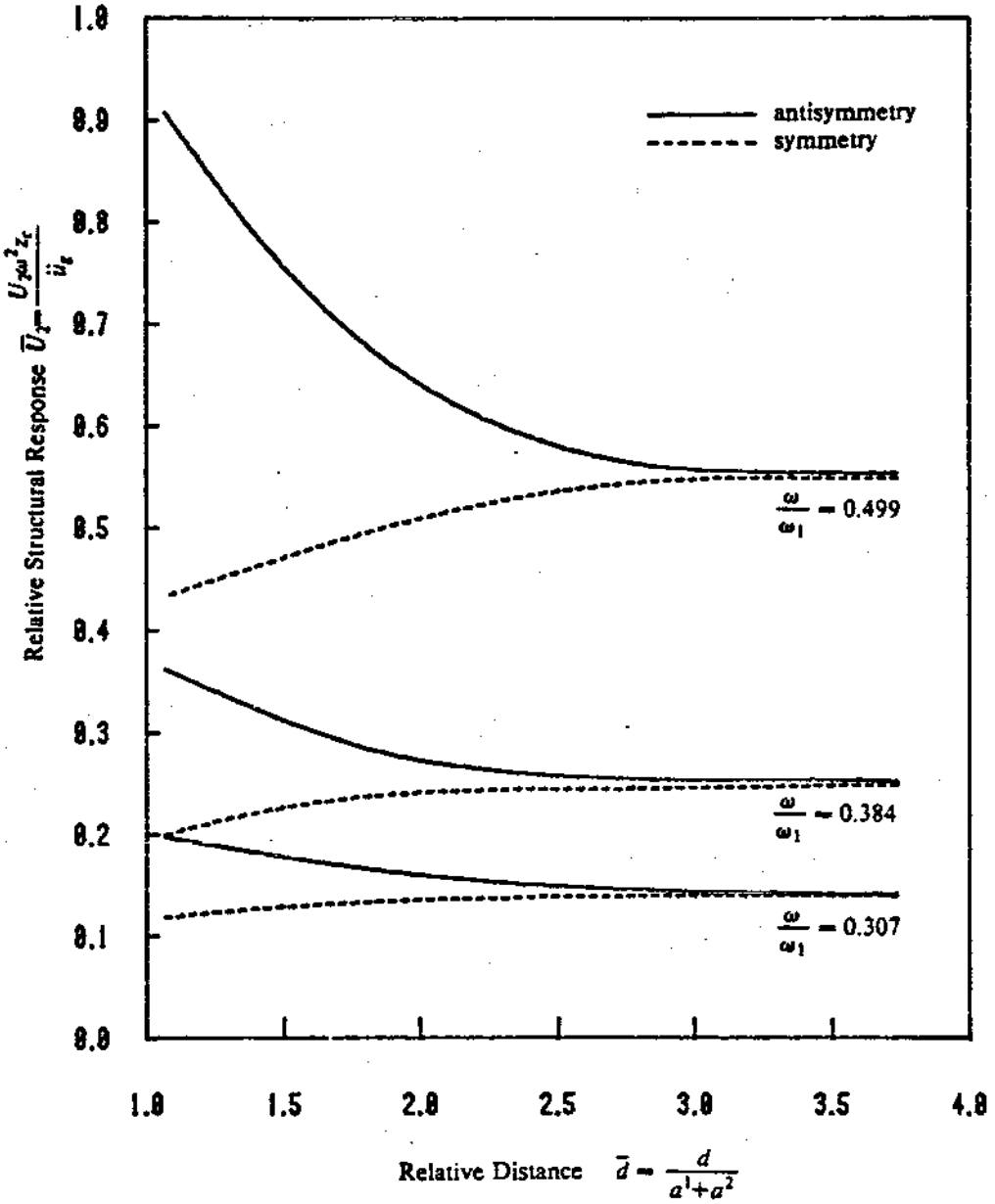

Figure 5.6 Relative Structural Response $\bar{U}_2$, ($\frac{h}{z_c}$=1.782)

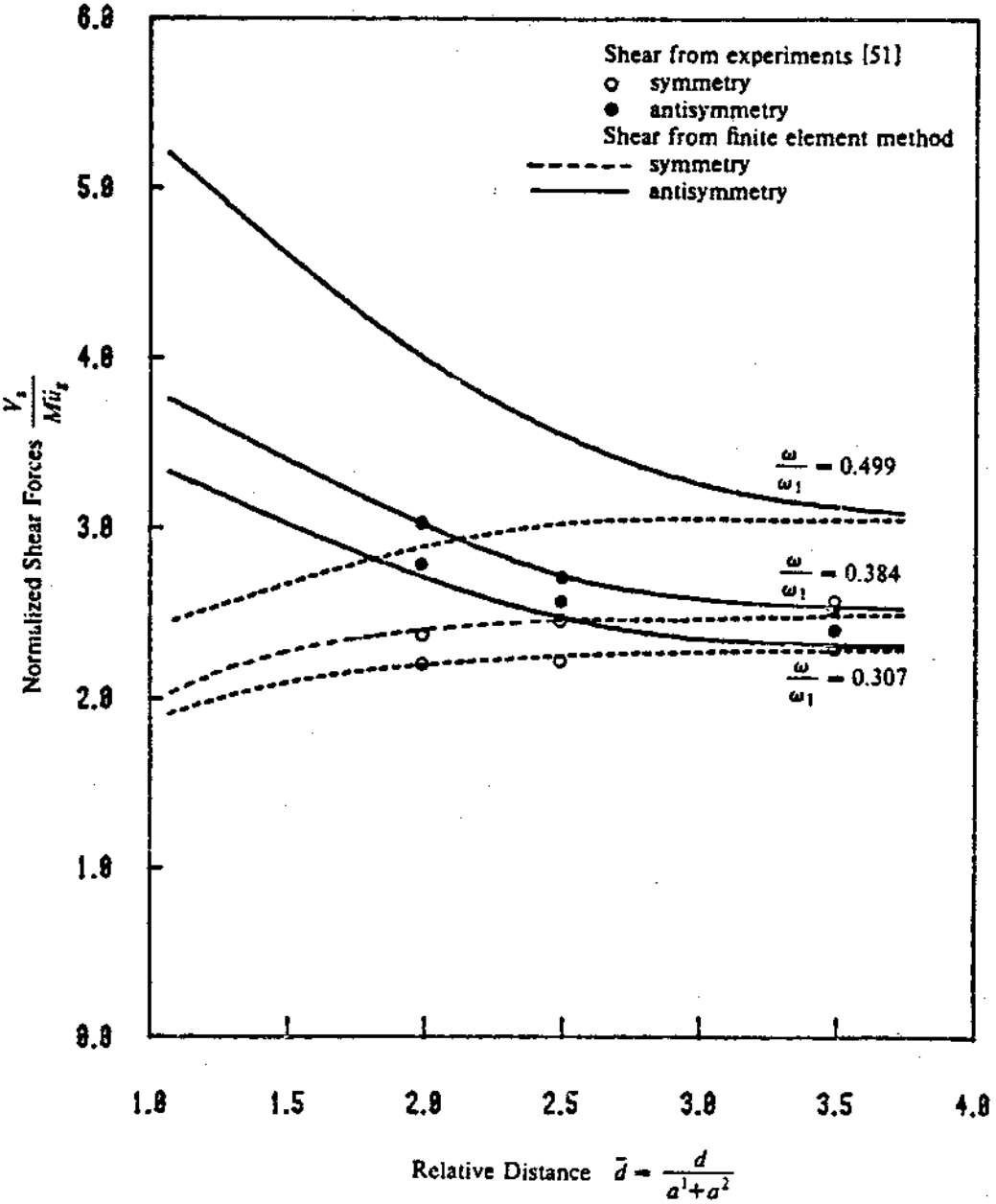

Figure 5.7 Normalized Shear Forces ($\frac{h}{z_c}$=1.782)

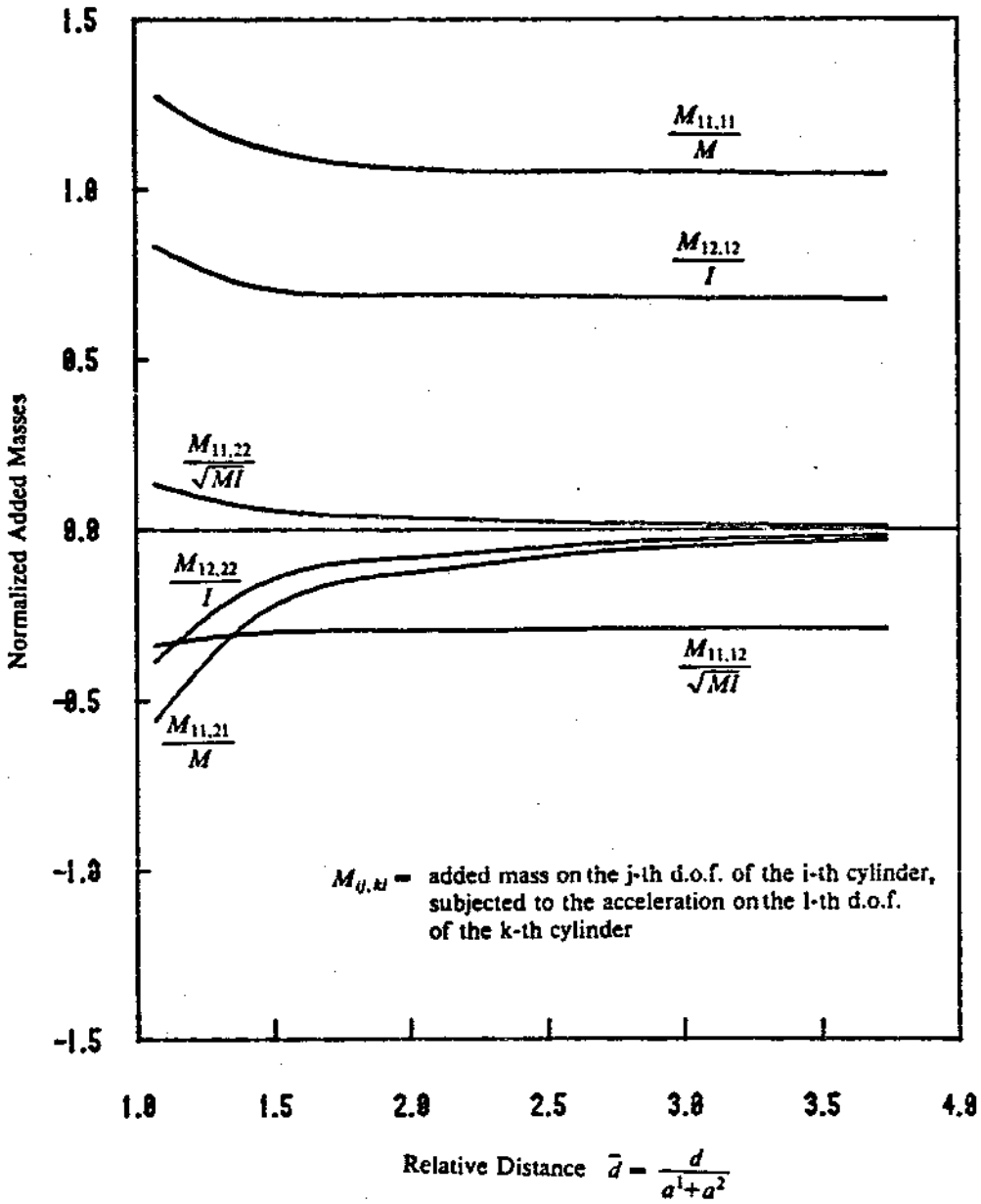

Figure 5.8 Normalized Added Masses - Symmetry ($\frac{h}{z_c}$=1.782)

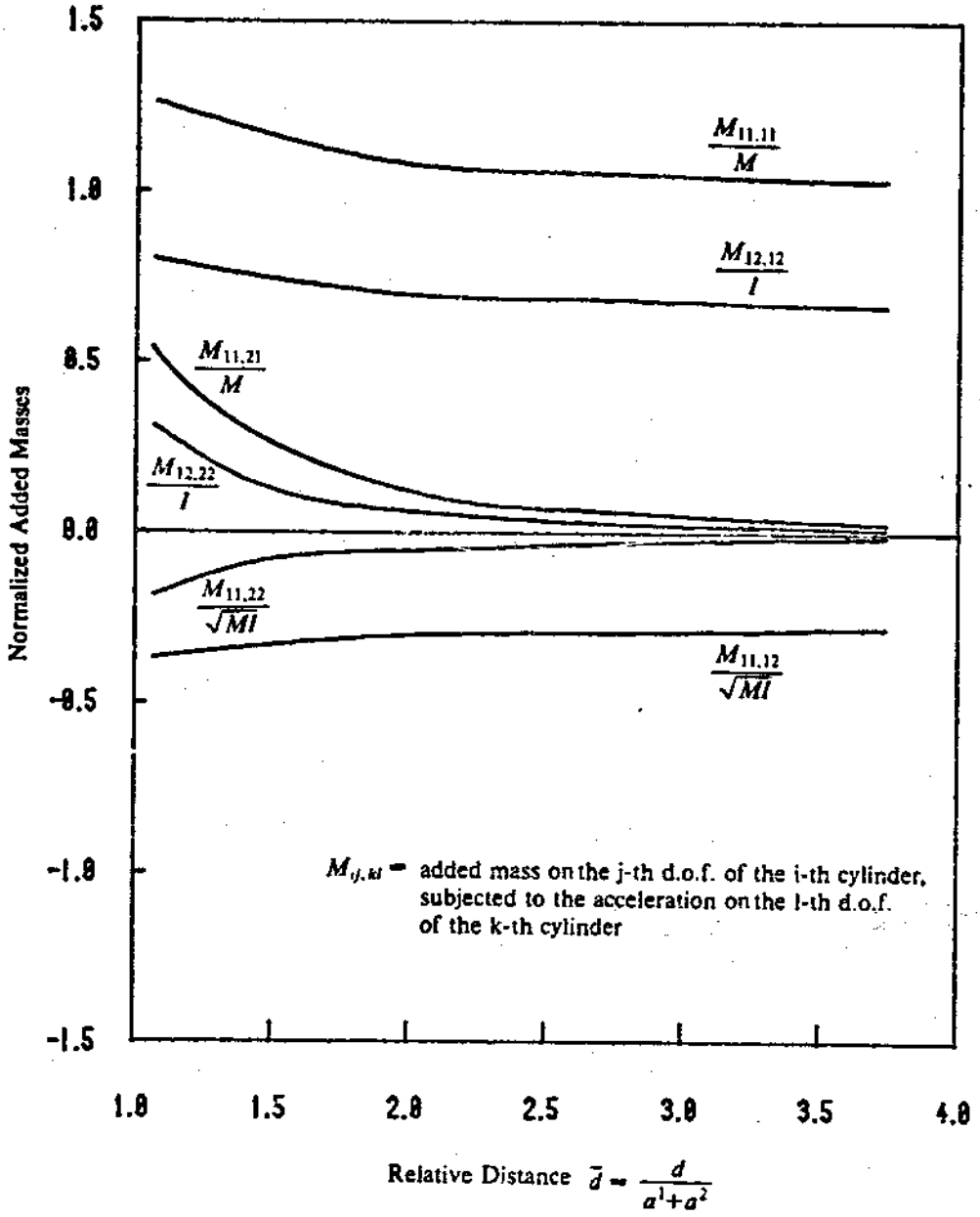

Figure 5.9 Normalized Added Masses - Antisymmetry ($\frac{h}{z_c}$=1.782)

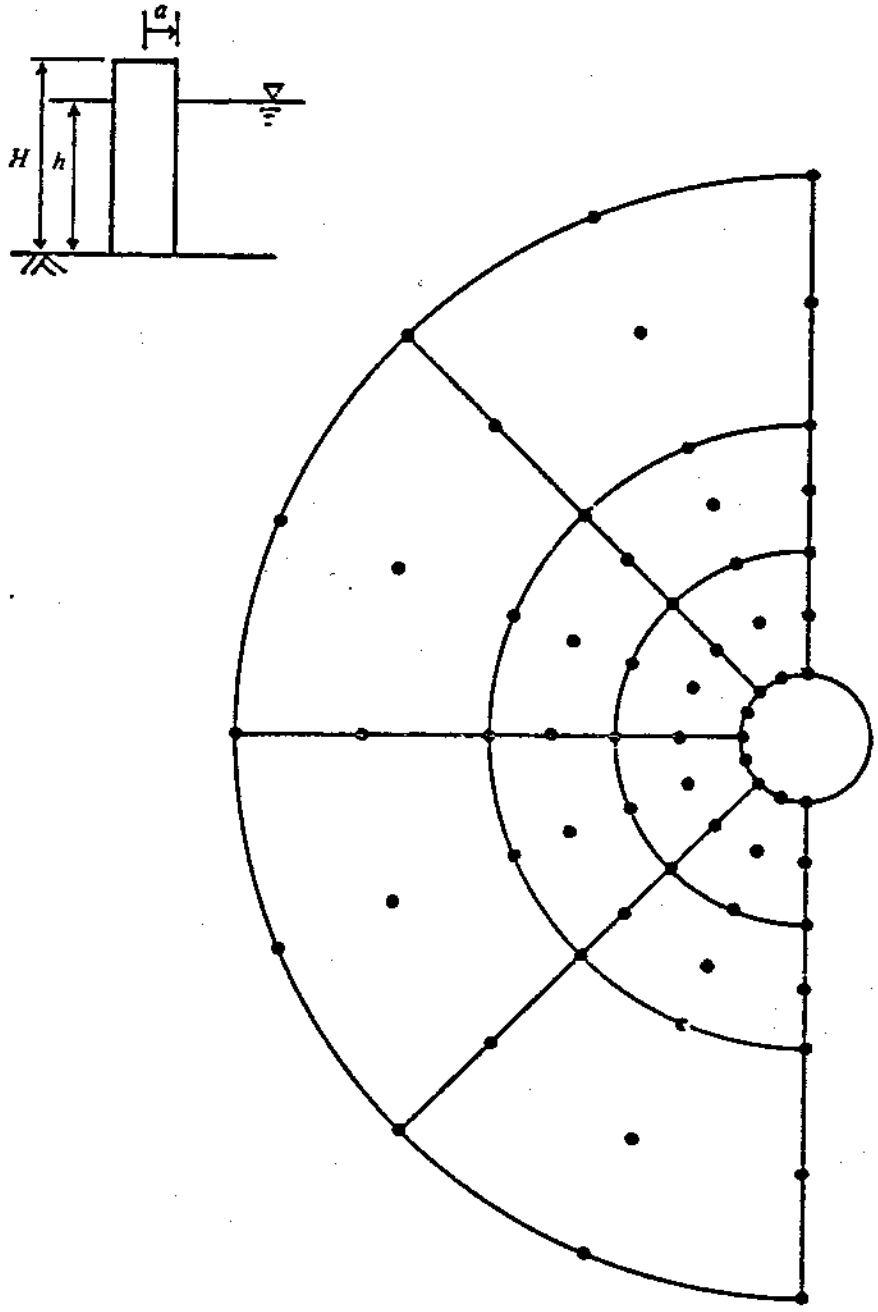

Figure 5.10 Finite Element Mesh in Example B

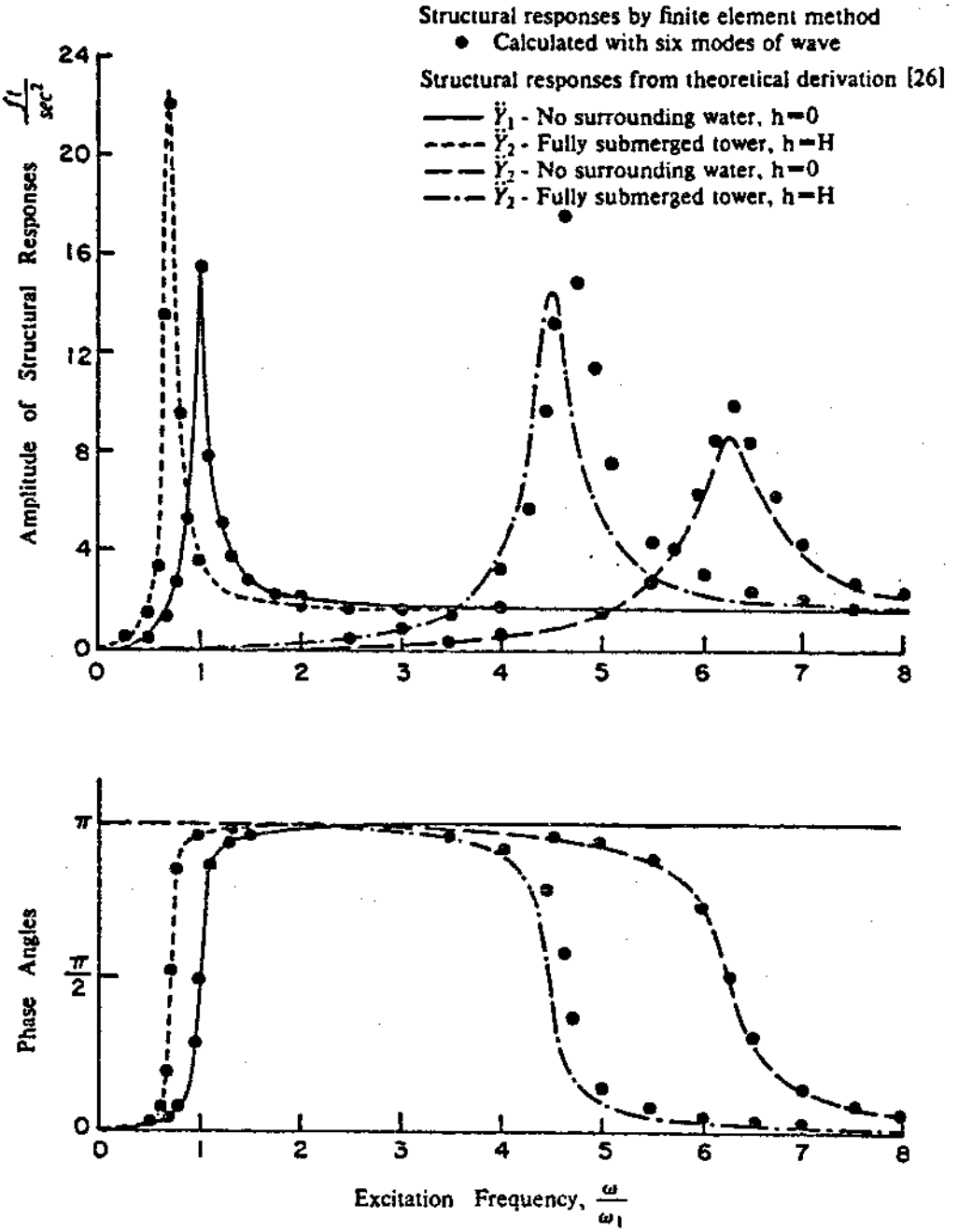

Figure 5.11 Comparison of Structural Responses

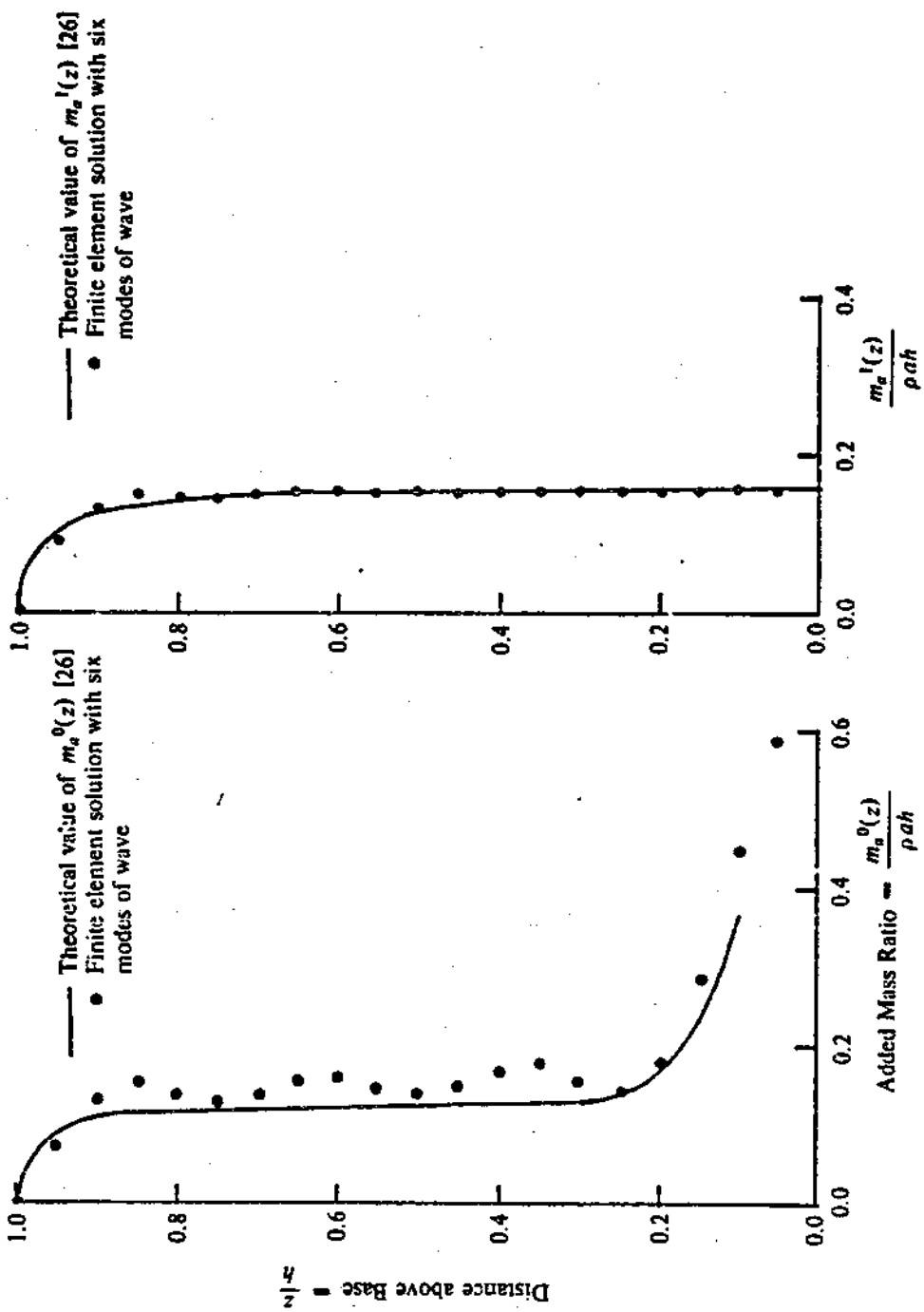

Figure 5.12 Comparison of Added Mass Distribution

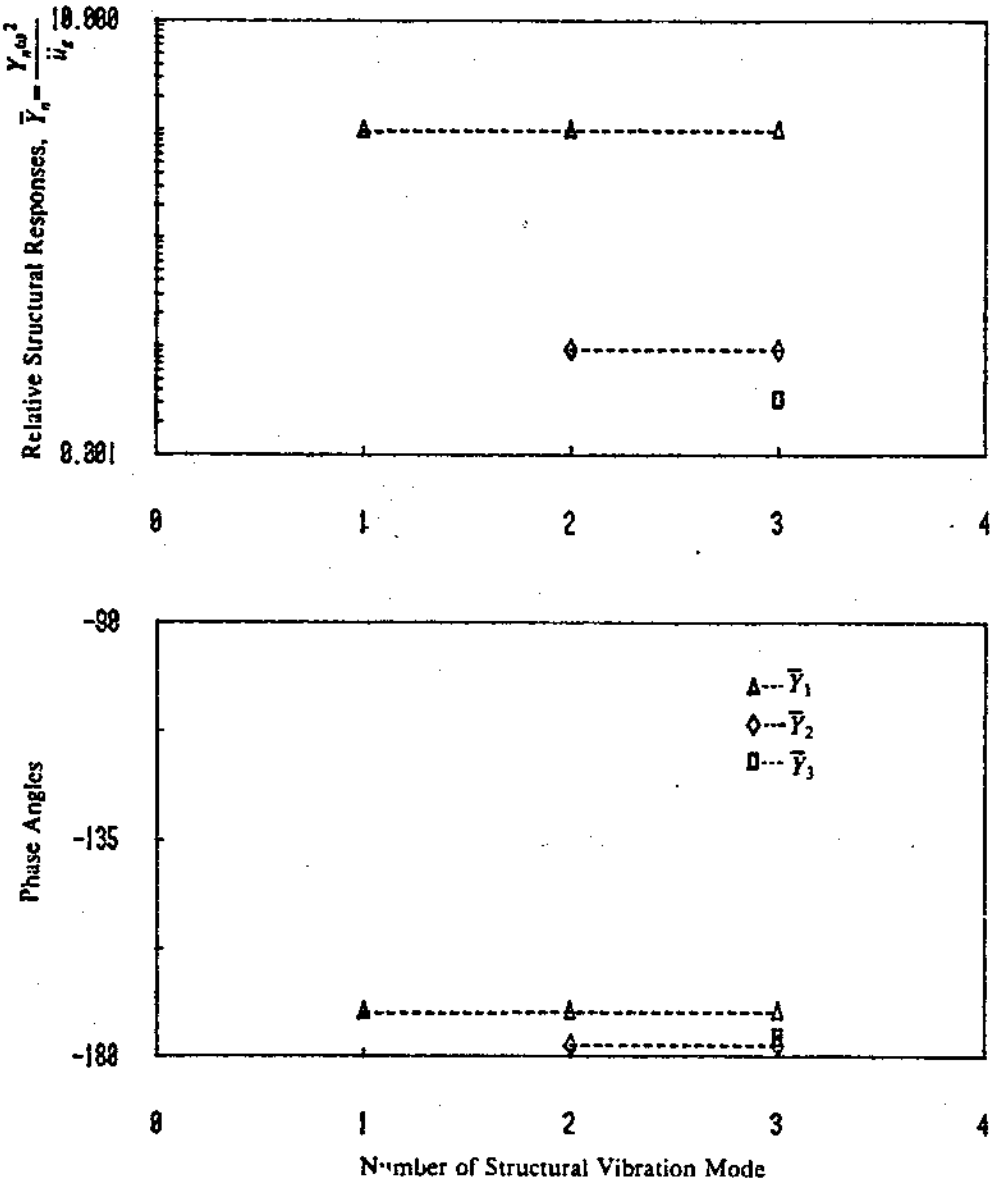

Figure 5.13 Convergence of Structural Responses ($\bar{d}$=1.333, $\frac{\omega}{\omega_1}$=0.616, $\frac{h}{H}$=1, *symmetry*)

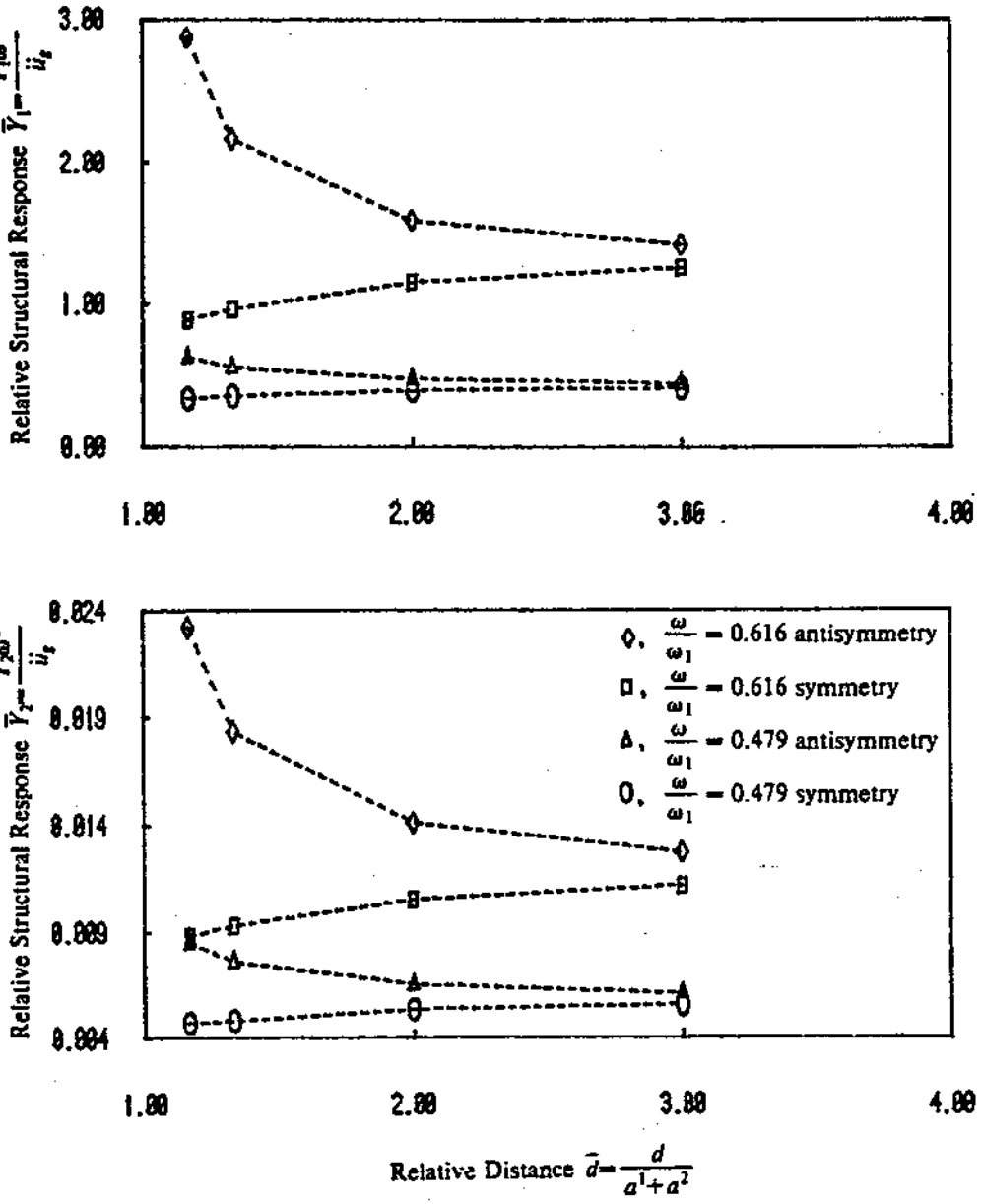

Figure 5.14 Decay of Structural Responses ($\frac{h}{H}$=1)

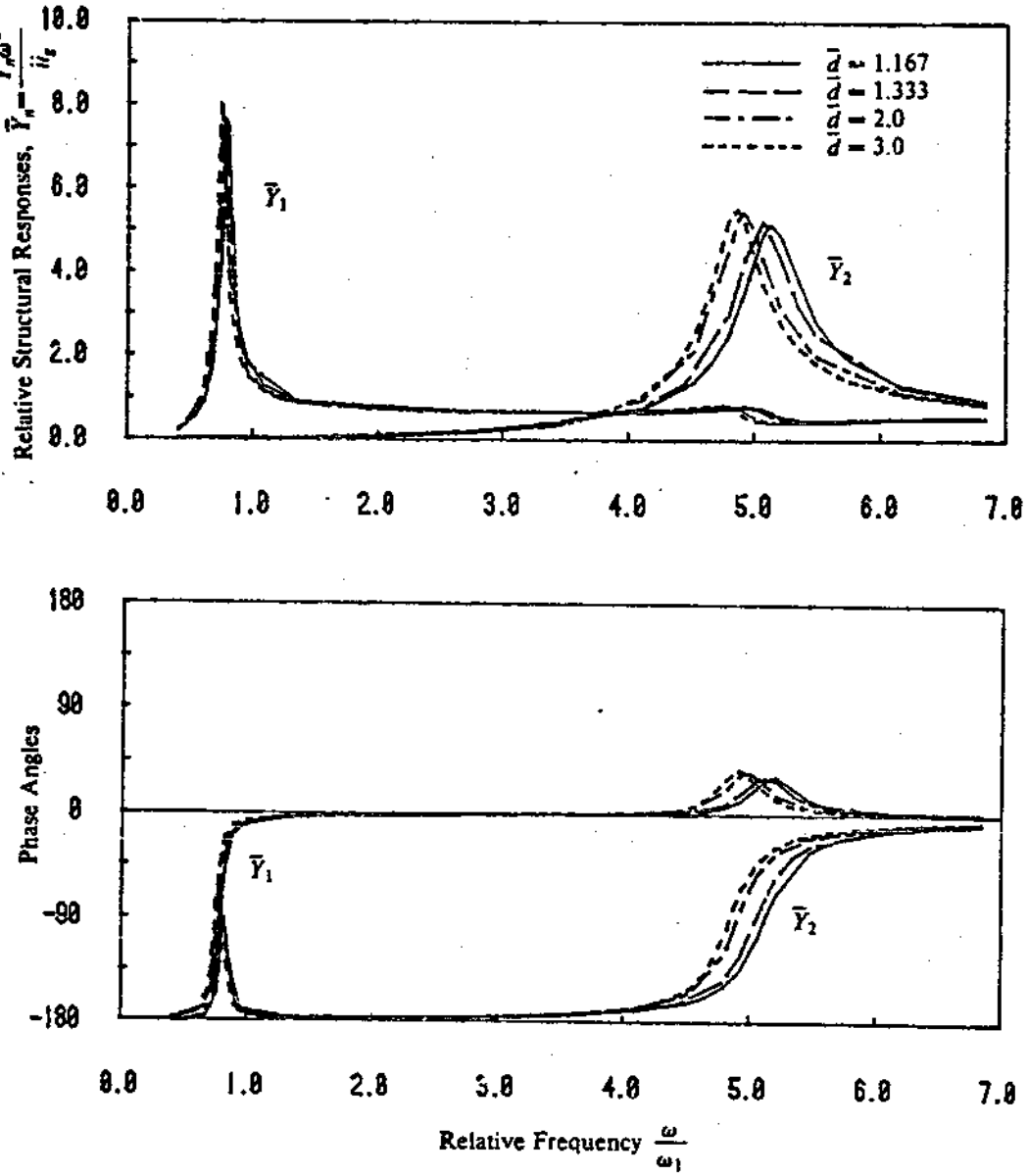

Figure 5.15 Symmetrical Structural Responses ($\frac{h}{H}$=1)

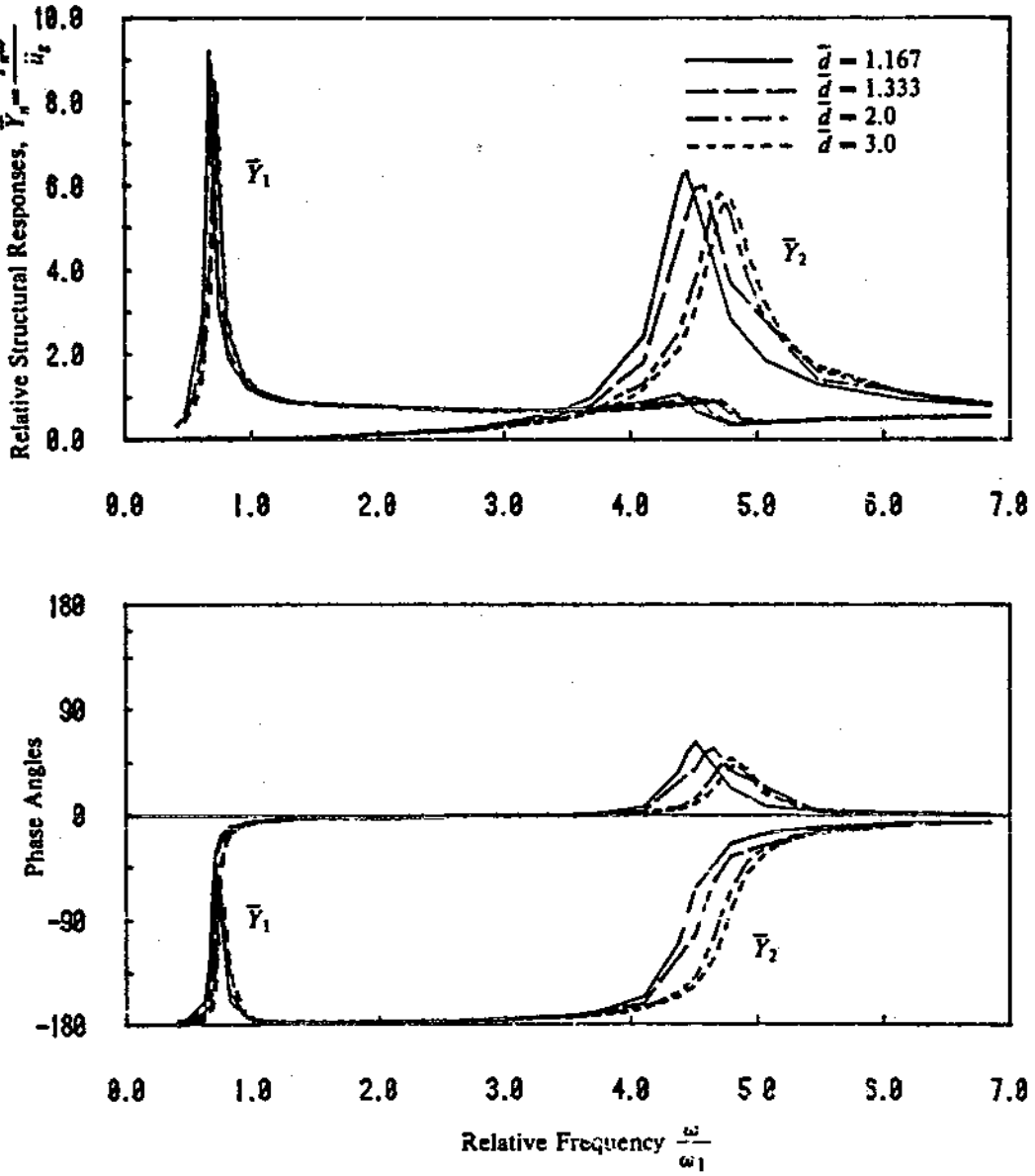

Figure 5.1c Antisymmetrical Structural Responses ($\frac{h}{H}$=1)

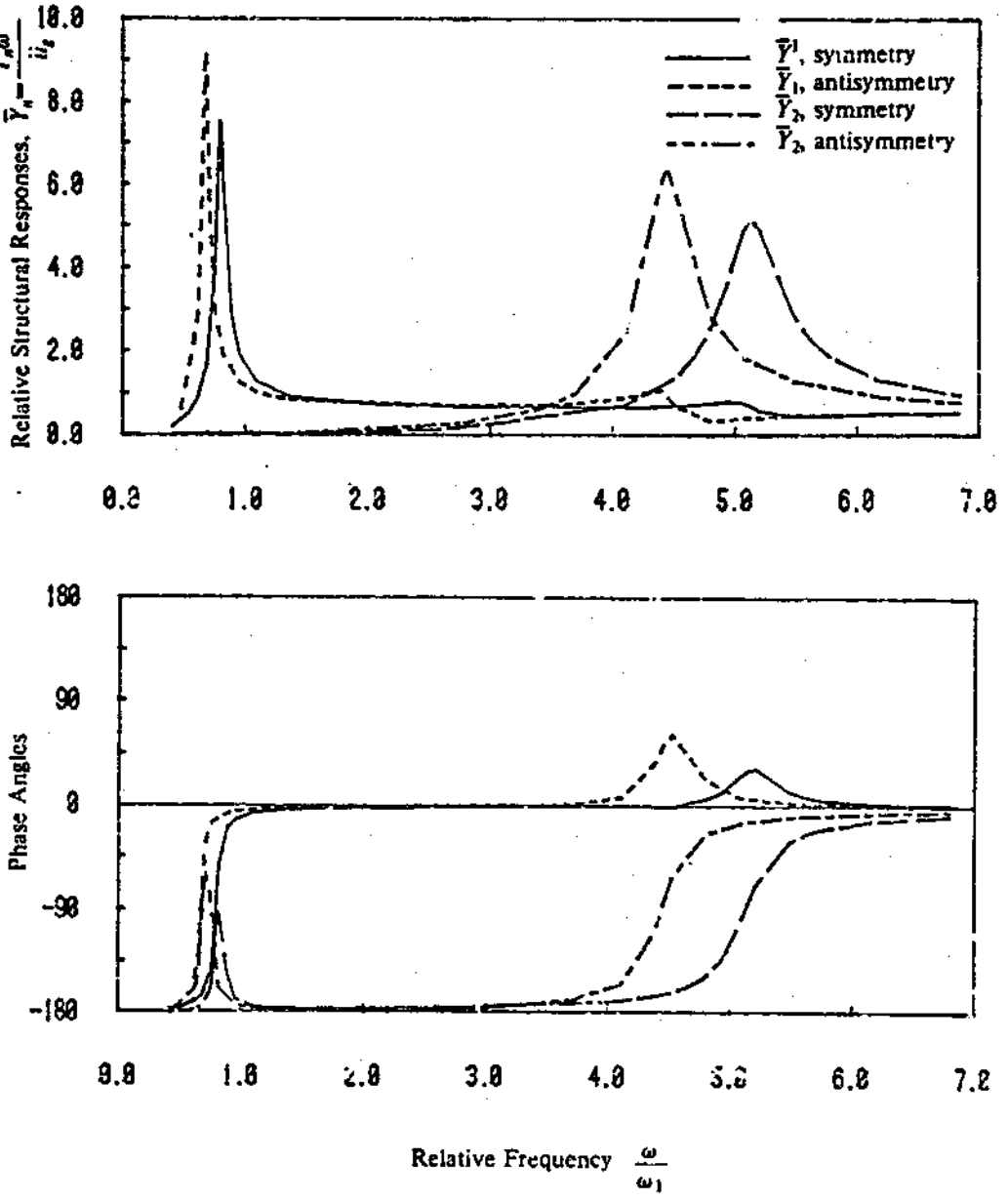

Figure 5.17 Structural Responses ($\bar{d}$=1.167, $\frac{h}{H}$=1)

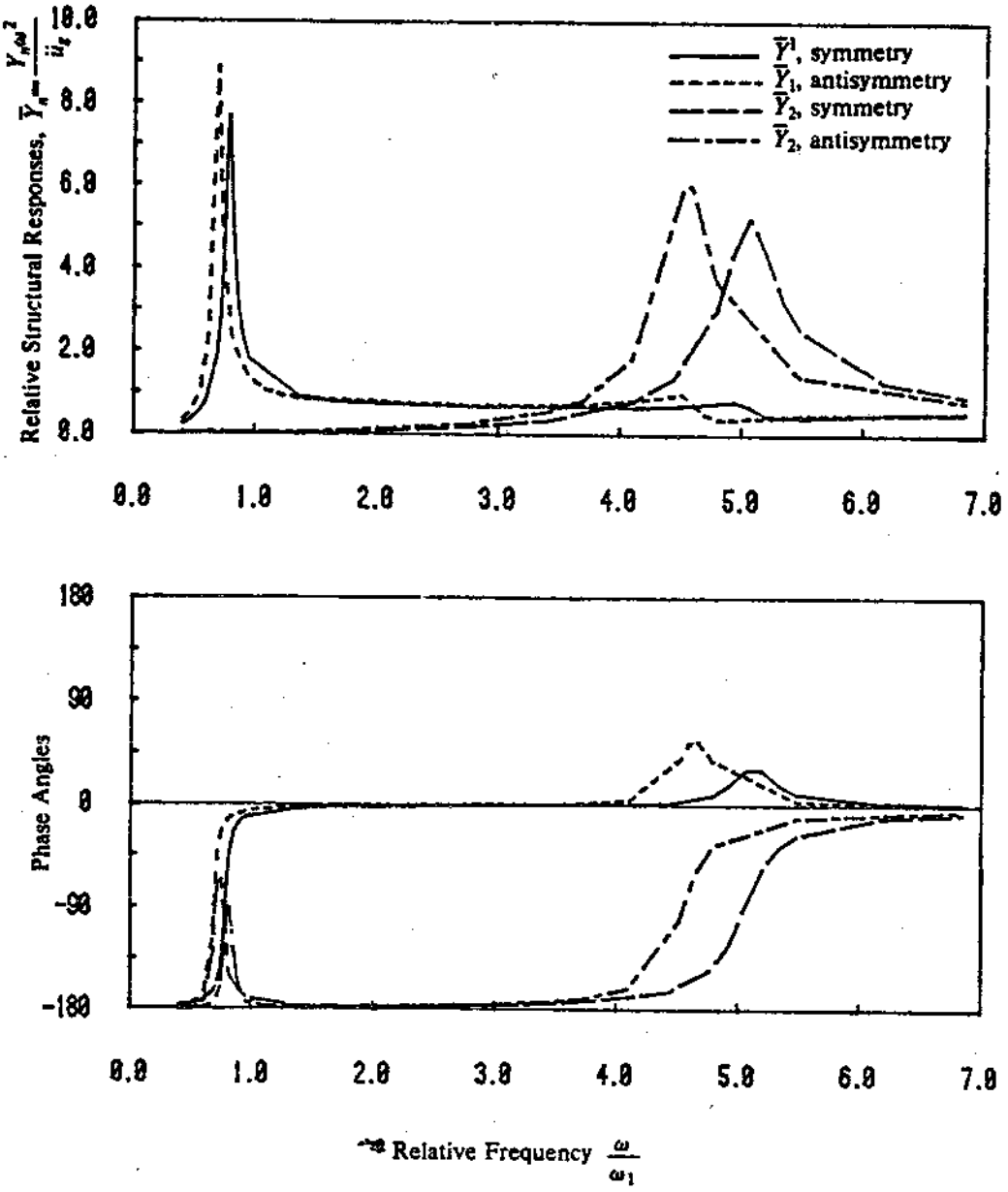

Figure 5.18 Structural Responses ($\bar{d}$=1.333, $\frac{h}{H}$=1)

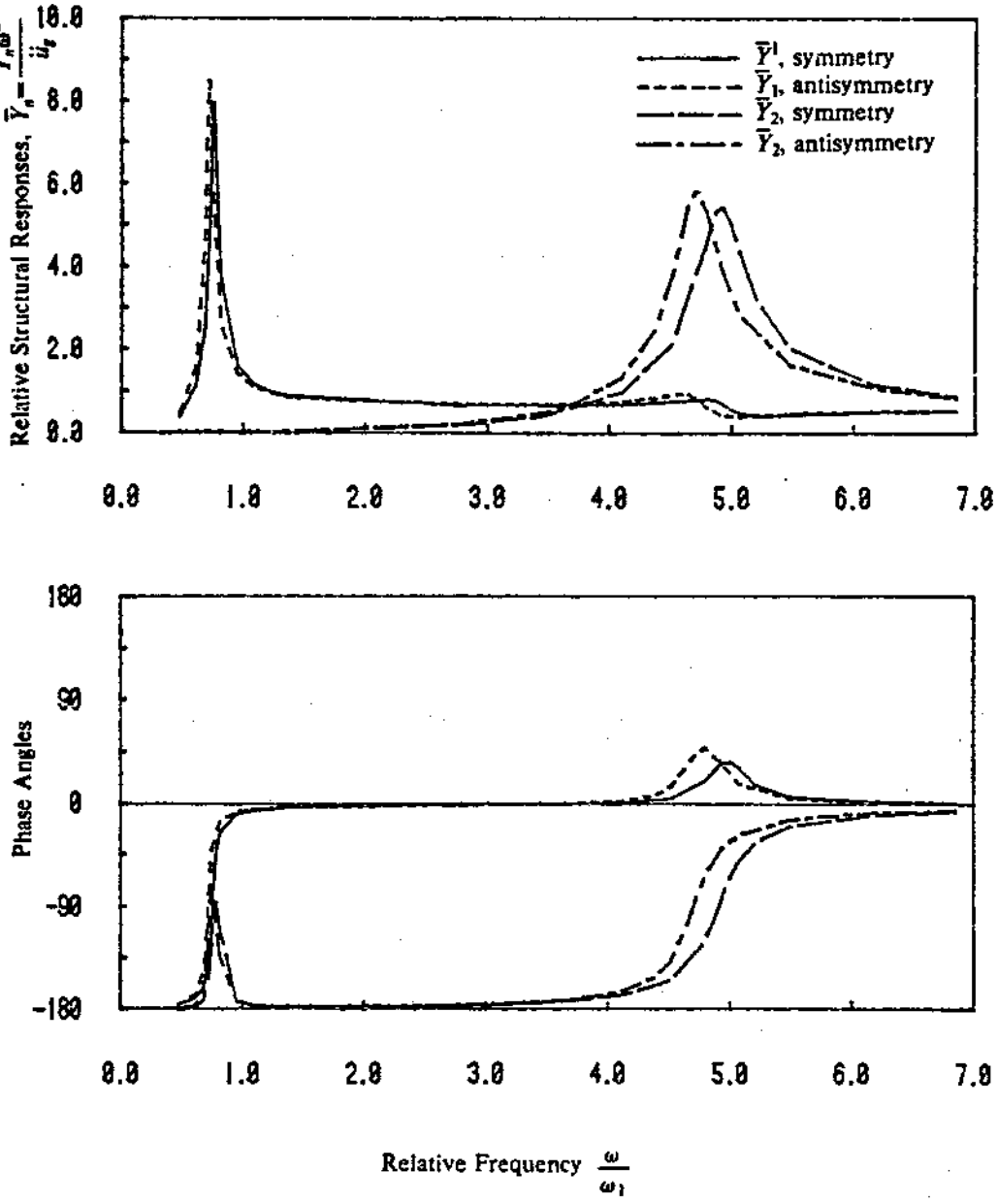

Figure 5.19 Structural Responses ($\bar{d}$=2.0, $\frac{h}{H}$=1)

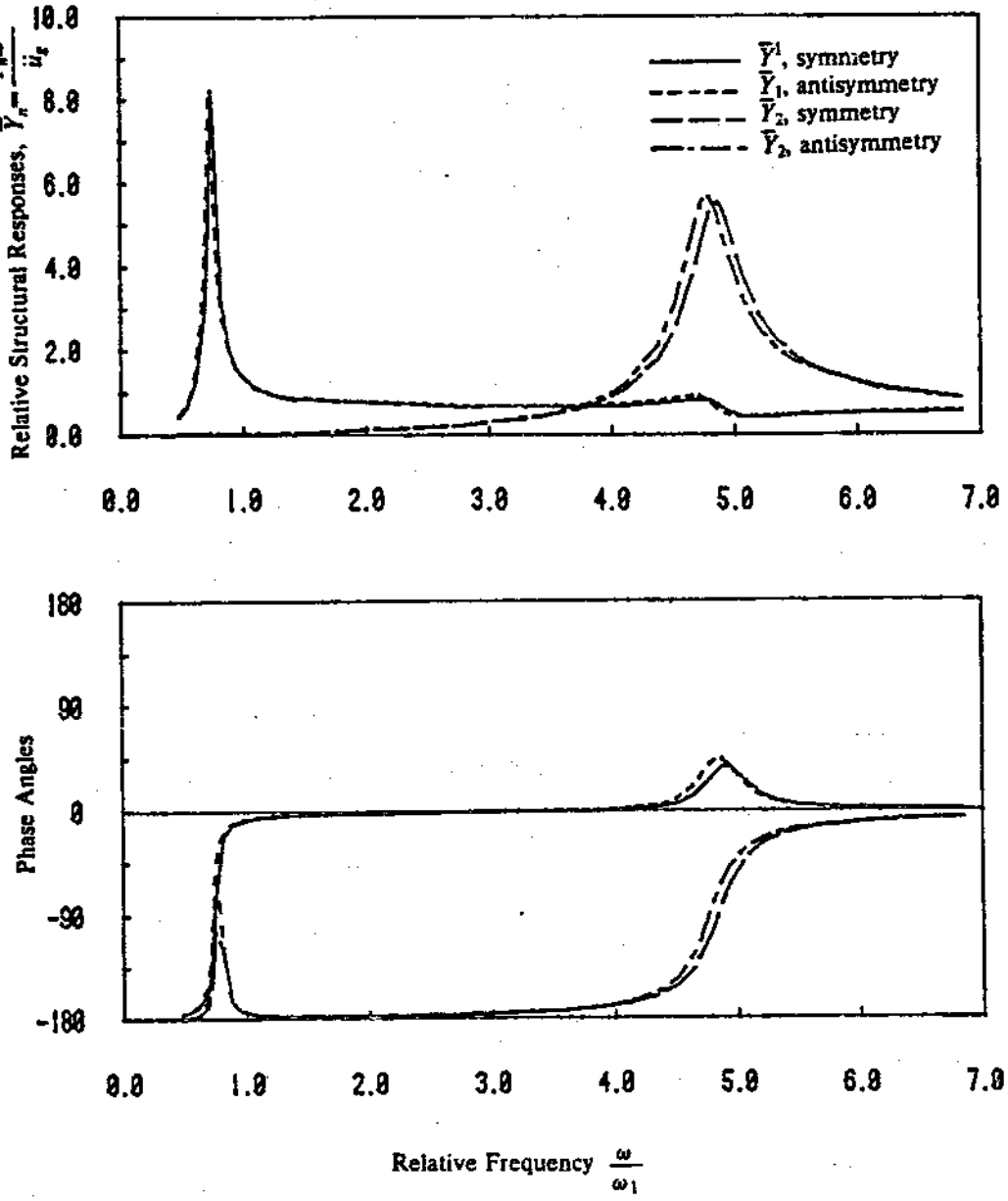

Figure 5.20 Structural Responses ($\bar{d}$=3.0, $\frac{h}{H}$=1)

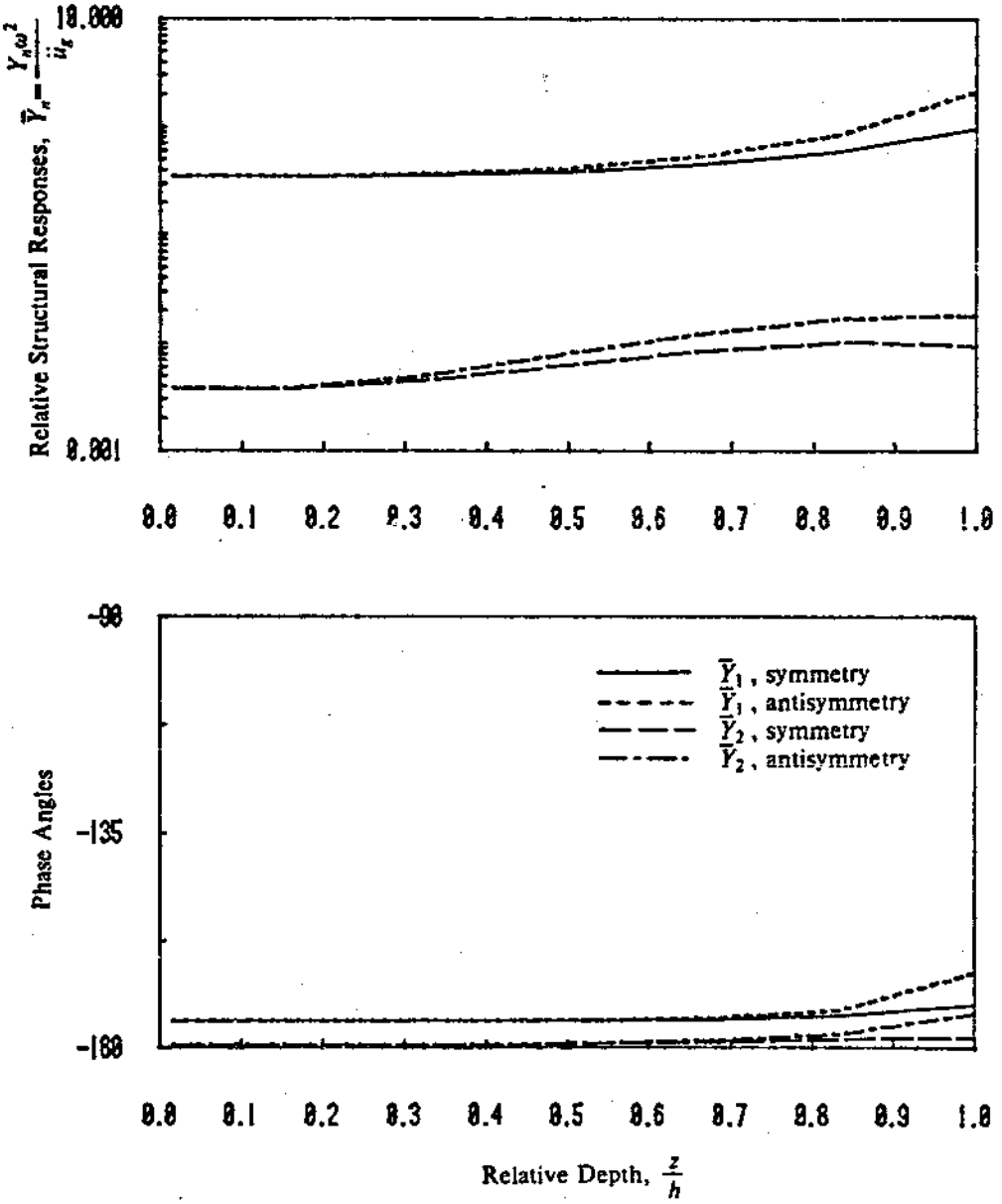

Figure 5.21 Structural Responses ($\bar{d}$=1.333, $\frac{\omega}{\omega_1}$=0.616)

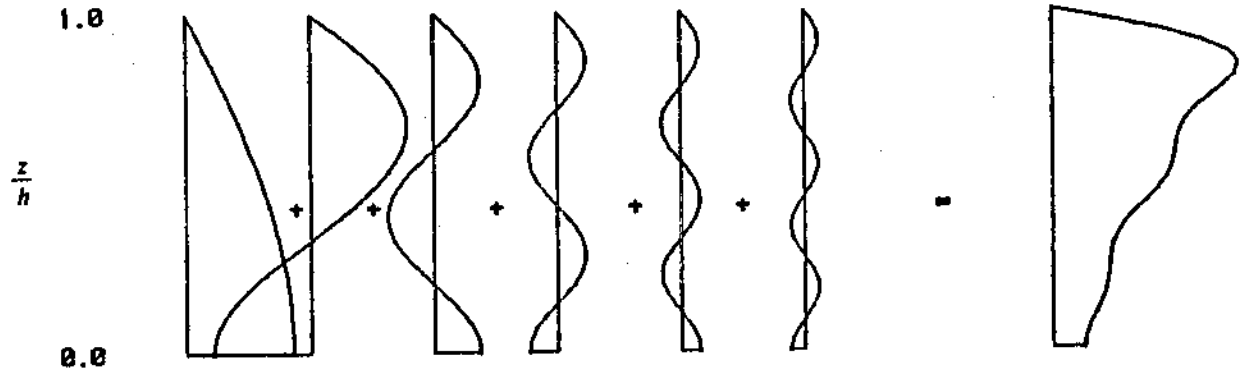

a. Re$\{\frac{p^J(z)}{\rho a h \ddot{u}_g}\}$

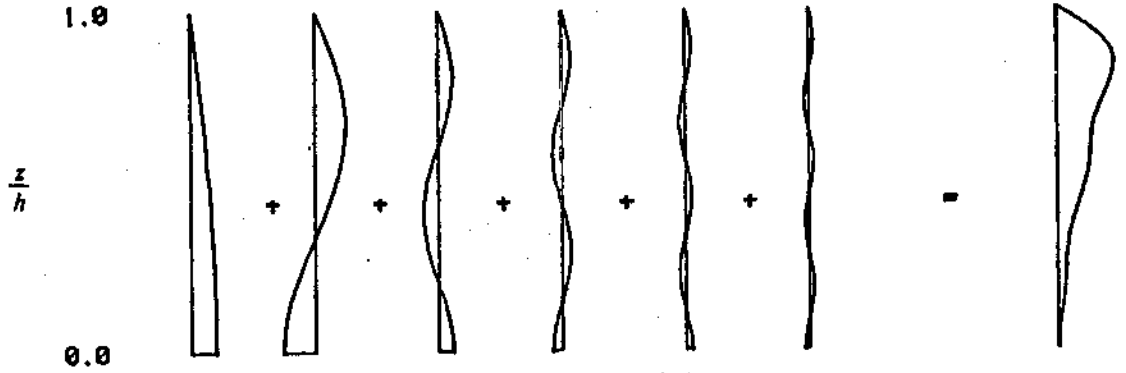

b. Im$\{\frac{p^J(z)}{\rho a h \ddot{u}_g}\}$

Figure 5.22 Hydrodynamic Forces Distribution ($\bar{d}$=1.167, $\frac{h}{H}$=1, $\frac{\omega}{\omega_1}$=0.616, *antisymmetry*)

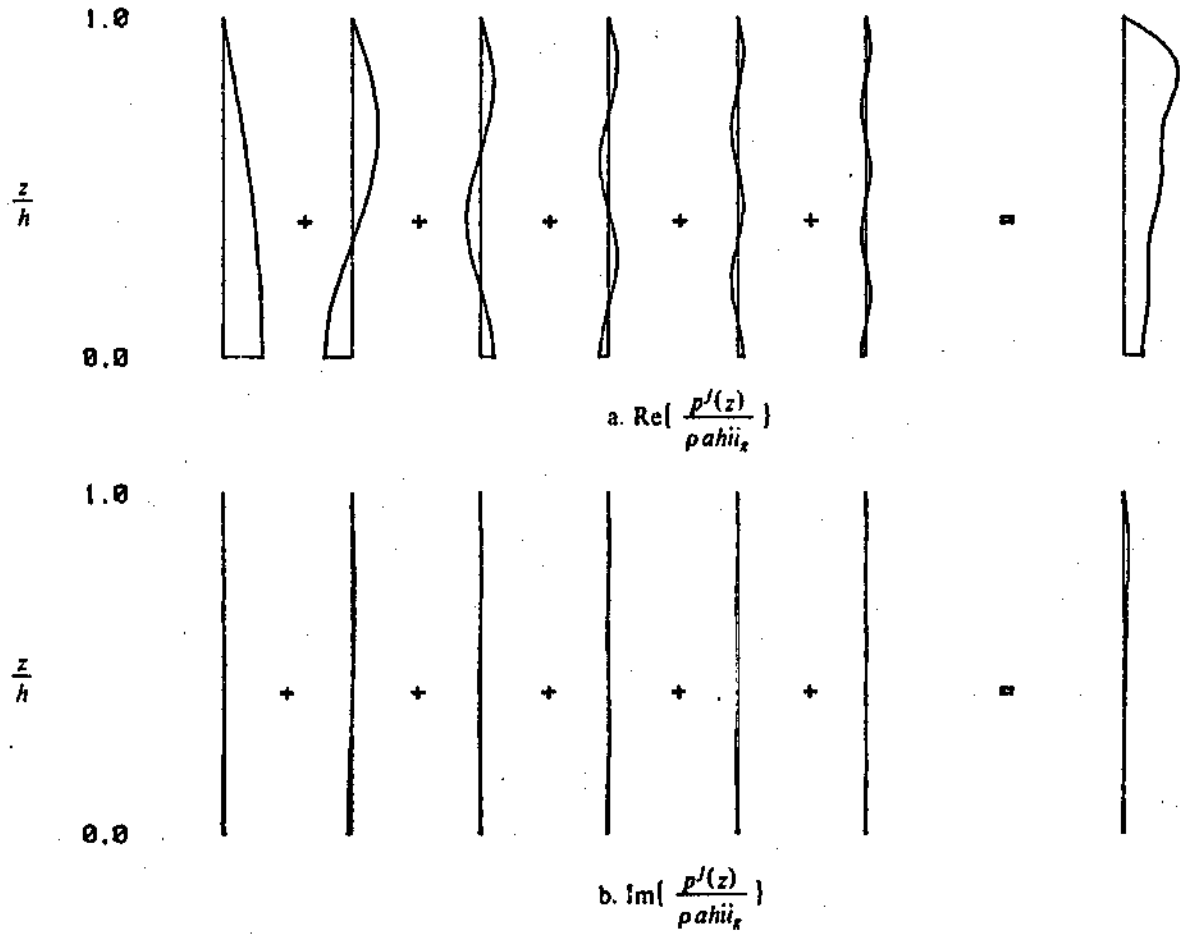

a. $\mathrm{Re}\{\frac{p^J(z)}{\rho a h i i_z}\}$

b. $\mathrm{Im}\{\frac{p^J(z)}{\rho a h i i_z}\}$

Figure 5.23 Hydrodynamic Forces Distribution ($\bar{d}$=1.167, $\frac{h}{H}$=1, $\frac{\omega}{\omega_1}$=0.616, *symmetry*)

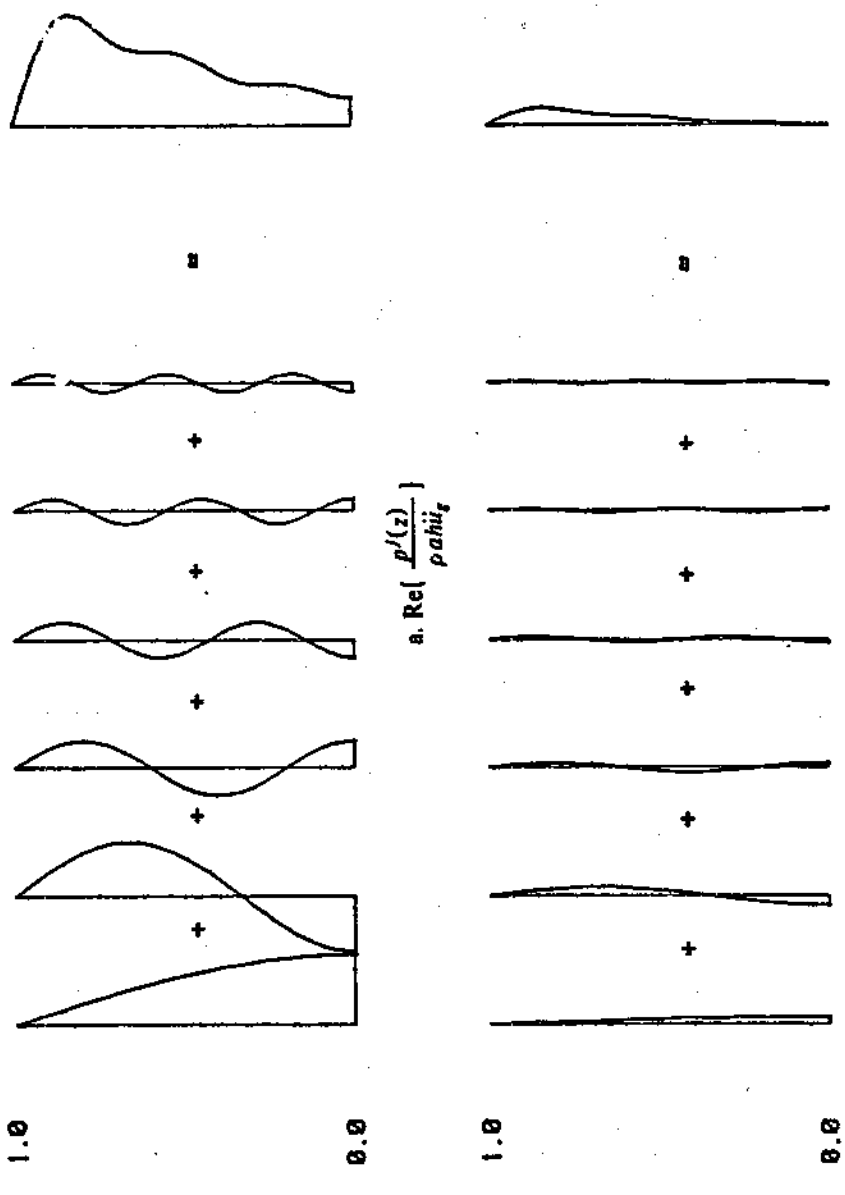

Figure 5.24 Hydrodynamic Forces Distribution ($\bar{d}$=3.0, $\frac{h}{H}$=1, $\frac{\omega}{\omega_1}$=0.616, *antisymmetry*)

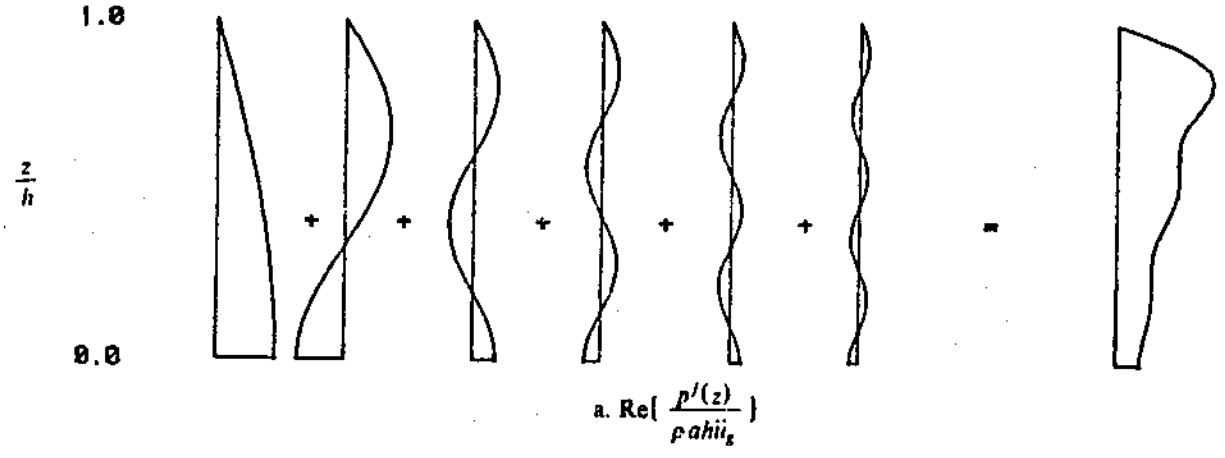

a. $\mathrm{Re}\{\frac{p^j(z)}{\rho a h i i_g}\}$

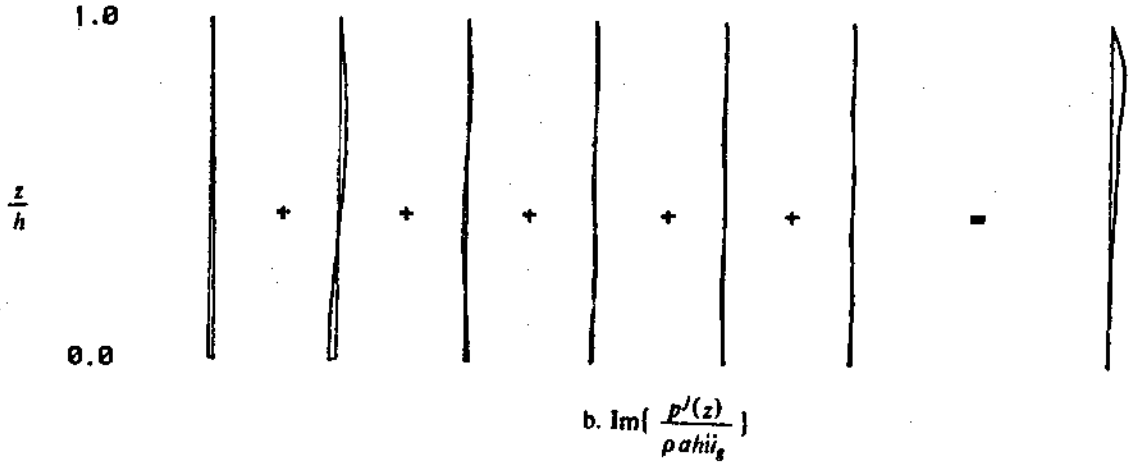

b. $\mathrm{Im}\{\frac{p^j(z)}{\rho a h i i_g}\}$

Figure 5.25 Hydrodynamic Forces Distribution ($\bar{d}$=3.0, $\frac{h}{H}$=1, $\frac{\omega}{\omega_1}$=0.616, *symmetry*)

Complex Amplitude of Hydrodynamic Forces ($\frac{p^j(z)}{\rho a h i i_z}$)				
Mode No.	$\bar{d} = 1.167$		$\bar{d} = 3.000$	
	Symmetry	Antisymmetry	Symmetry	Antisymmetry
1	0.219, 0.012	0.827, 0.193	0.334, 0.029	0.392, 0.039
2	-0.146,-0.016	-0.751,-0.244	-0.259,-0.039	-0.308,-0.051
3	0.074, 0.008	0.359, 0.115	0.134, 0.020	0.154, 0.025
4	-0.048,-0.005	-0.224,-0.072	-0.089,-0.013	-0.100,-0.017
5	0.034, 0.004	0.151, 0.049	0.063, 0.009	0.070, 0.012
6	-0.026,-0.003	-0.109,-0.035	-0.047,-0.007	-0.052,-0.009

Table 5.1 Complex Amplitude of Hydrodynamic Forces in Example C ($\frac{h}{H}$=1, $\frac{\omega}{\omega_1}$=0.616)

VI. CONCLUSIONS

According to the discussions in Chapters III, IV, and the examples in Chapter V, we have made the following conclusions:

1. An effective numerical procedure to investigate the hydrodynamic interaction between structures submerged in fluid induced by ground motion has been developed.
2. If the structures have uniform cross sections in the vertical direction, this boundary value problem can be reduced into two-dimensional one. Otherwise, a three-dimensional analysis is required for the non-axisymmetrical problem.
3. For high frequency ground excitation, the reduced boundary conditions are acceptable. However, a transmitting boundary and free surface condition should be considered for low frequency excitation such as incident waves.
4. In addition to the horizontal ground motion which has been considered in previous chapters, the vertical ground motion should also be taken into consideration. For a local earthquake, the effect of pressure waves which are transmitted from neighboring ground to the structure through water has not been well understood.
5. The agreement of the results from the experiments of physical model on an earthquake simulator and the numerical analysis has been shown in Example A in Chapter V. However, some minor discrepancies are observed. They may be caused by the following reasons: (1) the linearization of the boundary value problem in numerical analysis such that the hydrodynamic forces, which are along the center line connecting the centers of the cylinders and are induced by the ground motion perpendicular to this center line, are neglected, (2) the square basin being constructed to simulate the unbounded fluid domain such that the boundary conditions of experiments and numerical model are not exactly the same, (3) the uncertainties in laboratory works including the experimental equipments, techniques, and data reduction [51].

6. The numerical analysis to find the hydrodynamic forces on a non-axisymmetrical structure can also be applied to an axisymmetrical structure. For solving the structural responses of an axisymmetrical structure, it shows that the results from the theoretical analysis [26] and the numerical analsis are of great similarity. As the number of wave modes increases, the numerical analysis results approach to the theoretical analysis results asymptotically.

7. When the distance between cylinders is small, the structural responses induced by ground motion decrease in the symmetrical case and increase in the antisymmetrical case. Comparing to the structural responses when two cylinders are far from each other so that the interaction is no longer significant, a 50 percent variation for both symmetrical and antisymmetrical cases is illustrated within the examples in Chapter V. Generally speaking, the hydrodynamic interaction is negligible as the relative distance* exceeds 4; while it becomes relevant as the relative distance is less than 2. This phenomenon depends on the characteristics of structures, water depth, amplitude and frequency of ground excitation and the relative distance between cylinders.

8. In designing the offshore structure with two cylindrical legs, it is suggested that the center line of the cylinders should coincide with the direction of the expected major earthquake ground motion in order to decrease the interacted hydrodynamic forces.

9. For structures with more than two legs, the number of cylinders in previous chapters should be reset accordingly. The distribution of hydrodynamic pressures will become much more complicated and the interaction is expected to be significant, however, to the extent that can not be predicted from the examples in Chapter V.

* Relative distance is defined as the ratio of the distance between the centers of two cylinders to the sum of the [illegible] cylinders.

10. In order to obtain more realistic results, the cylinder with cylindrical shell should be considered. The conventional finite element method can be applied to the structures.

VII. REFERENCES

1. Sarpkaya, T., Isaacson, M., "Mechanics of Wave Forces on Offshore Structures", Van Nostrand Reinhold Co. 1981.
2. Shaw, T. L., editor, "Mechanics of Wave-Induced Forces on Cylinders", Pitman, England, 1979.
3. Lamb, H., "Hydrodynamics", 6 ed., Dover, 1945.
4. Milne-Thomson, L. M., "Theoretical Hydrodynamics", 5 ed., MacMillan, 1968.
5. Stoker, J. J., "Water Waves: The Mathematical The ry with Application", Interscience Publishers, 1957.
6. Morison, J. R., O'Brien, M. P., Johnson, J. W., Schaaf, S. A., "The Force Exerted by Surface Wave on Piles", Petroleum Transactions, AIME, Vol. 189, 1950.
7. Penzien, J., Tseng, W. S., "Seismic Analysis of Gravity Platforms Including Soil-Structure Interaction Effects", Offshore Technology Conference, OTC paper No. 2674, 1976.
8. Penzien, J., "Structural Dynamics of Fixed Offshore Structures", Behavior of Offshore Structures, Norwegian Institute of Technology, 1976.
9. Penzien, J., Tseng, W. S., "Three-Dimensional Dynamic Analysis of Fixed Offshore Platform", in Numerical Methods in Offshore Engineering, edited by Zienkiewicz, O. C., et. al., John Wiley and Sons, 1978.
10. Wade, B. G., Dwyer, M., "On the Application of Morison's Equation to Fixed Offshore Platforms", Offshore Tech. Conf., OTC paper No. 2723, 1976.
11. Keulegan, G. H., Carpenter, L. H., "Forces on Cylinders and Plates in A Oscillating Fluid", J. Research National Bureau of Standards, Vol. 60, No. 5, 1958.

12. McCamy, R. C., Fuchs, R. A., "Wave Forces on Piles: A Diffraction Theory", Beach Erosion Board, Technical Memorandum, No. 69, 1954.

13. Wehausen, J. V., Laitone, E. V., "Surface Waves", Encyclopedia of Physics, Vol. 9, Springer-Verlag, Berlin, 1960, pp. 446-778.

14. John, F., "On the Motion of Floating Bodies: II", Communication on Pure and Applied Mathematics, 1950, pp. 45-101.

15. Kim, W. D., "On The Harmonic Oscillations of a Rigid Body on a Free Surface", J. Fluid Mech., Vol. 21, 1965, pp. 427-451.

16. Black, J. L., Mei, C. C., Bray, M. C. G., "Radiation and Scattering of Water Waves by Rigid Bodies", J. Fluid Mech., Vol. 16, 1971, pp. 451-472.

17. Garrison, C. J., Rao, S. V., "Interaction of Waves with Submerged Objects", J. Waterways and Harbors Div., ASCE, Vol. 97, WW2, 1971, pp. 259-277.

18. Garrison, C. J., Chow, R. Y., "Wave Forces on Submerged Bodies", J. Waterways and Harbors Div. ASCE, Vol. 98, WW 3, 1972, pp. 375-392.

19. Garrison, C. J., "Hydrodynamics of Large Objects in the Sea: Part I. Hydrodynamic Analysis", J. Hydronautics, AIAA, Vol. 8, 1974, pp. 5-12.

20. Garrison, C. J., "Hydrodynamic Loading of Large Offshore Structures: Three-Dimensional Source Distribution Methods", in Numerical Method in Offshore Engineering, edited by Zienkiewicz, O. C., et. al., John Wiley and Sons, 1978.

21. Isaacson, M. de St. Q., "Wave Induced Forces in the Diffraction Regime", in Mechanics of Wave-Induced Forces on Structures, edited by Shaw, T. L., Pitman, England, 1979, pp. 68-89.

22. Webster, W. C., "The Flow About Arbitrary Three-Dimensional Smooth Bodies", J. Ship Research, Vol. 19, 1975, pp. 206-218.

23. Kioka, W., "A Green Function Method for Wave Interaction with a Submerged Body". Earthquake Engineering Research Center, Report No. 80-11, U. C. Berkeley, 1980.

24. Zienkiewicz, O. C., Irons, B. M., Nath, B., "Natural Frequencies of Complex Free or Submerged Structures by the Finite Element Method", Symp. Vibration in Civil Engng., London, 1965.

25. Zienkiewicz, O. C., Newton, R. E., "Coupled Vibrations in a Structure Submerged in a Compressible Fluid", Int. Symp. Finite Element Tech., Stuttgart, 1969, pp. 359-379.

26. Liaw, C. Y., Chopra, A. K., "Earthquake Response of Axisymmetric Tower Structures Surrounded by Water", Earthquake Engineering Research Center, Report No. 73-25, U. C. Berkeley, 1973.

27. Bai, K. J., Yeung, R. W., "Numerical Solutions to Free Surface Flow Problems", Tenth Symp. Naval Hydrodynamics, Dept. of Navy, ACR-204, 1974, pp. 609-947.

28. Bai, K. J., "A Localized Finite Element Method for the Uniform Flow Problem with a Free Surface", Proc. First Int. Conf. Num. Ship Hydro. David Taylor Naval Ship R&D Center, Bethesda, 1975.

29. Mei. C. C., "Numerical Methods in Water-Wave Diffraction and Radiation", Ann. Rev. Fluid Mech. V. 10, 1978, pp. 393-416.

30. Taylor, R. E., Zietsman, J., "A Comparison of Localized Finite Element Formulations for Two-Dimensional Wave Diffraction and Radiation Problem", Int. J. Num. Meth. Engng., V. 17, 1981, pp. 1355-84.

31. Chen, H. S., Mei, C. C., "Calculations of Two-Dimensional Ship Waves by a Hybrid Element Method Based on Variational Principles", Proc. First Int. Conf. Num. Ship Hydro., David Taylor Naval Ship R$D Center, Bethesda, 1975, pp. 95-111.

32. Mei, C. C., Chen, H. S., "A Hybrid Element Method for Steady Linearized Free Surface Flows", Int. J. Num. Meth. Engng., Vol. 10, 1976, pp. 1153-1175.

33. Bai, K. J., "A Localized Finite-Element Method for Steady Three-Dimensional Free-Surface Problem", Proc. Second Int. Conf. Num. Ship Hydro., U. C. Berkeley, 1977, pp. 78-87.

34. Hall, J. F., Chopra, A. K., "Dynamic Response of Embankment Concrete-Gravity and Arch Dams Including Hydrodynamic Interaction", Earthquake Engineering Research Center, Report No. 80-39, U. C. Berkeley, 1980.

35. Nilrat, F., "Hydrodynamic Pressure and Added Mass for Axisymmetric Bodies", Earthquake Engineering Research Center, Report No. 80-12, U. C. Berkeley, 1980.

36. Aranha, J. A., Mei, C. C., Yue, D. K. P., "Some Properties of a Hybrid Element Method for Water Waves", Int. J. Num. Meth. Engng., Vol. 14, 1979, pp. 1627-1641.

37. Zienkiewicz, O. C., Bettess, P., "Diffraction and Refraction of Surface Waves Using Finite and Infinite Elements", Int. J. Num. Meth. Engng., Vol. 11, 1977, pp. 1271-1290.

38. Bettess, P., "Infinite Elements", Int. J. Num. Meth. Engng., Vol. 11, 1977, pp. 54-64.

39. Spring, B. W., Monkmeyer, P. L., "Interaction of Plane Waves with a Row of Cylinders", Proc. Third Specialty Conf. Civil Engng. in the Ocean, ASCE, Newark, 1975.

40. Spring, B. W., Monkmeyer, P. L., "Interaction of Plane Waves with Vertical Cylinders", Proc. 14th Int. Conf. Coastal Engng. ASCE, Denmark, 1974, pp. 1828-1847.

41. Yamamoto, T., Nath, J. H., "Hydrodynamic Forces on Group of Cylinders", Offshore Tech. Conf., OTC Paper No. 2499, 1976, pp. 759-768.

42. Yamamoto, T., "Hydrodynamic Forces on Multiple Circular Cylinders", J. Hydraulic Div. ASCE, Vol. 102, HY9, 1976, pp. 1193-1210.

43. Isaacson, M. de St. Q., "Interference Effects Between Large Cylinders in Waves", Offshore Tech. Conf., OTC Paper No. 3067, 1978, pp. 185-192.

44. Isaacson, M. de St. Q., "Vertical Cylinders of Arbitrary Section in Waves", J. Waterway Port Coastal and Ocean Div., ASCE, Vol. 104, WW4, 1978, pp. 309-324.

45. Chakrabarti, S. K., "Wave Forces on Multiple Vertical Cylinders", J. Waterway Port Coastal and Ocean Div. ASCE, Vol. 104, WW2, 1978, pp. 147-161.

46. O'Brien, M. P., Morison, J. R., "The Forces Exerted by Waves on Objects", Fluid Mechanic Lab Rep. No. NR 083 008, Wave Investigation Technical Report, U. C. Berkeley, 1950.

47. Wiegel, R. L., "Oceanographical Engineering", Ch. 11, Wave Forces, Prentice Hall, 1964.

48. Bea, R. G., Lai, N. W., "Hydrodynamic Loading on Offshore Platforms", Offshore Tech. Conf., OTC Paper No. 3064, 1978.

49. Sarpkaya, T., "In-Line and Transverse Forces on Cylinders in Oscillatory Flow at High Reynolds Numbers", J. of Ship Research, Vol. 21, No. 4, 1977.

50. Wehausen, J. V. "Methods for Boundary-Value Problems in Free Surface Flows", Report 4622, David W. Taylor Naval Ship RSD Center, 1974.

51. Ansari, G. R., "A Laboratory Study of Submerged, Multi-body System in Earthquake", Ph.D. Thesis, Dept. Civil Engineering, U. C. Berkeley, 1982. (in preparation)

52. Bidde, D. D., "Wave Forces on a Circular Pile due to Eddy Shedding", Ph.D. Thesis, Dept. Civil Engineering, U. C. Berkeley, 1970.

APPENDIX A

REDUCED TWO-DIMENSIONAL PROBLEM

The two-dimensional boundary value problem reduced from three-dimensional Laplace's equation has been discussed by Wehausen [50]. Here, we will present the problem under the following two special cases:

i) low frequency excitation with linear wave theory,

ii) high frequency excitation without considering the gravity wave on the water surface.

1. Three-Dimensional Problem

For a three-dimensional problem, the Laplace's equation of hydrodynamic pressure in frequency domain governs. Thus, we have the following expression

$$\frac{\partial^2 p}{\partial x^2} + \frac{\partial^2 p}{\partial y^2} + \frac{\partial^2 p}{\partial z^2} = 0 \tag{A.1}$$

a. Boundary Conditions for Case i

The boundary condition at the bottom is given by

$$\frac{\partial p}{\partial z}(x,y,0) = 0 \tag{A.2}$$

The linear water surface condition is

$$\frac{\partial p}{\partial z}(x,y,h) - \frac{\omega^2}{g} p(x,y,h) = 0 \tag{A.3}$$

And the radiation condition at the far field is

$$\lim_{r\to\infty} r^{1/2}\left(\frac{\partial p}{\partial r}(r,z) - ikp(r,z)\right) = 0 \tag{A.4}$$

where $r = (x^2+y^2)^{1/2}$ and k comes from the dispersion relation

$$\omega^2 = kg \tanh kh \tag{A.5}$$

b. Boundary Conditions for Case ii

At the bottom we have the boundary condition

$$\frac{\partial p}{\partial z}(x,y,0) = 0 \tag{A.6}$$

The simplified free water surface condition is

$$p(x,y,h) = 0 \tag{A.7}$$

The condition at the far field becomes

$$\frac{\partial p}{\partial n}(r,z) = 0 \tag{A.8}$$

where n is normal to the boundary.

2. Separation of Variables

If the structure has uniform cross section, the three-dimensional problem can be reduced by the separation of variables,

$$p(x,y,z) = \bar{p}(x,y)\ \bar{f}(z) \tag{A.9}$$

Thus, Eq. (A.1) can be rewitten as

$$\frac{\nabla^2 \bar{p}(x,y)}{\bar{p}(x,y)} = -\frac{\bar{f}''(z)}{\bar{f}(z)} = \lambda \tag{A.10}$$

For the case of low frequency excitation, the boundary conditions (A.2) and (A.3) become

$$\frac{d\bar{f}}{dz}(0) = 0 \tag{A.11}$$

and

$$\frac{d\bar{f}}{dz}(h) - \frac{\omega^2}{g}\bar{f}(h) = 0 \tag{A.12}$$

For the case of high frequency excitation, the boundary conditions (A.5) and (A.6) become

$$\frac{d\bar{f}}{dz}(0) = 0 \tag{A.13}$$

and

$$\bar{f}(h) = 0 \tag{A.14}$$

a. If $\lambda = -k^2 < 0$

In this case, Eq. (A.10) becomes

$$\frac{d^2\bar{f}}{dz^2}(z) - k^2\bar{f}(z) = 0 \tag{A.15}$$

Providing the boundary conditions (A.11) and (A.12) for case i to Eq. (A.15), we get

$$\bar{f}(z) = c \cosh kz \tag{A.16}$$

with

$$\omega^2 = kg \tanh kh \tag{A.5}$$

where $c = 2c_1 = 2c_2$.

Similarly, substituting the boundary conditions (A.13) and (A.14) for case ii into Eq. (A.15), we obtain

$$\bar{f}(z) = 0 \tag{A.17}$$

Since the hydrodynamic pressure is not equal to zero in water, the assumption that $\lambda = -k^2 < 0$ does not apply to the case of high frequency excitation.

b. If $\lambda = k^2 > 0$

In this case, Eq. (A.10) becomes

$$\frac{d^2\bar{f}}{dz^2}(z) + k^2\bar{f}(z) = 0 \tag{A.18}$$

Substituting boundary conditions (A.11) and (A.12) for case i into Eq. (A.18), we get

$$\bar{f}(z) = c_3 \cos kz \tag{A.19}$$

with

$$\omega^2 = -kg \tan kh \tag{A.20}$$

Similarly, substituting the boundary conditions (A.13) and (A.14) for case ii into Eq. Eq. (A.18), we can find

$$k_i = \frac{(i-\frac{1}{2})\pi}{h} \quad \text{for } i \geq 1 \tag{A.21}$$

3. Two-Dimensional Problem

a. Case i of Low Frequency Excitation

From Eqs. (A.10) and (A.16), the following equation is obtained:

$$\nabla^2\bar{p}_0(x,y) + k_0^2\bar{p}_0(x,y) = 0 \tag{A.22}$$

with

$$p_0(x,y,z) = \bar{p}_0(x,y)\cosh k_0 z \tag{A.23}$$

where k_0 is given by the dispersion relation

$$\omega^2 = k_0 g \tanh k_0 h \tag{A.5}$$

From Eqs. (A.10), (A.19) and (A.20), we can derive

$$\nabla^2\bar{p}_i(x,y) - k_i^2\bar{p}_i(x,y) = 0 \tag{A.24}$$

with

$$p(x,y,z) = \sum_{i=1}^{n_2} c_i\bar{p}_i(x,y)\cos k_i z \tag{A.25}$$

where k_i is given by

$$\omega^2 = -k_i g \tan k_i h \tag{A.20}$$

Combining the above equations, we get

$$p(x,y,z) = c_0\bar{p}_0(x,y)\cosh k_0 z + \sum_{i=1}^{n_2} c_i\bar{p}_i(x,y)\cos k_i z \tag{A.26}$$

b. Case ii of High Frequency Excitation

From Eqs. (A.10) and (A.21), we have

$$\nabla^2 \bar{p}_i(x,y) - k_i^2 \bar{p}_i(x,y) = 0 \tag{A.27}$$

with

$$p(x,y,z) = \sum_{i=1}^{\infty} c_i \bar{p}_i(x,y) \cos k_i z \tag{A.28}$$

where

$$k_i = \frac{(i-\frac{1}{2})\pi}{h} \tag{A.21}$$

The hydrodynamic pressure in this case is independent of the frequency of excitation.

APPENDIX B

LOCALIZED FINITE ELEMENT METHOD FOR HIGH FREQUENCY EXCITATION

A reduced two-dimensional boundary value problem of hydrodynamic pressure in fluid domain can be solved by the localized finite element method which divides the fluid into inner and outer subdomains [27]. The following discussions of excitation in high frequency are based on the derivations in Chapter IV.

1. Inner and Outer Domains

As shown in Fig. 4.2, a transmitting boundary S_{tb} was located near the structure in order to separate the infinite fluid domain into inner domain R_1 and outer domain R_2. The truncated finite domain R_1 will be discretized into a number of finite elements which can be approached by the conventional finite element technique. The hydrodynamic pressure in the infinite outer domain R_2 will be represented by a finite number of eigenfunctions.

Let $\bar{p}_{1i}$ and $\bar{p}_{2i}$ denote the i-th mode hydrodynamic pressure in R_1 and R_2 respectively, then we have the following two-dimensional problems where the boundary conditions on water surface and the bottom are reduced.

In inner domain, we have $S = S_{f1} \bigcup S_{f2} \bigcup S_{tb}$ and

$$\nabla^2 \bar{p}_{1i}(x,y) - \lambda_i \bar{p}_{1i}(x,y) = 0 \tag{B.1}$$

with the interface boundary conditions

$$\frac{\partial p_1}{\partial n}(x,y,z) = -\rho \ddot{u}^j(z)\cos\bar{\theta} \qquad j=1,2$$

In the outer domain, we have $S = S_{tb} \bigcup S_f$ and

$$\nabla^2 \bar{p}_{2l}(x,y) - \lambda_l \bar{p}_{2l}(x,y) = 0 \tag{B.2}$$

with the far field boundary condition

$$\frac{\partial \bar{p}_{2l}}{\partial n}(x,y) = 0$$

On the transmitting boundary, two conditons are required as follows:

$$\bar{p}_{1l} = \bar{p}_{2l} \tag{B.3}$$

and

$$\frac{\partial \bar{p}_{1l}}{\partial n} = -\frac{\partial \bar{p}_{2l}}{\partial n}$$

where the normal vector n is taken outwards from each region.

If we take the cylindrical coordinates into consideration, then

$$\frac{\partial \bar{p}_{1l}}{\partial r} = \frac{\partial \bar{p}_{2l}}{\partial r} \tag{B.4}$$

With the transmitting boundary conditions, $\bar{p}_{1l}$ and $\bar{p}_{2l}$ will have unique solutions.

2. The Functional

Applying the principle of variation to the problem in the inner domain, the following functional is formulated for each mode of wave (see Chapter III and Appendix A):

$$F(\bar{p}_{1l},\bar{p}_{2l}) = \tfrac{1}{2}\int\int_{R_1}\left[(\nabla \bar{p}_{1l})^2 + \lambda_l \bar{p}_{1l}^2\right] dx\,dy - \sum_{j=1}^{2}\int_{S_{lj}} \bar{p}_{1l} f_l^j \, dS$$

$$+ \int_{S_{ab}} (\bar{p}_{1l} - \tfrac{1}{2}\bar{p}_{2l})\,\bar{p}_{2ln}\, dS \tag{B.5}$$

where $\bar{p}_{1in}, \bar{p}_{2in}$ denote $\frac{\partial \bar{p}_{1i}}{\partial n}, \frac{\partial \bar{p}_{2i}}{\partial n}$ respectively, and f_i' is shown in Eq. (4.29).

The variation of F is given by

$$\delta F = \iint_{R_1} (-\nabla^2 \bar{p}_{1i} + \lambda_i \bar{p}_{1i}) \delta \bar{p}_{1i} \, dx dy + \sum_{j=1}^{2} \int_{S_{ij}} (\bar{p}_{1in} - f_i') \delta \bar{p}_{1i} \, dS$$

$$+ \int_{S_\infty} \left[(\bar{p}_{1in} + \bar{p}_{2in}) \delta \bar{p}_{1i} + \bar{p}_{1i} \delta \bar{p}_{2in} - \tfrac{1}{2} (\bar{p}_{2i} \delta \bar{p}_{2in} + \bar{p}_{2in} \delta \bar{p}_{2i}) \right] dS \tag{B.6}$$

If the Green's Theorem is applied to $\bar{p}_{2i}$ and $\delta \bar{p}_{2i}$ in the outer domain, then we have

$$\iint_{R_2} \left[\nabla^2 \bar{p}_{2i} \delta \bar{p}_{2i} - \bar{p}_{2i} \nabla^2 (\delta \bar{p}_{2i}) \right] dx dy = \int_{S_2} (\bar{p}_{2in} \delta \bar{p}_{2i} - \bar{p}_{2i} \delta \bar{p}_{2in}) \, dS \tag{B.7}$$

By the basic assumption of potential flow theory, the integral on the left-hand side will vanish. Thus, the boundary integral on S_2 becomes

$$\int_{S_\infty} (\bar{p}_{2in} \delta \bar{p}_{2i} - \bar{p}_{2i} \delta \bar{p}_{2in}) \, dS = 0 \tag{B.8}$$

Substituting Eq. (B.8) into the variation of the functional, Eq. (B.6), we will obtain the same result as shown in Eq. (4.34). Since the variations $\delta \bar{p}_{1i}$, $\delta \bar{p}_{2i}$, $\delta \bar{p}_{1in}$ and $\delta \bar{p}_{2in}$ are arbitrary values, each integral in the above expression will disappear on the boundary or in the domain. Therefore, Eqs. (B.1) and (B.3) are obtained and the values of $\bar{p}_{1i}$, $\bar{p}_{2i}$ derived from the functional will be the solution of the boundary value problem.

3. Finite Element Technique

Let the inner domain R_1 be divided into a finite element mesh with nodal points in each element. Introducing the interpolation function associated with each node, each element can be represented as

$$\bar{p}_{1l} = \underline{N}\bar{p}_{1l} \tag{B.9}$$

where l is the number of wave mode and N is the shape function.

In the outer domain, a set of properly chosen eigenfunctions [34] will be used. For each i-th mode of wave, we have

$$p_2 = \sum_{l=1}^{n} \psi_l \bar{p}_{2l} \tag{B.10}$$

where

$$\bar{p}_{2l} = \sum_{i=0}^{n-1} \Psi_{il} \bar{p}'_{2l} \equiv \underline{\Psi}_l \bar{p}_{2l} \tag{B.11}$$

and

$$\Psi_{il} = e^{-k_l r} \cos(l\theta - \delta) \tag{B.12}$$

with $r = (x_2 + y_2)^{1/2}$ and ψ being the mode shape of wave as shown in Eq. (4.29).

From Eqs. (B.9)-(B.12), the stationary point of the functional, Eq. (B.5), with respect to $\bar{p}_{1l}$ and $\bar{p}_{2l}$ can be found by the following equations

$$\frac{\partial F(\bar{p}_{1l}, \bar{p}_{2l})}{\partial \bar{p}_{1l}} = 0 \tag{B.13.a}$$

and

$$\frac{\partial F(\bar{p}_{1l}, \bar{p}_{2l})}{\partial \bar{p}_{2l}} = 0 \tag{B.13.b}$$

Substituting Eqs. (B.10) and (B.11) into Eqs. (B.13.a) and (B.13.b), We obtain

$$\sum_e \iint_{R_1} (\nabla \underline{N}^T \nabla \underline{N} + \lambda_l \underline{N}^T \underline{N})\, dx dy \bar{p}_{1l} - \sum_e \int_{S_{ll}} \underline{N}^T \underline{\Psi}_{ln} dS \bar{p}_{2l} - \sum_{j=1}^{2} \sum_e \int_{S_{lj}} \underline{N}^T f_l^j dS = 0 \tag{B.14}$$

and

$$-\left[\sum_{e}\int_{S_{ib}} \underline{N}^T \underline{\Psi}_{in}\, dS\right]^T \bar{\underline{p}}_{1i} + \tfrac{1}{2}\int_{S_{ib}} (\underline{\Psi}_{in}{}^T \underline{\Psi}_i + \underline{\Psi}_i{}^T \underline{\Psi}_{in})\, dS \bar{\underline{p}}_{2i} = 0 \qquad \text{(B.15)}$$

If the cylindrical coordinates are applied to Eq. (B.4), then the results as shown in Eq. (4.40) is derived

$$\begin{bmatrix} \underline{A}_{11} & \underline{A}_{12} \\ \underline{A}_{21} & \underline{A}_{22} \end{bmatrix}_i \begin{Bmatrix} \bar{\underline{p}}_{1i} \\ \bar{\underline{p}}_{2i} \end{Bmatrix} = \begin{Bmatrix} \underline{b}_{1i} \\ \underline{b}_{2i} \end{Bmatrix} \qquad \text{(B.16)}$$

According to the decomposition procedures described in Chapter IV, Eq. (B.16) can be solved for the amplitude of hydrodynamic pressure for each mode of wave.

APPENDIX C

DYNAMIC RESPONSE OF A SINGLE FLEXIBLE CYLINDER SURROUNDED BY WATER

The analytic solution to the simple harmonic ground acceleration is presented here [26]. This solution is limited to the fundamental mode of structural vibration since the dynamic responses in modal coordinates do not remain uncoupled when hydrodynamic interaction is included.

1. Equation of Motion

Considering a linearly elastic cylinder governed by beam theory, the equation of motion in the first mode of vibration, subjected to horizontal ground acceleration $\ddot{u}_g(t)$, can be expressed in terms of the generalized coordinates,

$$M_1\ddot{Y}_1(t) + C_1\dot{Y}_1(t) + K_1Y_1(t) = -\ddot{u}_g(t)A_1 - F_1(t) \tag{C.1}$$

Let $\phi_1(z)$ and ω_1 denote the mode shape and frequency of structural vibration in the air respectively, $m(z)$ be the mass per unit length, and H be the height of cylinder. Thus, the generalized characteristics of the cylinder can be derived by

$$M_1 = \int_0^H m(z)\phi_1^2(z)\,dz \tag{C.2}$$

$$K_1 = \omega_1^2 M_1 \tag{C.3}$$

$$C_1 = 2\xi_1\omega_1 M_1 \tag{C.4}$$

$$A_1 = \int_0^H m(z)\phi_1(z)\,dz \tag{C.5}$$

and, the following equation can represent the generalized load which is associated with

hydrodynamic pressure acting on the surface of the cylinder

$$F_1 = \int_0^h \phi_1(z) \int_0^{2\pi} p(a,z,\theta,t)\, a\cos\theta\, d\theta\, dz \tag{C.6}$$

where $p(a,z,\theta,t)$ is the hydrodynamic pressure on the surface of the cylinder as $r = a$, and $p(a,z,\theta,t) = p(a,z,0,t)\cos\theta$.

The responses to harmonic ground acceleration $\ddot{u}_g(t) = e^{i\omega t}$ will be given by

$$\begin{aligned} Y_1(t) &= Y_1(\omega)\, e^{i\omega t} \\ \ddot{Y}_1(t) &= \ddot{Y}_1(\omega)\, e^{i\omega t} \\ \ddot{Y}_1(\omega) &= -\omega^2 Y_1(\omega) \end{aligned} \tag{C.7}$$

and the acceleration on the surface of the tower is

$$\ddot{u}(t) = [1 + \ddot{Y}_1(\omega)\phi_1(z)]\, e^{i\omega t}\cos\theta \tag{C.8}$$

2. Wave Equation

The hydrodynamic pressure in fluid domain can be treated as an axisymmetrical problem governed by the following wave equation in cylindrical coordinates

$$\frac{\partial^2 p}{\partial r^2} + \frac{1}{r}\frac{\partial p}{\partial r} + \frac{1}{r^2}\frac{\partial^2 p}{\partial \theta^2} + \frac{\partial^2 p}{\partial z^2} = \frac{1}{C^2}\frac{\partial^2 p}{\partial t^2} \tag{C.9}$$

with the boundary conditions

$$\frac{\partial p}{\partial z}(r,0,\theta,t) = 0 \tag{C.10}$$

$$\frac{\partial^2 p}{\partial t^2}(r,h,\theta,t) + g\frac{\partial p}{\partial z}(r,h,\theta,t) = 0 \tag{C.11}$$

$$\frac{\partial p}{\partial r}(a,z,\theta,t) = -\rho[1+\ddot{Y}_1(\omega)\phi_1(z)]\cos\theta e^{i\omega t} \tag{C.12}$$

$$\frac{\partial p}{\partial \theta}(r,z,0,t) = \frac{\partial p}{\partial \theta}(r,z,\pi,t) = 0 \tag{C.13}$$

where C is the velocity of sound in water, which is equal to 4720 fps, ρ is the mass density of water, and a is the radius of the cylinder.

The response to the harmonic ground acceleration will be

$$p(t) = p(\omega)e^{i\omega t} \tag{C.14}$$

and $p(\omega)$ can be decomposed into

$$p(\omega) = p_0 + \ddot{Y}_1(\omega)p_1 \tag{C.15}$$

where p_0 and p_1 are the values of p_k with $k = 0,1$ solving from the wave equation, Eq. (C.9), and the following boundary conditions

$$\frac{\partial p}{\partial z}(r,0,\theta,\omega) = 0$$

$$\frac{\partial p}{\partial z}(r,h,\theta,\omega) - \frac{\omega^2}{g}p(r,h,\theta,\omega) = 0 \tag{C.16}$$

$$\frac{\partial p}{\partial r}(a,z,\theta,\omega) = -\rho\phi_k(z)\cos\theta$$

$$\frac{\partial p}{\partial \theta}(r,z,0,\omega) = \frac{\partial p}{\partial \theta}(r,z,\pi,\omega) = 0$$

while $\phi_0(z) = 1$ and $\phi_1(z)$ is the first mode shape of the cylinder in the air.

3. Structural Response and Hydrodynamic Pressure

The complex frequency response function for the above problem is

$$\ddot{Y}_1(\omega) = \frac{A_1 + B_0(\omega)}{M_1\left[-1 + 2i\xi_1(\frac{\omega_1}{\omega}) + (\frac{\omega_1}{\omega})^2\right] - B_1(\omega)} \tag{C.17}$$

where

$$B_k = \int_0^h \phi_1(z)\int_0^{2\pi} p_k a\cos\theta\, d\theta\, dz \qquad k = 0,1 \tag{C.18}$$

For cylinder with no surrounding water, we have $B_k = 0$.

As mentioned in the previous section, p_k can be solved from Eqs. (C.9), (C.15) and (C.16) for a steady state solution as follows:

$$p_k(a,z,\theta,\omega) = 8\rho\{-\frac{\alpha_0}{\lambda_0}\frac{I_{k0}}{2\alpha_0 h+\sinh(2\alpha_0 h)}D_0(\lambda_0 a)\cosh(\alpha_0 z)\, e^{i\alpha_0 a} \tag{C.19}$$

$$-\sum_{m=1}^{m_1-1}\frac{\alpha_m}{\lambda_m}\frac{I_{km}}{2\alpha_m h+\sin(2\alpha_m h)}D_m(\lambda_m a)\cos(\alpha_m z)\, e^{i\alpha_m a}$$

$$+\sum_{m=m_1}^{\infty}\frac{\alpha_m}{\lambda_m'}\frac{I_{km}}{2\alpha_m h+\sin(2\alpha_m h)}E_m(\lambda_m' a)\cos(\alpha_m z)\}\cos\theta$$

where m_1 is the smallest integer value of m such that $\alpha_m > \frac{\omega}{C}$; α_0 and α_m are the solutions of

$$\alpha_0\tanh(\alpha_0 h) = \frac{\omega^2}{g}$$

$$\alpha_m\tan(\alpha_m h) = -\frac{\omega^2}{g}$$

moreover,

$$\lambda_0^2 = \frac{\omega^2}{C^2} + \alpha_0^2$$

$$\lambda_m^2 = \frac{\omega^2}{C^2} - \alpha_m^2$$

$$\lambda_m' = i\lambda_m$$

$$I_{k0} = \int_0^h \phi_k(z)\cosh(\alpha_0 z)\,dz$$

$$I_{km} = \int_0^h \phi_k(z)\cos(\alpha_m z)\,dz$$

$$[D_m(\lambda_m a)]^2 = \frac{[J_1(\lambda_m a)]^2 + [Y_1(\lambda_m a)]^2}{[J_0(\lambda_m a) - J_2(\lambda_m a)]_2 + [Y_0(\lambda_m a) - Y_2(\lambda_m a)]^2}$$

$$E_m(\lambda_m' a) = \frac{K_1(\lambda_m' a)}{K_0(\lambda_m' a) + K_2(\lambda_m' a)}$$

$$\tan(\epsilon_m a) = \frac{[Y_0(\lambda_m a) - Y_2(\lambda_m a)]J_1(\lambda_m a) - [J_0(\lambda_m a) - J_2(\lambda_m a)]Y_1(\lambda_m a)}{[J_0(\lambda_m a) - J_2(\lambda_m a)]J_1(\lambda_m a) + [Y_0(\lambda_m a) - Y_2(\lambda_m a)]Y_1(\lambda_m a)}$$

with J_n, Y_n being the Bessel functions of order n of the first and second kind respectively, and K_n being the modified Bessel function of order n of the second kind.

For high frequency vibration, the surface wave is ignored. The boundary condition at the free surface can be replaced by

$$p(r, h, \theta, \omega) = 0 \qquad \text{(C.20)}$$

If the compressibility of water is also neglected, the above solution, Eq. (C.19), can be simplified by substituting $C = \infty$ into the expressions. The simplified hydrodynamic pressures on the surface of the cylinder becomes

$$p_k(a,z,\theta,\omega) = 8\rho \sum_{m=1}^{\infty} \frac{I_{km}}{(2m-1)\pi} E_m(\lambda_m' a)\cos(\alpha_m z)\cos\theta \qquad \text{(C.21)}$$

in which $\lambda_m' = \alpha_m = \frac{(2m-1)\pi}{2h}$. The total hydrodynamic force per unit length in Z-direction will be computed from the following integral

$$p_k(z) = \int_0^{2\pi} p_k(a,z,\theta,\omega)\, a\cos\theta\, d\theta \qquad \text{(C.22)}$$

It is easy to see that p_k is now independent of the excitation frequency ω and in phase with the excitation for all frequencies.

APPENDIX D

THE COMPUTER PROGRAM HYDR

The purpose of thic computer program HYDR is to determine the elastic dynamic responses of two circular cylinders partially submerged in water to the horizontal earthquake ground motion.

As indicated before, both the waves at the free water surface and the compressibility of water are of little influence in the dynamic structural responses to the high frequency ground excitation. And hence, they are ignored.

This FORTRAN program is based on the numerical analysis described in Chapter III and IV, in which each cylinder with arbitrary radius is treated as either beam type flexible structure connected rigidly to the ground or rigid structure connected flexibly to the ground.

The surrounding water is treated as a reduced two-dimensional finite element system with self-generated mesh. Moreover, the principles of symmetry and antisymmetry are applied to the problem such that the fluid domain can be reduced to one half. As discussed in Chapter II, the unknown nodal hydrodynamic pressures are assigned to the finite element mesh. The pressure variation within each element is expressed in terms of nine-node nodal hydrodynamic pressures. Three-point Gaussian integration is also applied to the computation.

A flow diagram for the program HYDR is shown in Fig. D.1. In order to insure the convergence of the computation, two parameters are considered; namely the number of wave mode, n_w, and the number of structural vibration mode, n_s. As illustrated from the examples in Chapter V, the hydrodynamic pressure will converge by choosing $n_w \geqslant 6$. For the value of n_s, we will examine the characteristics of the structure. In the case of rigid cylinders connected flexibly to the ground, the value of n_s is set to be 2, which represents the translation and rotation of the structure. In the case of flexible cylinders connected rigidly to the ground, a small value of n_s is sufficient to achieve convergence if the cylinder is very stiff.

The X-axis of the coordinates system coincides with the line connecting the centers of

cylinders. For a horizontal ground motion with arbitrary direction, this boundary value problem is decomposed into the symmetrical and the antisymmetrical case with respect to the X-axis. The X-component of ground motion relates to the symmetrical case with a symmetrical stiffness matrix, while the Y-component relates to the antisymmetrical case with an asymmetrical stiffness matrix. A variable banded-matrix solver is used to solve the linear equations for both cases. The solution of the boundary value problem will be the combination of the results from these two cases.

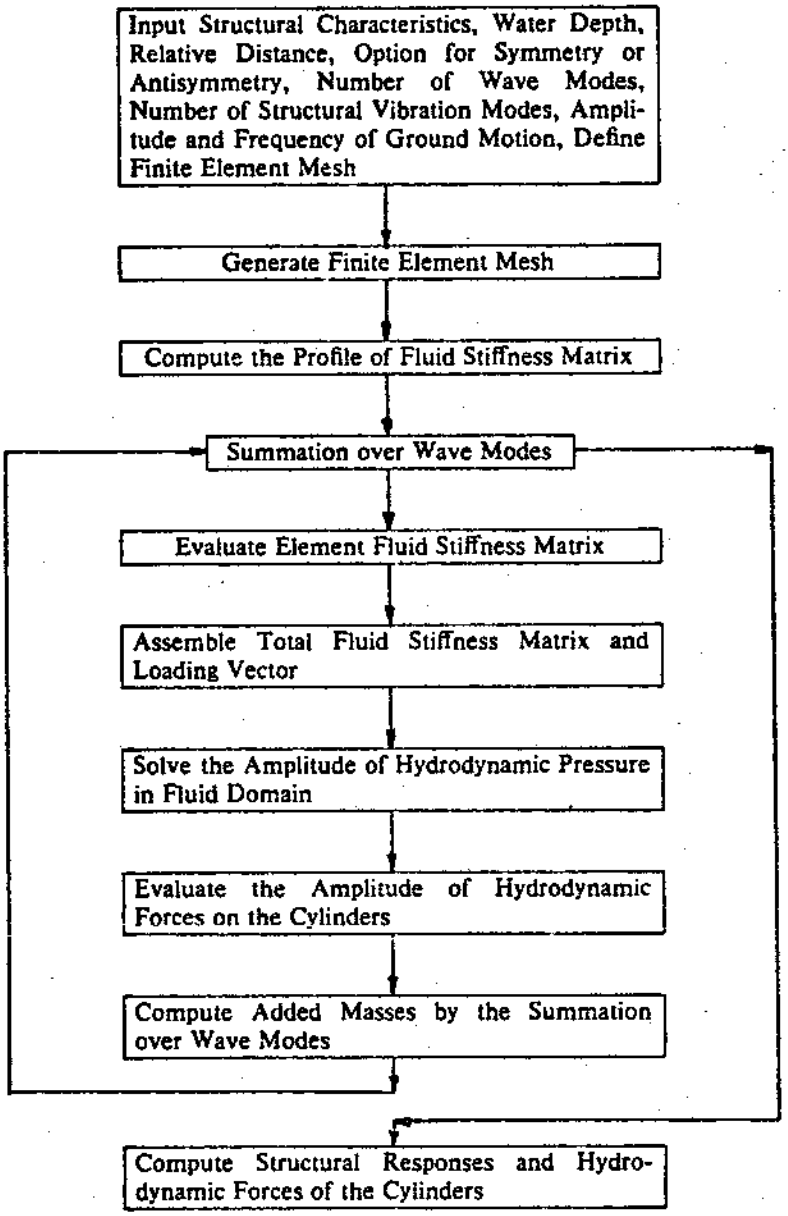

Figure D.1 Flow Diagram of Program HYDR

EARTHQUAKE ENGINEERING RESEARCH CENTER REPORTS

NOTE: Numbers in parentheses are Accession Numbers assigned by the National Technical Information Service; these are followed by a price code. Copies of the reports may be ordered from the National Technical Information Service, 5285 Port Royal Road, Springfield, Virginia, 22161. Accession Numbers should be quoted on orders for reports (PB --- ---) and remittance must accompany each order. Reports without this information were not available at time of printing. The complete list of EERC reports (from EERC 67-1) is available upon request from the Earthquake Engineering Research Center, University of California, Berkeley, 47th Street and Hoffman Boulevard, Richmond, California 94804.

UCB/EERC-77/01 "PLUSH - A Computer Program for Probabilistic Finite Element Analysis of Seismic Soil-Structure Interaction," by M.P. Romo Organista, J. Lysmer and H.B. Seed - 1977 (PB81 177 651)A05

UCB/EERC-77/02 "Soil-Structure Interaction Effects at the Humboldt Bay Power Plant in the Ferndale Earthquake of June 7, 1975," by J.E. Valera, H.B. Seed, C.F. Tsai and J. Lysmer - 1977 (PB 265 795)A04

UCB/EERC-77/03 "Influence of Sample Disturbance on Sand Response to Cyclic Loading," by K. Mori, H.B. Seed and C.K. Chan - 1977 (PB 267 352)A04

UCB/EERC-77/04 "Seismological Studies of Strong Motion Records," by J. Shoja-Taheri - 1977 (PB 269 655)A10

UCB/EERC-77/05 Unassigned

UCB/EERC-77/06 "Developing Methodologies for Evaluating the Earthquake Safety of Existing Buildings," by No. 1 - B. Bresler; No. 2 - B. Bresler, T. Okada and D. Zisling; No. 3 - T. Okada and B. Bresler; No. 4 - V.V. Bertero and B. Bresler - 1977 (PB 267 354)A08

UCB/EERC-77/07 "A Literature Survey - Transverse Strength of Masonry Walls," by Y. Omote, R.L. Mayes, S.W. Chen and R.W. Clough - 1977 (PB 277 933)A07

UCB/EERC-77/08 "DRAIN-TABS: A Computer Program for Inelastic Earthquake Response of Three Dimensional Buildings," by R. Guendelman-Israel and G.H. Powell - 1977 (PB 270 693)A07

UCB/EERC-77/09 "SUBWALL: A Special Purpose Finite Element Computer Program for Practical Elastic Analysis and Design of Structural Walls with Substructure Option," by D.Q. Le, H. Peterson and E.P. Popov - 1977 (PB 270 567)A05

UCB/EERC-77/10 "Experimental Evaluation of Seismic Design Methods for Broad Cylindrical Tanks," by D.P. Clough (PB 272 280)A13

UCB/EERC-77/11 "Earthquake Engineering Research at Berkeley - 1976," - 1977 (PB 273 507)A09

UCB/EERC-77/12 "Automated Design of Earthquake Resistant Multistory Steel Building Frames," by N.D. Walker, Jr. - 1977 (PB 276 526)A09

UCB/EERC-77/13 "Concrete Confined by Rectangular Hoops Subjected to Axial Loads," by J. Vallenas, V.V. Bertero and E.P. Popov - 1977 (PB 275 165)A06

UCB/EERC-77/14 "Seismic Strain Induced in the Ground During Earthquakes," by Y. Sugimura - 1977 (PB 284 201)A04

UCB/EERC-77/15 Unassigned

UCB/EERC-77/16 "Computer Aided Optimum Design of Ductile Reinforced Concrete Moment Resisting Frames," by S.W. Zagajeski and V.V. Bertero - 1977 (PB 280 137)A07

UCB/EERC-77/17 "Earthquake Simulation Testing of a Stepping Frame with Energy-Absorbing Devices," by J.M. Kelly and D.F. Tsztoo - 1977 (PB 273 506)A04

UCB/EERC-77/18 "Inelastic Behavior of Eccentrically Braced Steel Frames under Cyclic Loadings," by C.W. Roeder and E.P. Popov - 1977 (PB 275 526)A15

UCB/EERC-77/19 "A Simplified Procedure for Estimating Earthquake-Induced Deformations in Dams and Embankments," by F.I. Makdisi and H.B. Seed - 1977 (PB 276 820)A04

UCB/EERC-77/20 "The Performance of Earth Dams during Earthquakes," by H.B. Seed, F.I. Makdisi and P. de Alba - 1977 (PB 276 821)A04

UCB/EERC-77/21 "Dynamic Plastic Analysis Using Stress Resultant Finite Element Formulation," by P. Lukkunapvasit and J.M. Kelly - 1977 (PB 275 453)A04

UCB/EERC-77/22 "Preliminary Experimental Study of Seismic Uplift of a Steel Frame," by R.W. Clough and A.A. Huckelbridge 1977 (PB 278 769)A08

UCB/EERC-77/23 "Earthquake Simulator Tests of a Nine-Story Steel Frame with Columns Allowed to Uplift," by A.A. Huckelbridge - 1977 (PB 277 944)A09

UCB/EERC-77/24 "Nonlinear Soil-Structure Interaction of Skew Highway Bridges," by M.-C. Chen and J. Penzien - 1977 (PB 276 176)A07

UCB/EERC-77/25 "Seismic Analysis of an Offshore Structure Supported on Pile Foundations," by D.D.-N. Liou and J. Penzien 1977 (PB 283 180)A06

UCB/EERC-77/26 "Dynamic Stiffness Matrices for Homogeneous Viscoelastic Half-Planes," by G. Dasgupta and A.K. Chopra - 1977 (PB 279 654)A06

UCB/EERC-77/27 "A Practical Soft Story Earthquake Isolation System," by J.M. Kelly, J.M. Eidinger and C.J. Derham - 1977 (PB 276 814)A07

UCB/EERC-77/28 "Seismic Safety of Existing Buildings and Incentives for Hazard Mitigation in San Francisco: An Exploratory Study," by A.J. Meltsner - 1977 (PB 281 970)A05

UCB/EERC-77/29 "Dynamic Analysis of Electrohydraulic Shaking Tables," by D. Rea, S. Abedi-Hayati and Y. Takahashi 1977 (PB 282 569)A04

UCB/EERC-77/30 "An Approach for Improving Seismic - Resistant Behavior of Reinforced Concrete Interior Joints," by B. Galunic, V.V. Bertero and E.P. Popov - 1977 (PB 290 870)A06

UCB/EERC-78/01 "The Development of Energy-Absorbing Devices for Aseismic Base Isolation Systems," by J.M. Kelly and D.F. Tsztoo - 1978 (PB 284 978)A04

UCB/EERC-78/02 "Effect of Tensile Prestrain on the Cyclic Response of Structural Steel Connections, by J.G. Bouwkamp and A. Mukhopadhyay - 1978

UCB/EERC-78/03 "Experimental Results of an Earthquake Isolation System using Natural Rubber Bearings," by J.M. Eidinger and J.M. Kelly - 1978 (PB 281 686)A04

UCB/EERC-78/04 "Seismic Behavior of Tall Liquid Storage Tanks," by A. Niwa - 1978 (PB 284 017)A14

UCB/EERC-78/05 "Hysteretic Behavior of Reinforced Concrete Columns Subjected to High Axial and Cyclic Shear Forces," by S.W. Zagajeski, V.V. Bertero and J.G. Bouwkamp - 1978 (PB 283 858)A13

UCB/EERC-78/06 "Three Dimensional Inelastic Frame Elements for the ANSR-I Program," by A. Riahi, D.G. Row and G.H. Powell - 1978 (PB 295 755)A04

UCB/EERC-78/07 "Studies of Structural Response to Earthquake Ground Motion," by O.A. Lopez and A.K. Chopra - 1978 (PB 282 790)A05

UCB/EERC-78/08 "A Laboratory Study of the Fluid-Structure Interaction of Submerged Tanks and Caissons in Earthquakes," by R.C. Byrd - 1978 (PB 284 957)A08

UCB/EERC-78/09 Unassigned

UCB/EERC-78/10 "Seismic Performance of Nonstructural and Secondary Structural Elements," by I. Sakamoto - 1978 (PB81 154 593)A05

UCB/EERC-78/11 "Mathematical Modelling of Hysteresis Loops for Reinforced Concrete Columns," by S. Nakata, T. Sproul and J. Penzien - 1978 (PB 298 274)A05

UCB/EERC-78/12 "Damageability in Existing Buildings," by T. Blejwas and B. Bresler - 1978 (PB 80 166 978)A05

UCB/EERC-78/13 "Dynamic Behavior of a Pedestal Base Multistory Building," by R.M. Stephen, E.L. Wilson, J.G. Bouwkamp and M. Button - 1978 (PB 286 650)A08

UCB/EERC-78/14 "Seismic Response of Bridges - Case Studies," by R.A. Imbsen, V. Nutt and J. Penzien - 1978 (PB 286 503)A10

UCB/EERC-78/15 "A Substructure Technique for Nonlinear Static and Dynamic Analysis," by D.G. Row and G.H. Powell - 1978 (PB 288 077)A10

UCB/EERC-78/16 "Seismic Risk Studies for San Francisco and for the Greater San Francisco Bay Area," by C.S. Oliveira - 1978 (PB 81 120 115)A07

UCB/EERC-78/17 "Strength of Timber Roof Connections Subjected to Cyclic Loads," by P. Gülkan, R.L. Mayes and R.W. Clough - 1978 (HUD-000 1491)A07

UCB/EERC-78/18 "Response of K-Braced Steel Frame Models to Lateral Loads," by J.G. Bouwkamp, R.M. Stephen and E.P. Popov - 1978

UCB/EERC-78/19 "Rational Design Methods for Light Equipment in Structures Subjected to Ground Motion," by J.L. Sackman and J.M. Kelly - 1978 (PB 292 357)A04

UCB/EERC-78/20 "Testing of a Wind Restraint for Aseismic Base Isolation," by J.M. Kelly and D.E. Chitty - 1978 (PB 292 833)A03

UCB/EERC-78/21 "APOLLO - A Computer Program for the Analysis of Pore Pressure Generation and Dissipation in Horizontal Sand Layers During Cyclic or Earthquake Loading," by P.P. Martin and H.B. Seed - 1978 (PB 292 835)A04

UCB/EERC-78/22 "Optimal Design of an Earthquake Isolation System," by M.A. Bhatti, K.S. Pister and E. Polak - 1978 (PB 294 735)A06

UCB/EERC-78/23 "MASH - A Computer Program for the Non-Linear Analysis of Vertically Propagating Shear Waves in Horizontally Layered Deposits," by P.P. Martin and H.B. Seed - 1978 (PB 293 101)A05

UCB/EERC-78/24 "Investigation of the Elastic Characteristics of a Three Story Steel Frame Using System Identification," by I. Kaya and H.D. McNiven - 1978 (PB 296 225)A06

UCB/EERC-78/25 "Investigation of the Nonlinear Characteristics of a Three-Story Steel Frame Using System Identification," by I. Kaya and H.D. McNiven - 1978 (PB 301 363)A05

UCB/EERC-78/26 "Studies of Strong Ground Motion in Taiwan," by Y.M. Hsiung, B.A. Bolt and J. Penzien - 1978 (PB 298 436)A06

UCB/EERC-78/27 "Cyclic Loading Tests of Masonry Single Piers: Volume 1 - Height to Width Ratio of 2," by P.A. Hidalgo, R.L. Mayes, H.D. McNiven and R.W. Clough - 1978 (PB 296 211)A07

UCB/EERC-78/28 "Cyclic Loading Tests of Masonry Single Piers: Volume 2 - Height to Width Ratio of 1," by S.-W.J. Chen, P.A. Hidalgo, R.L. Mayes, R.W. Clough and H.D. McNiven - 1978 (PB 296 212)A09

UCB/EERC-78/29 "Analytical Procedures in Soil Dynamics," by J. Lysmer - 1978 (PB 298 445)A06

UCB/EERC-79/01 "Hysteretic Behavior of Lightweight Reinforced Concrete Beam-Column Subassemblages," by B. Forzani, E.P. Popov and V.V. Bertero - April 1979(PB 298 267)A06

UCB/EERC-79/02 "The Development of a Mathematical Model to Predict the Flexural Response of Reinforced Concrete Beams to Cyclic Loads, Using System Identification," by J. Stanton & H. McNiven - Jan. 1979(PB 295 875)A10

UCB/EERC-79/03 "Linear and Nonlinear Earthquake Response of Simple Torsionally Coupled Systems," by C.L. Kan and A.K. Chopra - Feb. 1979(PB 298 262)A06

UCB/EERC-79/04 "A Mathematical Model of Masonry for Predicting its Linear Seismic Response Characteristics," by Y. Mengi and H.D. McNiven - Feb. 1979(PB 298 266)A06

UCB/EERC-79/05 "Mechanical Behavior of Lightweight Concrete Confined by Different Types of Lateral Reinforcement," by M.A. Manrique, V.V. Bertero and E.P. Popov - May 1979(PB 301 114)A06

UCB/EERC-79/06 "Static Tilt Tests of a Tall Cylindrical Liquid Storage Tank," by R.W. Clough and A. Niwa - Feb. 1979 (PB 301 167)A06

UCB/EERC-79/07 "The Design of Steel Energy Absorbing Restrainers and Their Incorporation into Nuclear Power Plants for Enhanced Safety: Volume 1 - Summary Report," by P.N. Spencer, V.F. Zackay, and E.R. Parker - Feb. 1979(UCB/EERC-79/07)A09

UCB/EERC-79/08 "The Design of Steel Energy Absorbing Restrainers and Their Incorporation into Nuclear Power Plants for Enhanced Safety: Volume 2 - The Development of Analyses for Reactor System Piping,""Simple Systems" by M.C. Lee, J. Penzien, A.K. Chopra and K. Suzuki "Complex Systems" by G.H. Powell, E.L. Wilson, R.W. Clough and D.G. Row - Feb. 1979(UCB/EERC-79/08)A10

UCB/EERC-79/09 "The Design of Steel Energy Absorbing Restrainers and Their Incorporation into Nuclear Power Plants for Enhanced Safety: Volume 3 - Evaluation of Commercial Steels," by W.S. Owen, R.M.N. Pelloux, R.O. Ritchie, M. Faral, T. Ohhashi, J. Toplosky, S.J. Hartman, V.F. Zackay and E.R. Parker - Feb. 1979(UCB/EERC-79/09)A04

UCB/EERC-79/10 "The Design of Steel Energy Absorbing Restrainers and Their Incorporation into Nuclear Power Plants for Enhanced Safety: Volume 4 - A Review of Energy-Absorbing Devices," by J.M. Kelly and M.S. Skinner - Feb. 1979(UCB/EERC-79/10)A04

UCB/EERC-79/11 "Conservatism In Summation Rules for Closely Spaced Modes," by J.M. Kelly and J.L. Sackman - May 1979(PB 301 328)A03

UCB/EERC-79/12 "Cyclic Loading Tests of Masonry Single Piers: Volume 3 - Height to Width Ratio of 0.5," by P.A. Hidalgo, R.L. Mayes, H.D. McNiven and R.W. Clough - May 1979(PB 301 321)A08

UCB/EERC-79/13 "Cyclic Behavior of Dense Course-Grained Materials in Relation to the Seismic Stability of Dams," by N.G. Banerjee, H.B. Seed and C.K. Chan - June 1979(PB 301 373)A13

UCB/EERC-79/14 "Seismic Behavior of Reinforced Concrete Interior Beam-Column Subassemblages," by S. Viwathanatepa, E.P. Popov and V.V. Bertero - June 1979(PB 301 326)A10

UCB/EERC-79/15 "Optimal Design of Localized Nonlinear Systems with Dual Performance Criteria Under Earthquake Excitations," by M.A. Bhatti - July 1979(PB 80 167 109)A06

UCB/EERC-79/16 "OPTDYN - A General Purpose Optimization Program for Problems with or without Dynamic Constraints," by M.A. Bhatti, E. Polak and K.S. Pister - July 1979(PB 80 167 091)A05

UCB/EERC-79/17 "ANSR-II, Analysis of Nonlinear Structural Response, Users Manual," by D.P. Mondkar and G.H. Powell July 1979(PB 80 113 301)A05

UCB/EERC-79/18 "Soil Structure Interaction in Different Seismic Environments," A. Gomez-Masso, J. Lysmer, J.-C. Chen and H.B. Seed - August 1979(PB 80 101 520)A04

UCB/EERC-79/19 "ARMA Models for Earthquake Ground Motions," by M.K. Chang, J.W. Kwiatkowski, R.F. Nau, R.M. Oliver and K.S. Pister - July 1979(PB 301 166)A05

UCB/EERC-79/20 "Hysteretic Behavior of Reinforced Concrete Structural Walls," by J.M. Vallenas, V.V. Bertero and E.P. Popov - August 1979(PB 80 165 905)A12

UCB/EERC-79/21 "Studies on High-Frequency Vibrations of Buildings - 1: The Column Effect," by J. Lubliner - August 1979 (PB 80 158 553)A03

UCB/EERC-79/22 "Effects of Generalized Loadings on Bond Reinforcing Bars Embedded in Confined Concrete Blocks," by S. Viwathanatepa, E.P. Popov and V.V. Bertero - August 1979(PB 81 124 018)A14

UCB/EERC-79/23 "Shaking Table Study of Single-Story Masonry Houses, Volume 1: Test Structures 1 and 2," by P. Gülkan, R.L. Mayes and R.W. Clough - Sept. 1979 (HUD-000 1763)A12

UCB/EERC-79/24 "Shaking Table Study of Single-Story Masonry Houses, Volume 2: Test Structures 3 and 4," by P. Gülkan, R.L. Mayes and R.W. Clough - Sept. 1979 (HUD-000 1836)A12

UCB/EERC-79/25 "Shaking Table Study of Single-Story Masonry Houses, Volume 3: Summary, Conclusions and Recommendations," by R.W. Clough, R.L. Mayes and P. Gülkan - Sept. 1979 (HUD-000 1937)A06

UCB/EERC-79/26 "Recommendations for a U.S.-Japan Cooperative Research Program Utilizing Large-Scale Testing Facilities," by U.S.-Japan Planning Group - Sept. 1979(PB 301 407)A06

UCB/EERC-79/27 "Earthquake-Induced Liquefaction Near Lake Amatitlan, Guatemala," by H.B. Seed, I. Arango, C.K. Chan, A. Gomez-Masso and R. Grant de Ascoli - Sept. 1979(NUREG-CR1341)A03

UCB/EERC-79/28 "Infill Panels: Their Influence on Seismic Response of Buildings," by J.W. Axley and V.V. Bertero Sept. 1979(PB 80 163 371)A10

UCB/EERC-79/29 "3D Truss Bar Element (Type 1) for the ANSR-II Program," by D.P. Mondkar and G.H. Powell - Nov. 1979 (PB 80 169 709)A02

UCB/EERC-79/30 "2D Beam-Column Element (Type 5 - Parallel Element Theory) for the ANSR-II Program," by D.G. Row, G.H. Powell and D.P. Mondkar - Dec. 1979(PB 80 167 224)A03

UCB/EERC-79/31 "3D Beam-Column Element (Type 2 - Parallel Element Theory) for the ANSR-II Program," by A. Riahi, G.H. Powell and D.P. Mondkar - Dec. 1979(PB 80 167 216)A03

UCB/EERC-79/32 "On Response of Structures to Stationary Excitation," by A. Der Kiureghian - Dec. 1979(PB 80166 929)A03

UCB/EERC-79/33 "Undisturbed Sampling and Cyclic Load Testing of Sands," by S. Singh, H.B. Seed and C.K. Chan Dec. 1979(ADA 087 299)A07

UCB/EERC-79/34 "Interaction Effects of Simultaneous Torsional and Compressional Cyclic Loading of Sand," by P.M. Griffin and W.N. Houston - Dec. 1979(ADA 092 352)A15

UCB/EERC-80/01 "Earthquake Response of Concrete Gravity Dams Including Hydrodynamic and Foundation Interaction Effects," by A.K. Chopra, P. Chakrabarti and S. Gupta - Jan. 1980(AD-A087297)A10

UCB/EERC-80/02 "Rocking Response of Rigid Blocks to Earthquakes," by C.S. Yim, A.K. Chopra and J. Penzien - Jan. 1980 (PB80 164 002)A04

UCB/EERC-80/03 "Optimum Inelastic Design of Seismic-Resistant Reinforced Concrete Frame Structures," by S.W. Zagajeski and V.V. Bertero - Jan. 1980(PB80 164 635)A06

UCB/EERC-80/04 "Effects of Amount and Arrangement of Wall-Panel Reinforcement on Hysteretic Behavior of Reinforced Concrete Walls," by R. Iliya and V.V. Bertero - Feb. 1980(PB81 122 525)A09

UCB/EERC-80/05 "Shaking Table Research on Concrete Dam Models," by A. Niwa and R.W. Clough - Sept. 1980(PB81 122 368)A06

UCB/EERC-80/06 "The Design of Steel Energy-Absorbing Restrainers and their Incorporation into Nuclear Power Plants for Enhanced Safety (Vol 1A): Piping with Energy Absorbing Restrainers: Parameter Study on Small Systems," by G.H. Powell, C. Oughourlian and J. Simons - June 1980

UCB/EERC-80/07 "Inelastic Torsional Response of Structures Subjected to Earthquake Ground Motions," by Y. Yamazaki April 1980(PB81 122 327)A08

UCB/EERC-80/08 "Study of X-Braced Steel Frame Structures Under Earthquake Simulation," by Y. Ghanaat - April 1980 (PB81 122 335)A11

UCB/EERC-80/09 "Hybrid Modelling of Soil-Structure Interaction," by S. Gupta, T.W. Lin, J. Penzien and C.S. Yeh May 1980(PB81 122 319)A07

UCB/EERC-80/10 "General Applicability of a Nonlinear Model of a One Story Steel Frame," by B.I. Sveinsson and H.D. McNiven - May 1980(PB81 124 877)A06

UCB/EERC-80/11 "A Green-Function Method for Wave Interaction with a Submerged Body," by W. Kioka - April 1980 (PB81 122 269)A07

UCB/EERC-80/12 "Hydrodynamic Pressure and Added Mass for Axisymmetric Bodies," by F. Nilrat - May 1980(PB81 122 343)A08

UCB/EERC-80/13 "Treatment of Non-Linear Drag Forces Acting on Offshore Platforms," by B.V. Dao and J. Penzien May 1980(PB81 153 413)A07

UCB/EERC-80/14 "2D Plane/Axisymmetric Solid Element (Type 3 - Elastic or Elastic-Perfectly Plastic) for the ANSR-II Program," by D.P. Mondkar and G.H. Powell - July 1980(PB81 122 350)A03

UCB/EERC-80/15 "A Response Spectrum Method for Random Vibrations," by A. Der Kiureghian - June 1980(PB81122 301)A03

UCB/EERC-80/16 "Cyclic Inelastic Buckling of Tubular Steel Braces," by V.A. Zayas, E.P. Popov and S.A. Mahin June 1980(PB81 124 885)A10

UCB/EERC-80/17 "Dynamic Response of Simple Arch Dams Including Hydrodynamic Interaction," by C.S. Porter and A.K. Chopra - July 1980(PB81 124 000)A13

UCB/EERC-80/18 "Experimental Testing of a Friction Damped Aseismic Base Isolation System with Fail-Safe Characteristics," by J.M. Kelly, K.E. Beucke and M.S. Skinner - July 1980(PB81 148 595)A04

UCB/EERC-80/19 "The Design of Steel Energy-Absorbing Restrainers and their Incorporation into Nuclear Power Plants for Enhanced Safety (Vol 1B): Stochastic Seismic Analyses of Nuclear Power Plant Structures and Piping Systems Subjected to Multiple Support Excitations," by M.C. Lee and J. Penzien - June 1980

UCB/EERC-80/20 "The Design of Steel Energy-Absorbing Restrainers and their Incorporation into Nuclear Power Plants for Enhanced Safety (Vol 1C): Numerical Method for Dynamic Substructure Analysis," by J.M. Dickens and E.L. Wilson - June 1980

UCB/EERC-80/21 "The Design of Steel Energy-Absorbing Restrainers and their Incorporation into Nuclear Power Plants for Enhanced Safety (Vol 2): Development and Testing of Restraints for Nuclear Piping Systems," by J.M. Kelly and M.S. Skinner - June 1980

UCB/EERC-80/22 "3D Solid Element (Type 4-Elastic or Elastic-Perfectly-Plastic) for the ANSR-II Program," by D.P. Mondkar and G.H. Powell - July 1980(PB81 123 242)A03

UCB/EERC-80/23 "Gap-Friction Element (Type 5) for the ANSR-II Program," by D.P. Mondkar and G.H. Powell - July 1980 (PB81 122 255)A03

UCB/EERC-80/24 "U-Bar Restraint Element (Type 11) for the ANSR-II Program," by C. Oughourlian and G.H. Powell July 1980(PB81 122 293)A03

UCB/EERC-80/25 "Testing of a Natural Rubber Base Isolation System by an Explosively Simulated Earthquake," by J.M. Kelly - August 1980(PB81 201 360)A04

UCB/EERC-80/26 "Input Identification from Structural Vibrational Response," by Y. Hu - August 1980(PB81 152 308)A05

UCB/EERC-80/27 "Cyclic Inelastic Behavior of Steel Offshore Structures," by V.A. Zayas, S.A. Mahin and E.P. Popov August 1980(PB81 196 180)A15

UCB/EERC-80/28 "Shaking Table Testing of a Reinforced Concrete Frame with Biaxial Response," by M.G. Oliva October 1980(PB81 154 304)A10

UCB/EERC-80/29 "Dynamic Properties of a Twelve-Story Prefabricated Panel Building," by J.G. Bouwkamp, J.P. Kollegger and R.M. Stephen - October 1980(PB82 117 128)A06

UCB/EERC-80/30 "Dynamic Properties of an Eight-Story Prefabricated Panel Building," by J.G. Bouwkamp, J.P. Kollegger and R.M. Stephen - October 1980(PB81 200 313)A05

UCB/EERC-80/31 "Predictive Dynamic Response of Panel Type Structures Under Earthquakes," by J.P. Kollegger and J.G. Bouwkamp - October 1980(PB81 152 316)A04

UCB/EERC-80/32 "The Design of Steel Energy-Absorbing Restrainers and their Incorporation into Nuclear Power Plants for Enhanced Safety (Vol 3): Testing of Commercial Steels in Low-Cycle Torsional Fatigue," by P. Spencer, E.R. Parker, E. Jongewaard and M. Drory

UCB/EERC-80/33 "The Design of Steel Energy-Absorbing Restrainers and their Incorporation into Nuclear Power Plants for Enhanced Safety (Vol 4): Shaking Table Tests of Piping Systems with Energy-Absorbing Restrainers," by S.F. Stiemer and W.G. Godden - Sept. 1980

UCB/EERC-80/34 "The Design of Steel Energy-Absorbing Restrainers and their Incorporation into Nuclear Power Plants for Enhanced Safety (Vol 5): Summary Report," by P. Spencer

UCB/EERC-80/35 "Experimental Testing of an Energy-Absorbing Base Isolation System," by J.M. Kelly, M.S. Skinner and K.E. Beucke - October 1980(PB81 154 072)A04

UCB/EERC-80/36 "Simulating and Analyzing Artificial Non-Stationary Earthquake Ground Motions," by R.F. Nau, R.M. Oliver and K.S. Pister - October 1980(PB81 153 397)A04

UCB/EERC-80/37 "Earthquake Engineering at Berkeley - 1980," - Sept. 1980(PB81 205 674)A09

UCB/EERC-80/38 "Inelastic Seismic Analysis of Large Panel Buildings," by V. Schricker and G.H. Powell - Sept. 1980 (PB81 154 338)A13

UCB/EERC-80/39 "Dynamic Response of Embankment, Concrete-Gravity and Arch Dams Including Hydrodynamic Interaction," by J.F. Hall and A.K. Chopra - October 1980(PB81 152 324)A11

UCB/EERC-80/40 "Inelastic Buckling of Steel Struts Under Cyclic Load Reversal," by R.G. Black, W.A. Wenger and E.P. Popov - October 1980(PB81 154 312)A08

UCB/EERC-80/41 "Influence of Site Characteristics on Building Damage During the October 3, 1974 Lima Earthquake," by P. Repetto, I. Arango and H.B. Seed - Sept. 1980(PB81 161 739)A05

UCB/EERC-80/42 "Evaluation of a Shaking Table Test Program on Response Behavior of a Two Story Reinforced Concrete Frame," by J.M. Blondet, R.W. Clough and S.A. Mahin

UCB/EERC-80/43 "Modelling of Soil-Structure Interaction by Finite and Infinite Elements," by F. Medina - December 1980(PB81 229 270)A04

UCB/EERC-81/01 "Control of Seismic Response of Piping Systems and Other Structures by Base Isolation," edited by J.M. Kelly - January 1981 (PB81 200 735)A05

UCB/EERC-81/02 "OPTNSR - An Interactive Software System for Optimal Design of Statically and Dynamically Loaded Structures with Nonlinear Response," by M.A. Bhatti, V. Ciampi and K.S. Pister - January 1981 (PB81 218 851)A09

UCB/EERC-81/03 "Analysis of Local Variations in Free Field Seismic Ground Motions," by J.-C. Chen, J. Lysmer and H.B. Seed - January 1981 (AD-A099508)A13

UCB/EERC-81/04 "Inelastic Structural Modeling of Braced Offshore Platforms for Seismic Loading," by V.A. Zayas, P.-S.B. Shing, S.A. Mahin and E.P. Popov - January 1981(PB82 138 777)A07

UCB/EERC-81/05 "Dynamic Response of Light Equipment in Structures," by A. Der Kiureghian, J.L. Sackman and B. Nour-Omid - April 1981 (PB81 218 497)A04

UCB/EERC-81/06 "Preliminary Experimental Investigation of a Broad Base Liquid Storage Tank," by J.G. Bouwkamp, J.P. Kollegger and R.M. Stephen - May 1981(PB82 140 385)A03

UCB/EERC-81/07 "The Seismic Resistant Design of Reinforced Concrete Coupled Structural Walls," by A.E. Aktan and V.V. Bertero - June 1981(PB82 113 358)A11

UCB/EERC-81/08 "The Undrained Shearing Resistance of Cohesive Soils at Large Deformations," by M.R. Pyles and H.B. Seed - August 1981

UCB/EERC-81/09 "Experimental Behavior of a Spatial Piping System with Steel Energy Absorbers Subjected to a Simulated Differential Seismic Input," by S.F. Stiemer, W.G. Godden and J.M. Kelly - July 1981

UCB/EERC-81/10 "Evaluation of Seismic Design Provisions for Masonry in the United States," by B.I. Sveinsson, R.L. Mayes and H.D. McNiven - August 1981

UCB/EERC-81/11 "Two-Dimensional Hybrid Modelling of Soil-Structure Interaction," by T.-J. Tzong, S. Gupta and J. Penzien - August 1981(PB82 142 118)A04

UCB/EERC-81/12 "Studies on Effects of Infills in Seismic Resistant R/C Construction," by S. Brokken and V.V. Bertero - September 1981

UCB/EERC-81/13 "Linear Models to Predict the Nonlinear Seismic Behavior of a One-Story Steel Frame," by H. Valdimarsson, A.H. Shah and H.D. McNiven - September 1981(PB82 138 793)A07

UCB/EERC-81/14 "TLUSH: A Computer Program for the Three-Dimensional Dynamic Analysis of Earth Dams," by T. Kagawa, L.H. Mejia, H.B. Seed and J. Lysmer - September 1981(PB82 139 940)A06

UCB/EERC-81/15 "Three Dimensional Dynamic Response Analysis of Earth Dams," by L.H. Mejia and H.B. Seed - September 1981 (PB82 137 274)A12

UCB/EERC-81/16 "Experimental Study of Lead and Elastomeric Dampers for Base Isolation Systems," by J.M. Kelly and S.B. Hodder - October 1981

UCB/EERC-81/17 "The Influence of Base Isolation on the Seismic Response of Light Secondary Equipment," by J.M. Kelly - April 1981

UCB/EERC-81/18 "Studies on Evaluation of Shaking Table Response Analysis Procedures," by J. Marcial Blondet - November 1981

UCB/EERC-81/19 "DELIGHT.STRUCT: A Computer-Aided Design Environment for Structural Engineering," by R.J. Balling, K.S. Pister and E. Polak - December 1981

UCB/EERC-81/20 "Optimal Design of Seismic-Resistant Planar Steel Frames," by R.J. Balling, V. Ciampi, K.S. Pister and E. Polak - December 1981

UCB/EERC-82/01 "Dynamic Behavior of Ground for Seismic Analysis of Lifeline Systems," by T. Sato and A. Der Kiureghian - January 1982 (PB82 218 926) A05

UCB/EERC-82/02 "Shaking Table Tests of a Tubular Steel Frame Model," by Y. Ghanaat and R. W. Clough - January 1982 (PB82 220 161) A07

UCB/EERC-82/03 "Experimental Behavior of a Spatial Piping System with Shock Arrestors and Energy Absorbers under Seismic Excitation," by S. Schneider, H.-M. Lee and G. W. Godden - May 1982

UCB/EERC-82/04 "New Approaches for the Dynamic Analysis of Large Structural Systems," by E. L. Wilson - June 1982

UCB/EERC-82/05 "Model Study of Effects on the Vibration Properties of Steel Offshore Platforms," by F. Shahrivar and J. G. Bouwkamp - June 1982

UCB/EERC-82/06 "States of the Art and Practice in the Optimum Seismic Design and Analytical Response Prediction of R/C Frame-Wall Structures," by A. E. Aktan and V. V. Bertero - July 1982.

UCB/EERC-82/07 "Further Study of the Earthquake Response of a Broad Cylindrical Liquid-Storage Tank Model," by G. C. Manos and R. W. Clough - July 1982

UCB/EERC-82/08 "An Evaluation of the Design and Analytical Seismic Response of a Seven Story Reinforced Concrete Frame - Wall Structure," by A. C. Finley and V. V. Bertero - July 1982

UCB/EERC-82/09 "Fluid-structure Interactions: Added Mass Computations for Incompressible Fluid," by J. S.-H. Kuo - August 1982

UCB/EERC-82/10 "Joint-Opening Nonlinear Mechanism: Interface Smeared Crack Model," by J. S.-H. Kuo - August 1982

UCB/EERC-82/11 "Dynamic Response Analysis of Techi Dam," by R. W. Clough, R. M. Stephen and J. S.-H. Kuo - August 1982

UCB/EERC-82/12 "Analytical Earthquake Responses of R/C Coupled Wall-Frame Structures," by A. E. Aktan, V. V. Bertero and M. Piazza - August 1982

UCB/EERC-82/13 "Preliminary Report on the SMART 1 Strong Motion Array in Taiwan," by B. A. Bolt, C. H. Loh, J. Penzien, Y. B. Tsai and K. Yeh - August 1982

UCB/EERC-82/14 "Shaking-Table Studies of an Eccentrically X-Braced Steel Structure," by M.S. Yang - September 1982

UCB/EERC-82/15 "The Performance of Stairways in Earthquakes," by Catherine Roha, James W. Axley and Vitelmo V. Bertero - August 1982

UCB/EERC-82/16 "The Behavior of Submerged, Multiple Bodies in Earthquakes," by Wen-Gen Liao, September 1982